Formation of Defects at High Temperature Plastic Deformation of Gallium Arsenide

DISSERTATION

Zur Erlangung des akademischen Grades
doctor rerum naturalium (Dr. rer. nat.)

vorgelegt der

Mathematisch-Naturwissenschaftlich-Technischen Fakultät
(Mathematisch-naturwissenschaftlicher Bereich)
der Martin-Luther-Universität Halle-Wittenberg

von
Dipl. Phys. Vladimir V. Mikhnovich
geb. am 03. Oktober 1978 in Voskresensk, Russland

Gutachterin/Gutachter

1. PD Dr. Hartmut S. Leipner

2. Prof. Dr. Nikolai Bagraev

3. Prof. Dr. Jörg Weber

Halle (Saale), den 14 März 2006

urn:nbn:de:gbv:3-000010038
[http://nbn-resolving.de/urn/resolver.pl?urn=nbn%3Ade%3Agbv%3A3-000010038]

CONTENTS

1. INTRODUCTION

It's known that solids after being subjected to strong enough deformation alter their shape irreversibly. This phenomenon is generally called *plastic deformation* of solids. During many decades microscopic processes that take place in a crystal in the course of its deformation received studies of many scientists. At first they failed to explain the fact of existence of significantly lower experimental values of crystal strength in comparison with the theoretical value, which approximately equals to 10^{10} Pa [Ash79]. In some cases there was a difference of several orders between the two values. Low strength of well-prepared crystals was a mystery for throughout dozens of years. It was discovered, however, that the strength of relatively badly prepared crystals reaches closely the theoretical value. But it was also found out that the crystal strength decreased sharply after the improvement of its structure (for instance by means of annealing). In that case it would have been natural to suppose that the observed strength of more perfect samples should reach the theoretical value but the real situation was far different from that supposition.

In 1934 Taylor [Tay34], Orowan [Oro34] and Polyani [Pol34] tried to explain such crystal behavior with help of *dislocations*. They suggested that almost in all real crystals there are dislocations and their movement originates plastic deformation. However, the experimentally observed dependence of stress from deformation (*deformation curve*) when crystal is stretched cannot be explained only by means of glide of dislocations that were present in a crystal before the deformation. It turned out that it was possible to explain qualitatively the dependence of stress from deformation assuming that:

a) The concentration of dislocations can change if the deformation size is changed;
b) There are obstacles that impede the movement of dislocations and the influence of such obstacles can be higher or lower depending on the deformation size.

Exploring the crystal behavior Frank and Read came to conclusion that the dislocation line if it is fixed in two points bends in these two points. Increase in external stress applied to the dislocation leads to approaching of the bends to each other so that they annihilate and create a new dislocation cycle. The remaining segment of dislocation line can again bend until another dislocation cycle is created. These Frank-Read views allow us to propose an explanation for the increase in number (and, accordingly, in concentration) of dislocations in a crystal when it is being subjected to deformation. But concerning the mechanisms of movement of dislocations Peierls [Pei40] suggested a model according to which the dislocation line moves in the periodic potential with the *Burgers vector* periodicity. This means that during their movement dislocations have to overcome obstacles – a certain potential barriers. It turned out, however, that experimental values of dislocations velocity cannot be explained using this model only. And thus come to opinion that there are other obstacles that influence the movement of dislocations. Such obstacles are other dislocations and *defects* that exist in the initial non-deformed crystal. Other obstacles are defects that are not present in the initial crystal and that originate during the movement of dislocations in the process of deformation of the sample. Crystal lattice *vacancies* and *interstitials* are examples of such defects.

Seitz [Sei50] was the first who used the views of vacancies origination at time when dislocations move for experimental data interpretation (here the experimental data of

electrical conductivity measurement of NaCl plastically deformed crystals are meant; [Gyu 28] and [Ste33]). During the past years with help of different experimental methods scientists proved the origination of *point defects* in the course of plastic deformation in ion crystals, metals and semiconductors [Bro87].
Mott [Mot60] suggested the model of movement of *screw dislocation* by means of jogs creation. Jogs appear in the dislocation line but do not lie in the slip plane. The movement of jogs may be effected by emission or absorption of point defects (vacancies or interstitials). Such approach serves to explain the emergence of defects during the movement of dislocations. In [Sch65, Bar65, Mec80, Mil94] works also provide us with the quantitative models that explain the emergence of point defects during the movement of dislocations and the influence of the said defects on the dislocation motion.

Nevertheless, the existing qualitative models that explain the emergence of point defects during the movement of dislocations and the influence of these defects on the dislocation motion do not permit us, unfortunately, to make quantitative prognosis of the dependence of crystal stress from its deformation at different experimental conditions. Such conditions include temperature of the sample, deformation velocity, doping level and the alloy impurity type if a semiconductor material is tested. And so experimental studies of the influence of the plastic deformation on the crystal properties are still of current importance.

The purpose of the present thesis consists in acquiring more concrete information concerning the mechanism of the movement of dislocations and types of defects that appear during the process of dislocation motion on the basis of systematic experimental studies of the GaAs deformation. Experimental studies concerning the dependence of the stress of the samples from their deformation at different values of the deformation parameters (like temperature and deformation speed) were conducted in this paper. Moreover, the values of defects concentration that emerge in crystals during their deformation were analyzed later on. Different facets were considered when choosing the object of the study (GaAs samples in particular):

1. Semiconductor materials are easily processed.
2. GaAs materials are widely used in industrial microelectronics.
3. GaAs samples availability and operational experience with semiconductor material that our working group has are also of great importance.

To determine the concentration of defects introduced in samples during the deformation process the *positron annihilation spectroscopy* (PAS) method was used. This method is effective when studying defects with open volume (defects without positive atom nucleus) namely crystal lattice vacancies and their clusters that represent traps for positrons.
This method is a very important one in comparison with the other similar methods for types of defects identification because vacancies and their clusters represent one of the basic types of defects that emerge during the deformation of samples.

The second chapter of this paper deals with models of movement of dislocations and origination of defects during deformation of the samples. In the third chapter channels and models of positron annihilation in the GaAs samples are investigated. In the forth chapter the used experimental methods, preparation procedure of test samples and technical data of conducted experiments are described. The fifth chapter shows the results of deformation experiments. The sixth chapter shows the results of positron lifetime measurements by the PAS method. In the seventh chapter one can find analyses of the values of defects concentration that were introduced in samples during deformation.

2. PLASTIC DEFORMATION

During the deformation of a solid the measurable macroscopic magnitudes are: the force F applied to the sample and linear dimensions of the sample. The combination of these magnitudes allows us to calculate the average stress τ and average deformation ε:

$\tau = \frac{F}{A}$ (A is the sectional area that changes during the deformation process and to which the force F is applied), $\varepsilon = \Delta l / l$ (where $\Delta l, l$ are length variation and initial length of the test sample accordingly).If stretching (pressing) of the crystal occurs at constant deformation speed ($\dot{\varepsilon} = const$), then we speak about *dynamic regime of deformation* (and this very regime is studied further in the paper). It is supposed that in dynamic regime of tests the material preserves its elastic properties in the area of plastic deformation and it is believed, in this case, that the deformation consists of two parts [Rab79]:

$$\varepsilon = \varepsilon_{plast} + \varepsilon_{elast} . \tag{2.1}$$

The purpose of the most works dedicated to plastic deformation is to determine interactions between macroscopic magnitudes that characterize the properties of test material during deformation and microscopic magnitudes that characterize the movement of dislocations. In connection with this in the first part of the present chapter the deformation curve is analyzed qualitatively, i.e. macroscopic parameters of the deformation are examined. Then our attention switches to qualitative and quantitative models of the microprocesses that flow in different deformation stages. Finally models of kinetics of the origination of point defects are scrutinized.

2.1 Deformation curve during stretching

Deformation curve during stretching in dynamic regime conditions can be divided into several areas [Die56]. Figure 2.1 represents the qualitative dependence of stress τ from deformation ε. It should be noted that in real experiments these or that areas do not necessarily become apparent (in the figure 2.1 the most general situation is depicted).

Area of the first curve rise corresponds to the area of elastic deformation or the Hooke area. It is characterized by the linear dependence of stress from deformation and reversibility of the deformation process.

The area of elastic deformation borders with the area where the decrease in stress at the increase in stretching is observed. There the plastic deformation begins and the area is called *liquidity* area, τ_{ly}^{*} and τ_{ly} are accordingly called the upper and lower *yield stress*. It should be mentioned that the nature of dependence of τ from ε in that area to a considerable degree is determined by the initial state of the sample. For example it may be determined by the concentration of dislocations before the deformation. Moreover the dependence may take different values, e.g. constant stress can be traced during the deformation.

The area of *easy glide* denominated as stage I adjoins the liquidity area. In this phase dislocations are free to move almost in any direction in single slip system increasing the deformation without significant rise in stress [Lak80]. This phase is sometimes called the phase of insignificant *hardening*. It is also possible that the stress in that area remains the same. In the time of strong deformation the phase of multiple slip is seen meaning that dislocations move in two or more systems [Lak80] (phase II). In this phase the dislocation structure becomes very complicated and density of dislocations increases in comparison with its initial state.

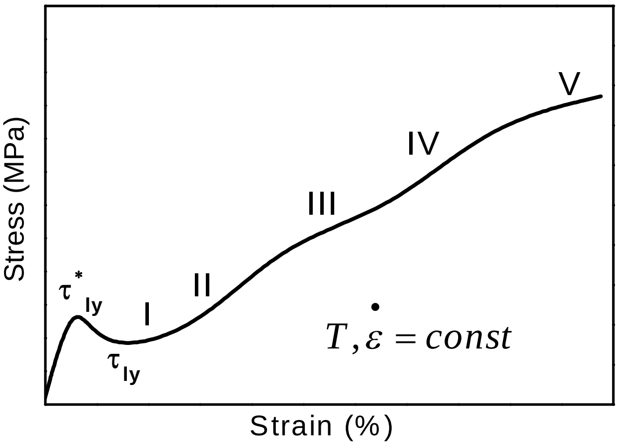

Fig. 2.1 Deformation curve during stretching in dynamic deformation conditions ($\dot{\varepsilon} = const$) [Sie93a].

Because of the dislocations interaction the resistance to their movement grows sharply and so the stress should also rise to ensure their motion. Phase II is called the hardening phase.

Phase III is called the phase of *dynamic recovery*. Such term was chosen to describe it because in this phase dislocations disappear and then appear again.

At high temperature deformation additional stages of hardening (IV) and recovery (V) may appear.

2.2 Movement of dislocations

Geometry. The plastic deformation is occurs due to dislocation motion. The simplest types of dislocations are *edge* and *screw dislocations*. The edge dislocation model is shown on figure 2.2. If we imagine extra crystalline half plane (on the picture it coincides with the upper half plane y, z; the z axis is directed vertically with respect to the picture plane) that is inserted into the lattice (its section is shown on the picture) then the edge line of that half plane (it coincides with the z axis on the picture) represents the edge dislocation. After the entire bypass about the dislocation line the lattice points displacement vector gains the increment $\vec{b}$. This vector is called the Burgers vector and it is equal to one of the lattice vectors. In case of the edge dislocation the Burgers vector is perpendicular to the dislocation line, in case of the screw dislocation the vector is parallel to the dislocation line.

In [Rab79] it is shown that if there are no defects in the crystal (vacancies and interstitials) then dislocations are able to move only in directions where the following is true:

$$(d\vec{u} \times d\vec{l})\vec{b} = 0 . \qquad (2.2)$$

Here $d\vec{l}$ is the dislocation line element, $d\vec{u}$ – vector of dislocation shift. It results from the (2.2) correlation that the edge dislocation is able to move only in the plane in which the dislocation is found and where the Burgers vector is present. On the contrary, according to the (2.2) equality the screw dislocation is able to move in any plane that contains the dislocation line because in this case the Burgers vector is parallel to the dislocation line. This means that in the process of its movement the dislocation line is able to move from one plane to another.

Theoretically possible directions of movement of dislocations were discussed above. However, the slip (displacement of separate crystal parts with regard to each other) in the crystal lattice is mainly realized along planes and directions with higher density of atoms where the magnitude of shear resistance is minimal.

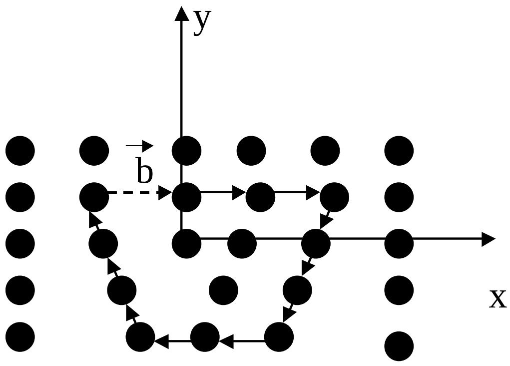

Fig. 2.2: Edge dislocation model. Contour is painted by continuous arrows. The Burgers vector $\vec{b}$ is painted by the dotted arrow. The dislocation line is placed vertically with respect to the plane of the draft.

This is because the distance between such neighboring atomic planes reaches its maximum and thus the bonds between them are extremely weak. The slip plane and the slip direction that lie in these planes constitute the slip system. It is possible that more than one slip system act in crystals simultaneously. For instance in crystals with face-centered cubic lattice the slip is effected in planes (111) [Lak80]. The more slip planes and directions exist in a crystal, the more it is exposed to plastic deformation. It must be noted, however, that the slip process should not be considered as a process of simultaneous displacement of one crystal part with relatively to the other. Such simultaneous shear would require far greater stress, probably hundred times as great as that at which the process of plastic deformation runs in reality. The real shear mechanism is quite different. The movement of dislocations at distances that are significantly greater than interatomic distances leads to the following. Two crystal parts that are divided by a plane in which dislocation moves come closer at the distance that equals to interatomic distance; and visible shear is detected after the repeated movement of dislocations on the slip plane.

Tangential stress σ that influences the dislocation in a certain slip system can be calculated by the formula $\sigma = \tau m_s$, and the *shear* γ of a crystal in the slip plane for the case of little deformations $(\varepsilon << 1)$ by $\gamma = \varepsilon / m_s$. Here m_s is the Schmidt factor and $m_s = \cos\Phi \cos\Psi$ (Φ is the angle between the deformation axis and the unit vector that is perpendicular to the slip plane; Ψ is the angle between the deformation axis and the Burgers vector). The Schmidt factor takes into account, in particular, direction of the influence of the external load on the crystal (using for this purpose the deformation axis) and the orientation of the slip plane (by means of orientation of the unit vector that is perpendicular to the slip plane).

Peierls potential. For the movement of the dislocation line along the lattice vector it is necessary to successively (as the dislocation moves) break the bond between the adjacent atoms on all dislocation length (see figure 2.2). To effect such movement the dislocation has to absorb large quantity of energy and that casts doubt on the mere possibility of the movement of dislocations itself. But in fact the dislocation can move consuming little energy. Peierls [Pei40] suggested the model that describes the movement of the dislocation according to which it moves in the periodic potential by the law:

$$W = W_0 \sin^2\left(\frac{\pi y}{a_p}\right) \tag{2.3}$$

At that the magnitude a_p is equal to the Burgers vector. The scheme on picture 2.3 shows the movement of the dislocation line in the potential (2.3). Kinks appear on the dislocation that lies in the slip plane. These kinks are able to appear as a result of thermogeneration.

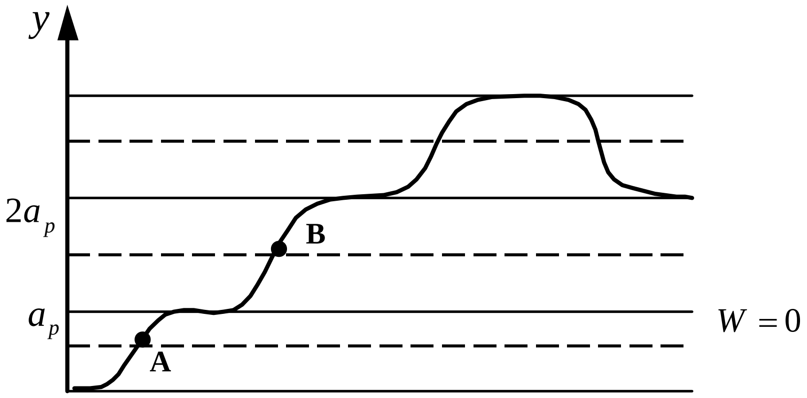

Fig. 2.3: Movement of dislocation line. Hatched and continuous lines represent maximum and minimum potential value. AB is the dislocation line segment and it is restricted by two fractures. According to [Kra84].

The movement is effected by the successive overcoming of barriers by segments (elements of the dislocation line that include two kinks). This process of segments flow over the barrier (like a wave) is much more beneficial from the energy point of view than the process of barrier overcoming by the whole dislocation at once. Such dislocations motion regime is generally called the *fracture movement* regime.

The studied qualitative model of the movement of dislocations – when dislocations cover large distances without any difficulties – can be used to explain phase I of crystal deformation (see figure 2.1).

Obstacles in the slip process. As a rule, crystals contain defects of different types that impede the movement of dislocations. These are impurity atoms, point defects and their clusters (existing both in the initial crystal and appearing during the deformation process), dislocations themselves.

The figure 2.4 shows the model that illustrates the stretching of the dislocation line that is fixed on obstacles (for example, on impurity atoms). In the first position the dislocation line is fixed.

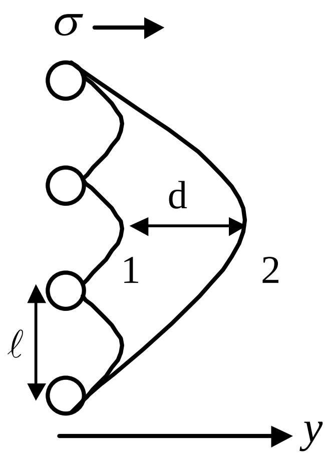

Fig. 2.4: Model for stretching of the dislocation line. Position 1 – dislocation line before tearing off from obstacles. Position 2 – dislocation line after tearing off from obstacles. According to [Kra 84].

If the external stress σ effecting the dislocation at the location of obstacles is strong enough then the dislocation stretches and tears off from the obstacles (position 2). In the time of further stretching the dislocation tears off from the layer of impurity atoms and hits upon the next layer of impurity atoms that are located more to the right along the y axis. Such dislocation motion regime is called the stretching regime.

Other dislocations can also be obstacles for the movement of dislocations due to their interaction. Interaction force between the two parallel screw dislocations related to the dislocation length unit near the isotropic medium is [Lan87]:

$$F_S = \mu \frac{b_1 b_2}{2\pi d_1}. \tag{2.4}$$

The similar magnitude for the two parallel edge dislocations that lie in the single slip plane is [Rab79]:

$$F_E = \mu \frac{b_1 b_2}{2\pi(1-\nu)d_1}. \tag{2.5}$$

At this μ is the shear modulus, ν is the Poisson coefficient, d_1 – distance between the dislocations, b_1, b_2 – absolute value of the Burgers vector of the first and the second dislocation accordingly. From (2.4) and (2.5) results that dislocations draw if Burgers vectors $(b_1 \times b_2 < 0)$ are pointed into opposite directions but if vectors $(b_1 \times b_2 > 0)$ are pointed into one direction then dislocations push off.

Mutual influence of dislocations on their movement can be more complicated. A crystal may have dislocations located in different slip planes and not in the single plane. Thus dislocations located in one slip plane are influenced by other dislocations located in other slip planes. Such influence can be illustrated in the following manner. Let a certain slip plane S_1 (figure 2.5) contain infinite number of identical parallel rectilinear edge dislocations removed on equal distance h one from another (dislocation lines are directed along the z axis).

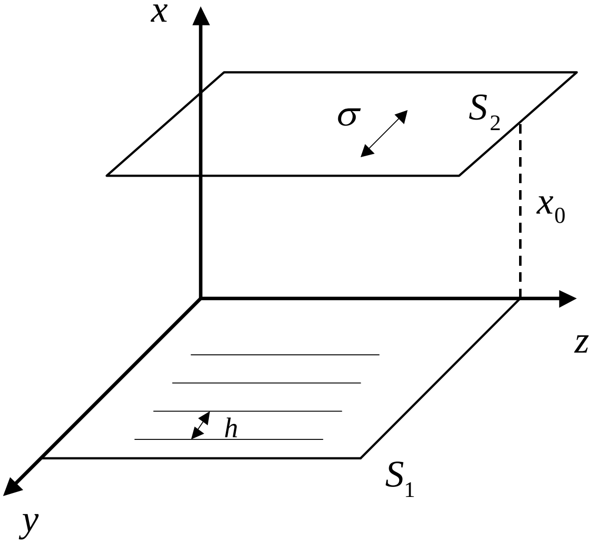

Fig. 2.5: Dislocation wall scheme. S_1 is the plane of arrangement of dislocations (dislocations are directed along the z axis and are shown by straight lines). S_2 is the plane of observation. x_0, h are the distances between the planes and dislocations accordingly. σ is the tangential stress.

Such dislocation system is called the *dislocation wall*. In the plane S_2 (the plane S_2 is parallel to the plane S_1 and is removed from it on the distance x_0) this dislocation wall creates tangential stress σ that works parallel the y axis. If there are dislocations in the plane S_2 then this stress effects their movement. In approximation the isotropic medium and there where the condition $x_0 >> h$ is realized the expression for σ is [Lan87]:

$$\sigma(y) = 4\pi^2 B \frac{bx_0}{h^2} \exp(-2\pi x_0 / h) \cos(2\pi y / h). \tag{2.6}$$

At this $B = \mu / 2\pi(1-\nu)$, b is the Burgers vector length for the edge dislocation.

Dislocation walls are comprised, as a rule, from dislocations of little mobility and represent obstacles for mobile dislocations. Dislocations of little mobility (as well as dislocation walls) located in different slip planes constitute the system of almost immobile *tree-like dislocations* that influence a lot the movement of mobile dislocations. Tree-like dislocations can appear both in the process of crystal growth and during crystal deformation. Increase in the concentration of the tree-like dislocations influences crystal strengthening that is noted in stage II of the deformation curve during stretching (see fig. 2.1).

2.3 Multiplication of dislocations

The concentration of dislocations is determined as the ratio of all dislocations length to the volume of the sample. This means that change in concentration of dislocations is not always connected with the change in number of separate dislocations because the change in total length of dislocations also means change in their concentration. In this aspect increase both in number of dislocations and their total length means multiplication. Let us focus on several mechanisms of multiplication of dislocations.

The dislocation line cannot simply end in a crystal: it rather appears on the surface of the crystal or forms a closed loop. For such dislocations the Burgers vector has constant value and direction throughout the entire dislocation line but the angle between the Burgers vector and the dislocation line element changes along the dislocation line. Proof of this statement can be found, for example, in [Lan87]. Mechanisms of multiplication of closed dislocations can be explain with help of the Frank -Read mechanisms.

Frank – Read Source. The figure 2.6 illustrates the multiplication of closed dislocation loops (closed dislocation cycles). The segment A of the dislocation line

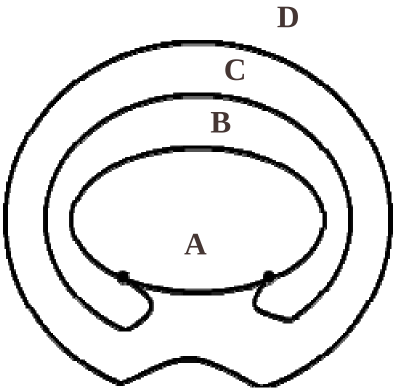

Fig.2.6: The Frank-Reed deformation source. Segment A of the dislocation stretches between the phases B and C. A new dislocation appears on the phase D.

(the initial dislocation itself is already a closed loop) that is fixed on two obstacles stretches under the influence of the external stress applied to it. As the stress increases the segment A progresses through several phases. The figure 2.6 represents two such phases B and C. The process enters into the phase D after the specific stress value has been achieved and there both dislocation line bends merge forming a single closed dislocation. The remaining part of the segment A of the initial dislocation line can again stretch and form a new dislocation.

The multiplication of dislocations and their movement in the Peierls potential serves to explain the nature of dependence of stress from crystal deformation in the liquidity area (see fig. 2.1). The stress in the elasticity area is high enough to allow dislocations to overcome obstacles there where the elasticity area borders the plasticity area [Ale68a].

Cross Slip. As has been described above (see chapter 2.2), the Burgers vector and direction of the dislocation line determine only one slip plane of the edge dislocation. During its movement the edge dislocation stays within the borders of the slip plane. Theoretically, any plane can be a slip plane for screw dislocations but in practice only planes with the densest concentration of dislocations participate in the slip process. It’s known that, theoretically, a screw dislocation can move freely in any direction so there are no restrictions for it to change slip planes. Such movement from one slip plane to another occurs under the influence of neighbouring dislocations and other obstacles on the viewed dislocation. In this case we observe what is called *double cross slip* of dislocations. The figure 2.7 illustrates this double cross slip.

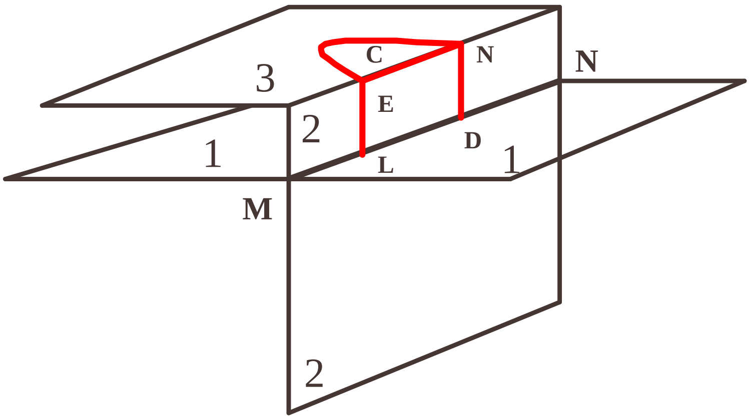

Fig. 2.7: Double cross slip of dislocations. MN- initial dislocation line. LE, ND-dislocation line segments. The segment C can act as at he Frank-Reed source.

The initial dislocation moves in the slip plane (1). Here MN is the dislocation line. At a certain moment a kink can appear in the screw dislocation. Kink represents a dislocation segments (LE, ND are dislocation segments) in the form of a step. The segment slip plane (2 is the segment slip plane) is perpendicular to the slip plane of the initial dislocation. The slip process in the plane (2) causes the segment to pass from this plane to the plane (3) which is parallel to the slip plane of the initial dislocation (1). The segment C can act here as the Frank-Read source. After the segment has moved to the plane (3) it can again return to the initial slip plane (1) and so the initial dislocation will continue its movement in the plane (1). In this very manner segments and dislocations slip in lateral planes (planes 2 and 1 respectively).

Destrengthening of the stress curve during stretching seen in the stage V (see fig. 2.1) associates with more rapid cross slip because, on the one hand, dislocations density increases and, on the other hand, the velocity of dislocations also increases as the cross slip helps to avoid obstacles during the slip process.

One must remember, however, that speaking about the multiplication of dislocations one should consider the possible reduction in density of dislocations due to annihilation. If the total Burgers vector of some of the interacting dislocations takes zero value then these dislocations will disappear.

2.4 Kinetics of the movement of dislocations

Qualitative analysis of the causes that influence the behaviour of the dependence of stress from crystal deformation has been already considered above (see chapters 2.2 and 2.3). To sum up we can say that the behaviour of dislocations, i.e. their movement and multiplication, determines significantly the behaviour of the deformation curve. This statement concerns both the dislocations that were present in the crystal long before the deformation and those that were emerged during the deformation process. To be able to analyze the behaviour of dislocations in a deformed crystal one needs certain equations that connect experimentally observed magnitudes, as well as those parameters that characterize the conditions at which the deformation process runs like deformation values, deformation velocity, and crystal temperature, with the magnitudes that characterize kinetics of the movement of dislocations, i.e. velocity and density. This chapter deals with these equations.

Effective Stress Model. It is very important to know what stress affects the dislocation line. Apart from the external stress on dislocation line is affected, stress fields of crystal dislocations. In [Ale68a] got expressions for stresses caused by dislocations with the density N_d:

$$\sigma_i^E = \left[\mu b/(2\pi(1-\nu)\right]N_d^{1/2}. \qquad (2.7)$$

$$\sigma_i^S = [\mu b/2\pi]N_d^{1/2}. \qquad (2.8)$$

The first equation serves to measure the stress in edge dislocations, the second is used in case of screw dislocations. To determine the stress applied to the dislocation line one should substitute the effective stress σ_{eff} for the external tangential stress σ that influences dislocations in a certain slip system [Haa62]:

$$\sigma_{eff} = \sigma - \sigma_i = \sigma - AN_d^{1/2}. \qquad (2.9)$$

Here the constant A includes different types of dislocations. The minus sign appears in the formula because dislocations strive to reduce overall stress in a crystal. Using (2.9) the only thing we can do is measure the maximum possible density of dislocations. Assuming $\sigma_{eff} = 0$ ($\sigma_{eff} \geq 0$) the maximum value of dislocations density will be $(\sigma / A)^2$. As a rule, it’s better to use (2.10) to determine the density of dislocations at a given external stress applied to the sample [Ger86]:

$$\tau = \alpha\mu b N_d^{1/2}. \qquad (2.10)$$

At this $\alpha -$is a constant determined by the geometry of the crystal structure and takes its values between 0.5 and 1 [Mec81].

Orowan Equation. Orowan [Oro40] was the first to view plastic deformation as a dynamic process. He supposed that plastic deformation is similar to other transport processes that run in a solid, for example, the process of movement of charge carriers. The difference is that in this case dislocations act as charge carriers. The following correlation was obtained to define the velocity of crystal shear along the dislocations slip plane:

$$\dot{\gamma} = bN_{dm}\upsilon \,. \tag{2.11}$$

Here υ is mobile dislocations velocity, N_{dm} is mobile dislocations density.

Dislocations Velocity. There are two models that relate between dislocation velocity to parameters that characterize experimental conditions: stress and temperature of the sample [Sch65], [Ale68a].

Schoeck [Sch65] followed thermodynamic understanding of the phenomenon and studied the changing of the thermodynamic Gibbs potential G (the Gibbs enthalpy) of a crystal during its deformation[1], i.e. studied the enthalpy difference ΔG before and after crystal deformation. In [Zon94] the equation for ΔG was given in its commonest form:

$$\Delta G = U - V_A \sigma_{eff} \,. \tag{2.12}$$

Here U is the energy barrier that dislocations have to pass during gliding. V_A is *the activation volume* of the movement of dislocations [Wee83a]:

$$V_a = bdl \,. \tag{2.13}$$

Here l is the length of a dislocation element fixed on the two nearest obstacles (see fig. 2.4); d is the stretching amplitude of that dislocation element in lateral direction with respect to the element line at the moment it tears off from obstacles under the influence of the external stress.

In [Wee83a] relying on the Schoeck model [Sch65] the following was obtained to define dislocation glide velocity:

$$\upsilon = lf \exp(-\Delta G / k_B T). \tag{2.14}$$

At this $f -$ is the oscillation frequency of the dislocation line, k_B is the Boltzmann constant. Later, assuming that the activation volume does not depend on the external stress

---

[1] The enthalpy G for deformed crystal is G=E-TS-$\sigma_{ik} u_{ik}$. [Lan87]. Here E, T, S are internal energy, temperature and enthalpy of a deformed crystal accordingly; σ_{ik} is the external stress tensor, it functions in the x_k coordinate direction in the plane perpendicular to the x_i coordinate; u_{ik} is the deformation tensor which is $u_{ik} = \frac{1}{2}(\frac{\partial u_i}{\partial x_k} + \frac{\partial u_k}{\partial x_i})$; u_j shows the crystal points displacement along the x_j axis.

and taking into consideration 2.9, 2.12 and 2.14 the following expression is derived to connect dislocation velocity υ with stress σ: $\upsilon \sim \exp(\sigma)$. However, it was experimentally found out that the functional dependence between υ and σ is expressed like $\upsilon \sim \sigma^m$, where *rate of stress indicator* m takes values from 1 to 2 (for semiconductor materials) [Sch67].

In [Ale68a] Alexander and Haasen suggested a model for movement of dislocations velocity assuming that dislocations move in the fracture regime (see fig. 2.3). Taking into consideration this supposition and with regard to the assumption that fractures appear due to thermal activation (by means of passing some of oscillating atoms' energy to dislocations) dislocations velocity is given by:

$$\upsilon = B\sigma^m \exp(-U / k_B T)\,. \tag{2.15}$$

Here U is the *activation energy* of movement of dislocation which is the sum of formation energy and double fractures migration energy. $B-$ is the empiric constant. Rate of stress indicator takes values from 1 to 1.5.

If we use the Schoeck model to describe movement of dislocations velocity, then V_A and U will be the parameters to characterize the movement of dislocations. But if, on the contrary, we take the Alexander and Haasen model [Ale68a] for this purpose , then m and U will be the parameters to characterize the movement of dislocations.

Let's determine the activation volume V_A of the movement of dislocations. Using the Orowan equation (2.11) for expressing υ we'll have: $\upsilon = \dot{\gamma}/(bN_{d_m})$. Given that $\gamma = \varepsilon / m_s$ we come to $\dot{\gamma} = \dot{\varepsilon}/ m_s$. Now for movement of dislocations velocity we arrive at $\upsilon = \dot{\varepsilon}/(m_s bN_{d_m})$. Substituting this expression for velocity into (2.14) and finding the logarithm of the expression we get:

$$\ln \dot{\varepsilon} = \ln(m_s N_{d_m} blf) - \frac{\Delta G}{k_B T}\,.$$

Using (2.12) for ΔG and (2.9) for σ_{eff} we see that:

$$\ln \dot{\varepsilon} = \frac{\sigma V_A}{k_B T} - \frac{U + A V_A N_d^{1/2}}{k_B T} + \ln(m_s N_{d_m} blf)\,.$$

Assuming that the dislocations density N_d does not depend on σ the following is obtained:

$$\frac{V_A}{k_B T} = \left(\frac{\partial \ln \dot{\varepsilon}}{\partial \sigma} \right)_{T=const}$$

Taking into account that $\sigma = \tau m_s$ ($\tau -$ is the external stress applied in a certain direction) we arrive at:

$$V_A = \frac{k_B T}{I}\,. \tag{2.16}$$

Here

$$I = m_s \left(\frac{\partial \tau}{\partial \ln \dot{\varepsilon}} \right)_{T=const} . \qquad (2.17)$$

Let's express rate of stress indicator m. Substituting the above found expression for velocity $\upsilon = \dot{\varepsilon}/(m_s b N_{d_m})$ into (2.15) and taking the logarithm we'll finally have:

$$\ln \dot{\varepsilon} = m \ln \sigma + \ln(m_s b N_{d_m} B) - \frac{U}{k_B T} .$$

Assuming that the density of dislocations is a constant value and taking into account that $\sigma = \tau m_s$ we arrive at the expression for *m*:

$$m = \left(\frac{\partial \ln \dot{\varepsilon}}{\partial \ln \tau} \right)_{T=const} . \qquad (2.18)$$

It is possible to determine V_A and m but first we need to determine experimentally the dependence of τ from $\dot{\varepsilon}$. But to do this it's necessary for the value of dislocations density to be a constant. Changing the stretching velocity the density of dislocations can also change. This means that at the chosen experimental conditions for determining the values V_A and m stretching velocity should be changed abruptly. Then the abrupt changing of $\dot{\varepsilon}$ prevents the changing of dislocations density because the necessary processes have very little time to run smoothly till the end.

Unfortunately, it's impossible to determine the value of U in this case. For example, if the above described method to determine U is used then, assuming that the Alexander and Haasen model [Ale68a] is right, we have:

$$\left[\frac{\partial \ln \dot{\varepsilon}}{\partial \left(\frac{1}{k_B T} \right)} \right]_{N_d=const} = m \left[\frac{\partial \ln \tau}{\partial \left(\frac{1}{k_B T} \right)} \right]_{N_d=const} - U .$$

As the strain rate $\dot{\varepsilon}$ does not depend on parameter T under the experimental conditions, we arrive at:

$$U = m \left[\frac{\partial \ln \tau}{\partial \left(\frac{1}{k_B T} \right)} \right]_{N_{d=const}} .$$

The assumption that the Schoeck model [Sch65] is right gives the following expression for U:

$$U = V_A m_s \left[\tau + \frac{1}{k_B T} \frac{\partial \tau}{\partial \left(\frac{1}{k_B T} \right)} \right]_{N_{d=const}} .$$

It results from these formulae, deduced for activation energy U of the movement of dislocations, that to define the value of U under the given experimental conditions it's necessary to change abruptly the crystal temperature. Such change, however, should be made so that the density of dislocations retains its constant value, but it's technically impossible as the speed of crystal warming has its limit. So a different method is used to define the activation energy U of the movement of dislocations. In [Ale68b] the relation between the liquidity lower limit τ_{ly} (see fig. 2.1) and U was derived as:

$$\tau_{ly} = C \dot{\varepsilon}^{1/(2+m)} \exp\left[\frac{U}{(2+m) k_B T} \right]. \tag{2.19}$$

Here C is an empiric constant. Using (2.19) we come to:

$$\ln \tau_{ly} = \frac{1}{(2+m)} \ln \dot{\varepsilon} + \frac{U}{(2+m) \kappa_B T} + \ln C.$$

Hence, for U and m we have:

$$U = (2+m) \left[\frac{\partial \ln \tau_{ly}}{\partial \left(\frac{1}{k_B T} \right)} \right]_{\dot{\varepsilon}=const} . \tag{2.20}$$

$$\frac{1}{2+m} = \left(\frac{\partial \ln \tau_{ly}}{\partial \ln \dot{\varepsilon}} \right)_{T=const} . \tag{2.21}$$

Thus, from experiments for dependence of the lower yield stress τ_{ly} from the strain rate $\dot{\varepsilon}$ at a maintained temperature we can define using (2.21) the rate of stress indicator m value. Later, having defined the experimental dependence of τ_{ly} from the crystal temperature T at a constant strain rate $\dot{\varepsilon}$, it is possible to find $U/(2+m)$ using (2.20). Finally, from these experiments we are able to find U and m but not the value of the activation volume V_A of movement of dislocations. To determine V_A one must first experimentally determine the dependence of τ from $\dot{\varepsilon}$ changing abruptly the value of $\dot{\varepsilon}$ during one experiment. At the same time the temperature of a sample must be kept constant during the experiment. Then the value of V_A is derived using (2.16) and (2.17).

Moreover, these very experiments help to define the value of m using (2.18); in this case it's unnecessary to conduct experiments with abrupt changing of $\dot{\varepsilon}$ for determination of m because as has been stated above the value of m may be obtained from other experiments. However, the comparison of the values of m obtained by two above described methods is of great interest.

2.5 Formation of point defects

2.5.1 Models

Dislocations Climb. When (2.2) is true a dislocation moves conservatively in a slip plane. But when the (2.2) correlation doesn't apply dislocations may come out of the slip plane by means of climb and such movement of dislocations is considered to be nonconservative. Such kind of movement can be realized as long as a crystal lattice contains vacancies (defects) and interstitials capable of moving freely due to disproportional distribution of the thermal oscillation energy between atoms. We can imagine a defect located within a dislocation neighbourhood to move, such movement having diffusion inherent characteristics. The dislocation starts moving and follows the defect leaving its own slip plane. However, in most cases such movement of dislocations can be seen only at extremely high temperatures.

As a matter of principle, dislocations climb is a mechanism that may be used for generation of point defects because such movement of dislocations may be effected by means of emission or absorption of point defects. The emission of point defects, in its turn, may be explained the following way. A crystal lattice vacancy adjoining the dislocation can be rapidly transported along the dislocation line with help of diffusion and drifting movement in the mechanical stress field created by the dislocation [Cui96]. The dislocation line is a 'narrow gully' for vacancies [Mec80]. This can be explained by creation of alternate mechanical stress in anisotropic environment by the dislocation. The stress causes the dislocation to move to those areas containing the dislocation line where the crystal is compressed. As a result, crystal stress there where the dislocation rests now relaxes a little. The emission of crystal lattice vacancies can be affected only when reduction in the energy of the system (comprising vacancies with the dislocation) is higher than the energy required to form crystal lattice vacancies. The reduction is possible due to partial relaxation of stress in the locality of vacancies.

In [Wee83b] the following expression was obtained for the concentration of a point defect near dislocations that move according to the climb mechanism:

$$C - C_0 = C_0 \exp(-E / k_B T) \exp(\pm \sigma b^3 L / d k_B T) . \qquad (2.22)$$

Here C is the concentration of vacancies near the dislocation; C_0 is the concentration of vacancies at the thermodynamic equilibrium of the crystal away from dislocations (there where there's no influence of dislocations on the concentration of vacancies); E is the vacancy formation energy; σ is the mechanical stress caused by the dislocation; L, d denote the average way of the dislocation line before annihilation with another dislocation during dislocation glide and climb accordingly. The plus (minus) sign in the second exponential member corresponds to the emission (absorption) of crystal lattice vacancies by the dislocation.

Phase III on the deformation curve during stretching (see fig.2.1) is explained by dislocations climb [Haa89].

Fracture Resistance. In case a screw dislocation is studied, there is one more reason (in addition to that considered above) that causes emission and absorption of defects. During its movement a screw dislocation experiences a kink in certain cases. Such kinks on the dislocation line can be of different nature. Some appear due to double cross slip of dislocations (see fig. 2.7). The influence of mechanical stress fields of other dislocations on the given dislocation can, in particular, be the reason why a screw dislocation travels to a neighbouring slip plane, such movement being caused by double cross slip.

But there is another reason for appearance of kinks. Kinks may appear by virtue of crossing of two screw dislocations. Figure 2.8 (the scheme was taken from [Hub98]) illustrates how kinks appear.

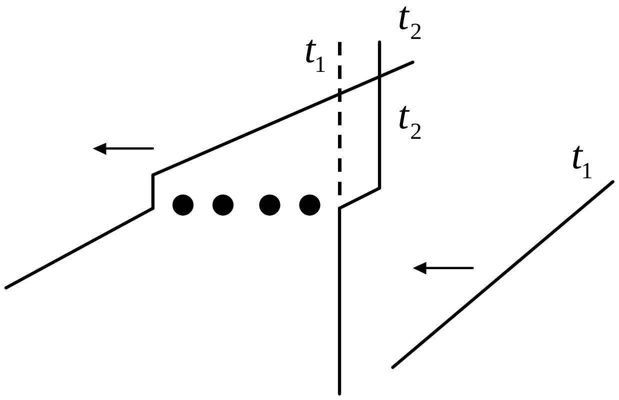

Fig. 2.8: Crossing of two screw dislocations (t_1 is the time moment before crossing, t_2 is the time moment after crossing).

As after the passage of a dislocation one-crystal part (that one above the dislocation slip plane) displaces with regarding to the other part of the crystal (that one under the slip plane) on the Burgers vector, the dislocation line itself also moves, i.e. a kink appears.

Mott [Mot60] suggested a model explaining how a screw dislocation moves having gained impulse of a kink during emission or absorption of point defects. A kink in a dislocation line is a graded dislocation segment. The kink slip plane is perpendicular to the screw dislocation slip plane. The screw dislocation kink affects nonconcervative climb motion. Such nonconservative motion can be realized by emission or absorbing point defects and such dislocation movement mechanism is called *fracture resistance*. Series of defects may be formed by means of fracture resistance. But such defects configuration (series) is sometimes unstable. As a result, two-dimensional or three-dimensional defects clusters may originate. In particular, three-dimensional vacancies clusters are constituted.

2.5.2 Kinetics of formation of point defects

Both processes that lead to defects emergence and processes that are responsible for their annihilation should be taken into consideration when analyzing the kinetics of formation of point defects. There are different ways of annihilation of vacancies and interstitials (interstice atoms):

1. Recombination of crystal lattice vacancies with interstitials.
2. Interaction of vacancies and interstitials with dislocations and atoms of different impurity (in this case other point defects emerge).

To make the annihilation of vacancies and interstitials possible it is required that they be mobile at crystal deformation temperature. Further on, for formation of stable defects – complex of a vacancy (interstitial atom) and an impurity atom – it's necessary that the annealing temperature of such complex be higher than the deformation temperature, or else these complex will not be formed. The difficulty to conduct analysis of the annihilation process in this case lies in the impossibility to use experimental data obtained for an undeformed crystal. The point is that dislocation mechanical stress may significantly influence the defects formation processes in a deformed crystal (there is no such influence in an undeformed crystal).

Formation of point defects velocity

Two completely different approaches are used to determine the velocity of formation of vacancies and interstitial atoms during the movement of dislocations. The Mott [Mot60] and Popov [Pop90] models study macroscopic processes, while the Estrin-Mecking model [Mec80] uses energetic considerations rather than macroscopic ones.

A kink generates point defects during screw dislocation glide and it is believed to be the initial moment of the formation of point defects velocity model. Mott was the first who paid attention to screw dislocations glide that contain kinks [Mot60]. Taking into consideration processes of kinks creation resulting from crossing of gliding screw dislocations with noncoplanar slip system dislocations (tree-like dislocations), and their annihilation or merger, Mott proposed the following:

$$\frac{\partial C_V}{\partial \gamma} = \frac{\xi^{1/2}}{2\sqrt{2}} b N_d^{1/2}. \qquad (2.23)$$

Here C_V is the relative concentration of vacancies (ratio of the true concentration of vacancies to the concentration of lattice atoms), $\xi -$ is the ratio of tree-like dislocations density to the general density of dislocations. Popov proceeds from the same considerations as Mott but examines the conservative movement of kinks along the screw dislocation in more detail [Pop90]. In that model it's assumed that to form point defects it is necessary for the following to be true:

$$\upsilon > \upsilon_j b / \lambda_j. \qquad (2.24)$$

If (2.24) is not right, defects cannot be formed. Here υ_j is the kinks glide velocity, $\upsilon -$ is the movement of dislocations velocity, λ_j is the distance between kinks on the dislocation line. The (2.24) condition was obtained proceeding from the following suppositions. To form defect it is necessary that a dislocation has covered the distance Δl before kinks annihilation. This distance is larger than the Burgers vector length. The time required for two neighbouring kinks to annihilate can be measured up by $t = \lambda_j / \upsilon_j$. During this time the dislocation has to cover $\Delta l = \upsilon\lambda_j / \upsilon_j > b$. Hence we have (2.24). When (2.24) is true we get [Pop90]:

$$\frac{\partial C_{I,V}}{\partial \gamma} = \frac{1}{2} P_j^{1/2} \xi^{1/2} b N_d^{1/2} (\upsilon / \upsilon_j)^{1/2}. \qquad (2.25)$$

Here $C_{I,V}$ is the relative concentration of interstitial atoms (I) and vacancies (V), P_j is density of tree dislocations that create kinks on a screw dislocation to the general density of dislocations. Unfortunately, the dependence of $\partial C_{I,V} / \partial \gamma$ from parameters that characterize experimental conditions (from strain rate $\overset{\bullet}{\varepsilon}$ and temperature of the sample) cannot be valued by (2.23) and (2.25). It's quite difficult to use these formulae to make practical evaluations. To determine the formation of point defects velocity the authors of [Mec80] and [Mil93, Mil94] proceeded from energetic considerations. It is assumed that the formation energy E_k of the type k point defect (a crystal lattice vacancy or an interstitial) is proportional to μb^3. The starting point in the Estrin-Mecking model is the fact that a certain amount of work done during the deformation of a crystal is used to form point defects. The equation for the formation of point defects velocity P is noted as:

$$P = \frac{\chi \tau \overset{\bullet}{\varepsilon}}{\alpha_1 \mu b^3}. \qquad (2.26)$$

Here α_1 is a constant, $\chi -$ is the portion of the overall work done that is spent on formation of point defects. This formula is preferential to (2.23) and (2.25) when making practical evaluations because here we have the apparent dependence of P from τ and $\overset{\bullet}{\varepsilon}$.

Point defects annihilation velocity

The already formed crystal lattice vacancies and interstice atoms can react with impurity atoms during the diffusion process thus constituting new point defects. These processes together with vacancies and interstitials generation processes determine the value of concentration of vacancies and interstitials. Generation velocities have been treated before in the present paper. Here let's consider interaction velocities of vacancies and interstitials with impurity atoms.

A number of scientific works were dedicated to studies of velocities of diffusionally controlled reactions in a solid state. These are reactions velocities of which are limited by the diffusion process of the reaction components. Notable are [Vin72a, Vin72b, Vin75], [Koz81] works. The [Koz81] findings are given below because this paper takes account of the other mentioned works' findings. Velocities of diffusionally controlled reactions in semiconductor materials between two components (at least one of them must be mobile) were examined in [Koz81]. The coulomb interaction between the components having charge condition spectrum in the semiconductor band – gap was taken consideration of in the work. The following was obtained for velocity of reactions:

$$\frac{1}{\iota} = \frac{1}{4\pi} \int_{r_0}^{\infty} \frac{\exp\left\{\dfrac{U(r)}{k_B T}\right\}}{D(r) r^2} dr. \qquad (2.27)$$

$$U(r) = \sum_{i,j} U_{ij}(r) f_{ij}(r). \qquad (2.28)$$

$$D(r) = \sum_{i,j} (D_i + D_j)\, f_{ij}(r). \tag{2.29}$$

$$f_{ij}(r) = F_{ij}\, f_{i,j-1}(r) + \Phi_{ij}\, f_{i-1,j}\,. \tag{2.30}$$

$$\sum_{i,j} f_{ij}(r) = 1\,. \tag{2.31}$$

Here ι is the reaction velocity; r is the distance between the reacting defects; r_0 is the reaction radius (the distance at which the components must come closer so that the reaction will run and a new defect will form); D_i is the diffusion coefficient of the reaction first component in the charge condition i; D_j is the diffusion coefficient of the reaction second component in the charge condition j; U_{ij} is the coulomb interaction energy between the reacting components having ie and je charges (e is the electron charge); $f_{ij}(r) -$ is the probability that at the distance r between the interacting components one of them is found in the charge condition i and the other one is found in the charge condition j; $U(r) -$ is the average energy of electrostatic interaction between the reaction components removed on the distance r; $D(r) -$ is the average total diffusion coefficient of the two components removed on the distance r; F_{ij} and Φ_{ij} are the functions of the distance r between the reaction components, electrons and holes concentration, crystal temperature, energy levels in the semiconductor band – gap (of the charge condition spectrum) for each reaction component; all charge conditions of the reaction components are summed.

Qualitatively the reaction process can be explained the following way. The reaction components are found initially at the distance $r >> r_0$. This distance is taken equal to the infinity, so in the (2.27) integral the integration upper limit is infinity. The components have ie and je charges. For instance, if the first component is in the single negative charge condition and the second one is in the single positive charge condition, then $i = 1$ and $j = -1$. As defects come closer, it may turn out that at a certain distance r between the components the condition having different i and j values will be more beneficial from the energetic point of view. If the components continue their approaching motion the values of i and j can again change. So f_{ij} depends on the distance r and the components' mutual diffusion coefficient and the interaction energy between them is characterized by average values (see (2.28) and (2.29) equations). In case the reaction components are neutral (when $U_{ij} = 0$ and, hence, $U = 0$ and $D = const$) we get the common formula for the velocity of diffusionally controlled (diffusionally limited) reaction:

$$\iota = 4\pi (D_1 + D_2) r_0\,. \tag{2.32}$$

Here D_1, D_2 are the diffusion coefficients of the first and the second components accordingly. From (2.27) results that if one component attracts the other ($U_{ij} < 0$ and hence $U < 0$) the reaction velocity value is higher then the similar magnitude in case the components are neutral. And vice versa: if one component repulsion the other ($U_{ij} > 0$ and hence $U > 0$) the reaction velocity value is less then the similar magnitude in case the components are neutral. In other words, attraction between the components speeds the reaction up, while repulsion slows it.

The discussed reaction velocity model can be applied to the case of formation of defects located in the field of dislocation mechanical stress. First, however, the influence of dislocation stress on energy levels values and on activation energies of the reaction components migration in various charge conditions must be considered in the $(2.27 \div 2.30)$ equations. The model as it is cannot be applied to practical estimation of reactions velocity values that run in the field of dislocation mechanical stress. In [Mec80] a model of annihilation velocity of vacancies that are situated in the dislocation neighbourhood was proposed:

$$A = \beta(C - C_0). \qquad (2.33)$$

Here A is the annihilation velocity, $C -$ is the relative concentration of vacancies, C_0 is the relative concentration of vacancies (away from dislocations) in the crystal thermodynamic equilibrium. The constant β is calculated by the following expression [Mec80]:

$$\beta = \frac{D_V}{C_0 b^3 \lambda^2}. \qquad (2.34)$$

Here D_V is the vacancy diffusion coefficient, $\lambda -$ is the average distance between annihilation centers.

Stationary concentration

The stationary concentration of vacancies is reached when vacancies emission velocity is equal to annihilation velocity. In the framework of the Estrin-Mecking model [Mec80], the stationary concentration can be determined from $P = A$ assuming that only dislocations constitute annihilation centers (see (2.26) and (2.34) equations). Then:

$$\Delta C = C_0 \frac{\chi \lambda^2 \tau \dot{\varepsilon}}{\alpha_1 D_V \mu} \qquad (2.35)$$

Here $\Delta C = C - C_0$ is the surplus relative concentration of vacancies.

Let’s multiply the numerator and the denominator in the right part of the equation by the density of dislocations N_d. After that, let’s express the density of dislocations in the denominator with help of (2.10): $N_d = (\tau / \alpha \mu b)^2$. Then the following expression is obtained for ΔC:

$$\Delta C = C_0 \frac{\chi \alpha^2 \lambda^2 b^2 N_d}{\alpha_1 D_V} \left(\frac{\mu}{\tau} \right) \dot{\varepsilon} \sim \lambda^2 N_d \frac{\dot{\varepsilon}}{\tau}. \qquad (2.36)$$

From (2.15) results that $\tau \sim \upsilon^{1/m}$ (m is the rate of stress indicator) and from (2.11) and $\dot{\gamma} = \dot{\varepsilon} / m_s$ results that $\upsilon = \dot{\varepsilon} / (m_s b N_{d_m})$. Thus $\tau \sim (\dot{\varepsilon} / N_{d_m})^{1/m}$. Finally we come to:

$$\Delta C \sim \lambda^2 N_d N_{d_m}^{1/m} \overset{\bullet}{\varepsilon}^{(1-\frac{1}{m})} . \tag{2.37}$$

Here $N_{d_m} -$ is the density of mobile dislocations. From (2.35) results that at a constant deformation velocity

$$\Delta C \sim \tau \lambda^2 . \tag{2.38}$$

From (2.37) results that, given that the density of dislocations has a constant value, the dependence of ΔC from $\overset{\bullet}{\varepsilon}$ is:

$$\Delta C \sim \overset{\bullet}{\varepsilon}^{1-\frac{1}{m}} . \tag{2.39}$$

2.6 Dislocations in the diamond structure

The diamond lattice can be viewed as superposition of two face-centered cubic lattices displaced with respect to each other in the direction of the volume diagonal for ¼ of its length. If, in this case, the diamond lattice contains atoms of two different types, then we deal with zinc blende structure. The *GaAs* lattice is the blende type lattice.

Plastic deformation occurs as a result of shear in a certain crystallographic plane in a certain direction in that plane. The combination of the slip plane and the slip direction in that plane is called the slip system. Slip plane is a plane with the densest packing of atoms (because distances between such planes are maximal) and slip direction is a direction for which distances between adjacent atoms centers in a slip plane are minimal. The diamond lattice does not possess all the properties of cube symmetry. However, by its macroscopic parameters a diamond crystal has cube symmetry [Ans78]. That's why here let's consider slip systems and as an example take face-centered lattice. Figure 2.9 represents the plane (111) and all the possible slip directions in it. Slip planes are planes NAC, MDB, EDB. So we have four systems of physically equivalent planes: {111} slip systems each having three slip directions. Thus, in the general case a face-centered lattice can have up to twelve slip systems.

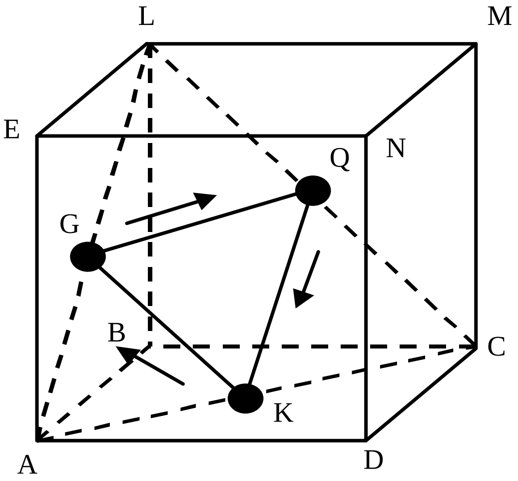

Fig. 2.9: Slip systems and slip directions scheme. The ALC plane is the (111) slip plane. QK, KG, GQ directions are the slip directions in the ALC plane (atoms in the cube vertices and in the middle of the AEND, DNMC, ELMN facets are not shown on the scheme).

The real quantity of slip systems under specific experimental conditions may be less then their maximum theoretically possible number. This can be explained the following way. It has been discussed above that the relation between the external stress (τ) and the tangential stress (σ) affecting a dislocation (and causing its movement) in the slip plane is expressed like: $\sigma = \tau m_s$. The Schmidt factor (m_s) value is determined by direction of the unit vector which is perpendicular to the slip plane, the Burgers vector plane and by stretching direction. If we have such stretching direction that for any slip systems m_s=0 then in this slip system $\sigma = 0$ and there's no dislocation glide in it. Hence, the quantity of real slip systems will be less then their theoretically possible quantity. For example, in a diamond lattice there are 8 slip systems for the [100] stretching direction (four slip plane systems and two slip directions in slip planes), four slip systems for the [110] direction. Since the GaAs lattice is nothing more nor less than superposition of two face-centered lattices with different atoms (Ga and As), two types of dislocations exist there: 60^0-degree $\alpha-$dislocations (in Ga atoms lattice) and 60^0-degree β-dislocations (in As atoms lattice) [Mat74]. There are two possible positions of slip planes in the diamond structure [Ale68a]: slip planes can be situated between plane couples, or, in the other case, between planes within one couple. That makes the diamond structure so peculiar. In the slip regime complete dislocations can dissociate for two partial dislocations. As a result, the atomic structure deformation reduces. The greater part of dislocations in the diamond lattice decomposes (dissociates) for partial dislocations. During dissociated screw dislocation cross slip dislocation line segments that stay in the cross slip plane constitute 60^0-degree dislocations. If two screw dislocations cross we have the similar situation: 60^0-degree jumps appear on both screw dislocations after their crossing.

Conclusions

Proceeding from the above-explained material, we may conclude that two principal factors – changing in the density of dislocations (both mobile and immobile) and their velocity – determine the nature of experimentally observed deformation curves during stretching of a sample. In all probability we can state that nowadays there are clear and understandable notion concerning reasons that lead to changes in the values of the discussed dislocation characteristics during plastic deformation of crystals. To be more precise, impurity, point defects and their clusters, and other dislocations influence the movement of dislocations velocity. The fact that defects impeding the movement of dislocations appear during the proper movement of dislocations (in the process of kinks climb in screw dislocations) complicates studies of the matter. The concentration of dislocations changes as a result of movement of dislocations as well (double cross slip of dislocations). It's comprehensible that to be able to quantitatively interpret experimental data and to make prognosis concerning the behaviour of deformation curves under these or that experimental conditions (like sample temperature and stretching velocity) we need equations that connect together concentration of defects, macroscopic parameters $(\tau, \varepsilon, \dot{\varepsilon}, T)$, and parameters that characterize the movement of dislocations (υ, N_d, N_{d_m}). Such equations are those discussed earlier in this work: (2.10), (2.11), ($2.15 \div 2.17$), ($2.19 \div 2.21$), (2.38), (2.39). Unfortunately, these do not form a closed system. For example, there's no evident connection between concentration of defects and movement of dislocations velocity. Later, if in the (2.15) equation for movement of dislocations velocity we substitute τ for σ using $\sigma = \tau m_s$ and then make use of (2.10), we'll arrive at:

$$\upsilon \sim N_d^{m/2} \exp(-U / k_B T) .$$

This means that υ grows as N_d ($m > 0$) grows. In reality, however, υ should decrease with the increases of N_d because dislocations are obstacles for movement of mobile dislocations. Thus, the movement of dislocations activation energy U should rise as density of dislocation N_d increase. The activation energy should rise if concentration of defects increases, too, because they are obstacles for the movement of dislocations. In this situation the use of V_A, m, U parameters for description of the movement of dislocations is justified only if these parameters depend very little on those that characterize experimental conditions ($\overset{\bullet}{\varepsilon}$, T).

[Hub98] provides us with findings of systematic experimental research of GaAs deformation curves at the crystal temperature range of $= T(400 \div 800)^0 C$ and strain rate of $\overset{\bullet}{\varepsilon} \approx (10^{-5} \div 10^{-3}) s^{-1}$. In particular, for an undoped GaAs during stretching the following results were obtained (the crystal was stretched in the [110] direction) [Hub98]: in the range of $\overset{\bullet}{\varepsilon} \approx (10^{-5} \div 10^{-4}) s^{-1}$ at $T = 400^0 C$, $500^0 C, 600^0 C\ 800^0 C$ the research gave $2 + m = 4{,}5 \pm 0{,}6$, $3.0 \pm 0.4, 3.7 \pm 0.3,$ 3.9 ± 0.3 values accordingly; $U/(2+m) \approx 0.44 eV$ ($\overset{\bullet}{\varepsilon} = 8 \cdot 10^{-5} s^{-1}$). Thus, very weak relation between rate of stress indicator (m) value and the value of the activation energy (U) of the movement of dislocations was determined. These experimental data prove that the use of m and U parameters and, perhaps, V_A is justified. It’s sad, however, that in [Hub98] and in other works there are no data for the values of V_A in a vast range of $\overset{\bullet}{\varepsilon}$ and T parameters.

[Hub98] also proved that there is influence from part of doped impurity on the value of U, i.e. defects influence significantly the processes of movement of dislocations. It was stated above, however, that the system of expressions describing processes of movement of dislocations doesn’t directly connect the values of U and concentration of defects. This fact does not allow us to determine the value of concentration of defects (leaving alone their type) directly from the experimental data obtained for crystal deformation. That’s why to determine the concentration and type of defects in deformed crystal scientists use additional experimental methods. The PAS method (that is further treated in detail) was used in the present paper. Using experimental data obtained by the PAS method it will be possible to make a conclusion concerning the applicability of (2.38) and (2.39) when determining functional relation between concentration of defects and τ with $\overset{\bullet}{\varepsilon}$.

3. POSITRON ANNIHILATION SPECTROSCOPY

3.1 Positronium in vacuum

During interaction of an electron with a positron a hydrogen-like system – *positronium* - can emerge. There are two types of positronium: *parapositronium* (system of an electron and a positron with antiparallel spins) and *orthopositronium* (system of an electron and a positron with parallel spins). It was demonstrated in the work [Ber68], that levels of positronium energy could be classified in accordance with the value of complete spin S. Since for parapositronium $S=0$, it could be only in one state (i.e. parapositronium constitutes *singlet state* with spin projection $S_z=0$). For orthopositronium $S=1$, that's why it could be in three states (i.e. orthopositronium constitutes *triplet state* with spin projection $S_z=-1,0,1$).

Positron annihilation is accompanied by emission of one, two or more $\gamma-$quanta. One-photon annihilation of an electron-positron pair is possible only in presence of any third substance (electron, atom), which perceives recoil momentum. This could be explained in the following way: during annihilation of an electron-positron pair the energy conservation law and the impulse conservation law, are implemented. If we consider an electron-positron pair within the system of center of inertia (in such a coordinate system positronium is stationary, its components have speeds different from zero), positronium momentum is equal to zero. After annihilation total momentum of the system will be equal to the momentum of $\gamma-$quantum (one-photon annihilation) differ from zero, which is impossible due to the momentum conservation law. Thus one more substance shall be present, which as a result of positronium annihilation acquires a momentum so as to complete momentum of $\gamma-$quantum and this substance is equal to zero. At this point we will consider positronim without any other solid, that's why process of one-photon annihilation will be excluded. During positronium annihilation C charge parity [Ber68] of the system shall be preserved. Positronium charge parity [Ber68] is as follows: $C=(-1)^{l+s}$ ($l,s-$orbital moment and positronium spin, accordingly), and system's charge of parity is as follows: $C=(-1)^N$ ($N-$number of photons). Since positronium orbital moment has the only value [Ber68] $l=0$, positronium charge of parity $C=(-1)^S$. As to parapositronium $(S=0)$ $C=1$ and, consequently, annihilation occurs with formation of even number of photons. For orthopositronium $(S=1)$ $C=-1$. Thus, ortopositronium's annihilation is accompanied by emission of odd number of photons. Hence, the main process-determining *lifetime of positronium* is two-photon annihilation in case of parapositronium and three-photon annihilation in case of ortopositronium [Ber68] (processes with a great number of photons are not considered, because they are less likely). Let's determine lifetime of positronium for the case $\upsilon_{e,p}/C<<1$ (C - light speed, υ_e and υ_p - speed of electron and positron in positronium). Equations for sections of two-photon $\sigma_{2\gamma}$ and three-photon $\sigma_{3\gamma}$ annihilations in the system of center of inertia have are the following [Ber68]:

$$\sigma_{2\gamma}=\pi\left(\frac{e^2}{m_ec^2}\right)\frac{c}{\upsilon}, \qquad (3.1)$$

$$\sigma_{3\gamma} = \frac{4(\pi^2 - 9)c}{3\upsilon}\alpha\left(\frac{e^2}{m_e c^2}\right)^2. \qquad (3.2)$$

Where $\upsilon -$ relative velosity of electron and positron in positronium, $\alpha = e^2/(\hbar c)$, m_e - electron mass.

Normalized to unity wave function of positronium ground state is as follows:

$$\Psi(r) = (\pi a^3)^{-1/2}\exp(-r/a). \qquad (3.3)$$

where $a = 2\hbar^2/(m_e e^2) \approx 10^{-10} m - Bohr\ radius$ of positronium. Possibility of two-photon annihilation of parapositronium w_0 is as follows [Ber68]:

$$w_0 = 4|\Psi(0)|^2 \upsilon\sigma_{2\gamma}. \qquad (3.4)$$

Substitute into equation (3.4) values $\sigma_{2\gamma}$ and $|\Psi(0)|^2$ from equations (3.1) and (3.3) we can get the following for parapositronium lifetime:

$$\tau_{2\gamma} = \frac{1}{w_0} = \frac{2\hbar}{m_e c^2 \alpha^5} \approx 1.23\times 10^{-10} s. \qquad (3.5)$$

Energy E_0 of positronium ground state and level width Γ_0 are as follows:

$$|E_0| = \frac{m_e e^4}{4\hbar^2} \approx 6.8 eV.$$

$$\Gamma_0 = \hbar/\tau_{2\gamma} \approx 5.4\times 10^{-6} eV.$$

Hence, level width is small as compared to $|E_0|$. Namely this fact allows considering positronium as a quasistationary system. For three-photon ortopositronium annihilation life time $\tau_{3\gamma} \approx 1{,}4\times 10^{-7} s$ [Ber68]. In this case level width is also small as compared to ground state energy and orthoposirtonium can be considered as a quasistationary system.

3.2 Positronium in crystals

Results represented in the foregoing section cannot be directly used to evaluate positronium lifetime in crystals. Electron density in positronium atom $|\Psi(0)|^2$ according to equation (3.3) depends on Bohr radius of positronium: $|\Psi(0)|^2 \sim a^{-3}$. To acquire expression for $|\Psi(0)|_S^2$ in crystal we should place in the above mentioned expression for Bohr radius of positronium $m^* = m_- m_+/(m_- + m_+)$ instead of $m_e/2$ and multiply Bohr radius of positronium by ε_0. At this point m_- and m_+ - effective mass of electron and positron in crystal, ε_0 static permittivity of crystal. Then we get the following:

$$\left|\Psi(0)\right|_S^2 = \chi_S \left|\Psi(0)\right|^2. \qquad (3.6)$$

Where $\chi_S = 8[m^* /(m_e \varepsilon_0)]^3$.
As a consequence of this *annihilation rate* of positronium in crystal $\lambda_{2\gamma(3\gamma)}$ and vacuum $\lambda^0_{2\gamma(3\gamma)}$ are connected as follows:

$$\lambda_{2\gamma(3\gamma)} = \chi_S \lambda^0_{2\gamma(3\gamma)}. \qquad (3.7)$$

In this case $\lambda^0_{2\gamma} = 1/\tau_{2\gamma}$ and $\lambda^0_{3\gamma} = 1/\tau_{3\gamma}$ (values of $\tau_{2\gamma}$ and $\tau_{3\gamma}$ were represented in the foregoing section). We can calculate binding energy $\left|E_S\right|$ of positronium in crystal by using expression for the same value in vacuum $\left|E_0\right|$, if we decrease $\left|E_0\right|$ by ε_0^2 (binding energy of electron in hydrogen-like atom placed in a medium with permittivity ε_0 decreases by ε_0^2) and replace $m_e/2$ by m^*. Then we get the following:

$$\left|E_S\right| = \frac{m^* e^4}{2\hbar^2 \varepsilon_0^2} = 2\frac{m^*}{m_e \varepsilon_0^2}\left|E_0\right|. \qquad (3.8)$$

Let's evaluate χ_S and $\left|E_S\right|$ values for GaAs. Provided that $\varepsilon_0 \approx 12.53$ [Gri91], $m_- \approx 0.065 m_e$ [Ask85] and assuming that $m_+ \sim m_e$ (quite good approximation for metals [Are83]), we get the following: $\left|E_S\right| \approx 5.5 \times 10^{-3} eV$, $\chi_S \approx 10^{-6}$. It follows that $\left|E_S\right| << \hbar\omega_0$, where $\hbar\omega_0$ - energy of *deformation optical phonon* ($\hbar\omega_0 \approx 0.036 eV$ [Gri91]). Hence during interaction with phonons positronium is able to dissociate (decompose into free positron and electron). Dissociation possibility $\sim \exp(-\left|E_S\right|/k_B T)$. Therefore we could expect that positronium exists in quasistable state under $T < \left|E_S\right|/k_B \approx 60K$. At high temperatures positronium is most likely unstable. Further taking into account equations (3.5), (3.7) и χ values we can get the following: $\lambda_{2\gamma} \approx 0.8 \times 10^4 s^{-1}$.
Thus positronium *spontaneous annihilation* is a very slow process (with characteristic time of annihilation $\sim 10^{-4} s$) and most probably is not an important channel of positron annihilation (at this point we should take into account that in GaAs without any defects characteristic time of annihilation is about $10^{-10} s$).

There is one more channel of positronium annihilation (in addition to spontaneous positronium annihilation which was examined earlier) – positronium annihilation by its interaction with an electron of lattice atom (or with a free electron). Reaction is carried out in accordance with the following model: $P_S + e \rightarrow 2\gamma + e$ ($P_S -$ positronium, $e -$ free electron of conduction band or electron of lattice atom). Such a process is called *pick-off annihilation* of positronium [Are83] (this process can be observed in particular in ionic crystals). *Pick-off annihilation* takes place in case if positronium is in quasistable state. It was demonstrated earlier that most probably this condition is implemented at low temperatures. At temperatures at which positronium is most probably unstable ($T \geq \left|E_S\right|/k_B$) *pick-off annihilation* is improbable. However the following needs to be explained. It was noted earlier that positronium dissociation at temperatures determined is caused by its interaction with phonons. However if characteristic time τ_p of energy transfer from phonon to positronium (period between collisions of positronium and phonons) is higher than characteristic time of *pick-off annihilation* τ_{pick}, for process of time of *pick-off annihilation* positronium could be considered nevertheless stable. Time $\tau_{pick} \geq 10^{-10}\,s$ (since it was experimentally determined in crystals without any defects that time of positrons annihilation is about $10^{-10}\,s$). Time τ_p is unknown. However if we assume that collision rate of phonons and positronium coincides in order of magnitude with collision rate of phonons and free electrons (approximately $10^{13}\,s^{-1}$), then we can get the following: $\tau_p \sim 10^{-13}\,s$ .Consequently, $\tau_p << \tau_{pick}$. Hence, *pick-off annihilation* does not contribute to positron annihilation under $T \geq |E_S|/k_B$. According to the above mentioned analysis spontaneous positronium annihilation in GaAs does not substantially contribute to positron annihilation, *pick-off annihilation* of positronium can affect processes of positron annihilation only at low temperatures of crystal: under $T \leq |E_S|/k_B$.

3.3 Annihilation of free positrons

Positron and electron in crystal are sometimes in *zone state* and sometimes – in *bound state* constituting positronium (at this point crystal without any defects is considered). Possible channels of positron annihilation through formation of positronium (with subsequent annihilation of related positron and electron in positronium) were discussed earlier. At this point we consider two channels of free positron annihilation with electrons: annihilation with free electrons of conduction band and electrons of lattice atom. Annihilation rate of positron with free electrons is as follows:

$$\lambda_{2\gamma,n} = \sigma_{2\gamma} \upsilon n. \tag{3.9}$$

where $\sigma_{2\gamma}$ is determined in accordance with equation (3.1), $\upsilon -$ relative speed of electron and positron in system of center of inertia, $n -$ concentration of free electrons. By using equations (3.4) and (3.9) we can get the following:

$$\lambda_{2\gamma,n} = \frac{n}{4|\Psi(0)|^2} w_0 .$$

Since $|\Psi(0)|^2 = (\pi a^3)^{-1}$ and $w_0 = 1/\tau_{2\gamma}$ (see equations (3.3) and (3.5)), we can finally get the following:

$$\lambda_{2\gamma,n} = \frac{\pi a^3 n}{4} \tau_{2\gamma}^{-1}. \tag{3.10}$$

It was demonstrated earlier that $a \approx 10^{-10}\,m,\ \tau_{2\gamma} = 1.23 \times 10^{-10}\,s.$ (3.5). By real concentration of dopants concentration of free electrons does not exceed value of $10^{19}\,cm^{-3}$. As a result we can get the following: $\lambda_{2\gamma,n} \leq 10^5\,s^{-1}$. Hence lifetime of positrons caused by annihilation at free electrons is as follows: $1/\lambda_{2\gamma,n} \geq 10^{-5}\,s.$ This value is considerably higher than values acquired during the experiment (approximately$10^{-10}s$). Thus this channel can be considered inessential for annihilation. To evaluate positron annihilation rate at electrons of lattice atoms equation (3.9) is usually used [Are83]. At the same electrons concentration n is interpreted as an effective value n_{ef}. Let’s demonstrate that the mechanism under consideration can substantially contribute to positron annihilation. In accordance with equation (3.10), given that $n = n_{ef}$, we can get the following:

$$\lambda_{2\gamma,n_{ef}} = \frac{\pi a^3 n_{ef}}{4}\tau_{2\gamma}^{-1}. \qquad (3.11)$$

Let’s assume that $n_{ef} = Zn_A$ ($n_A -$ concentration of crystal atoms; $Z -$number of electrons in atom equal to atomic number). For GaAs $n_A = 4.4\times10^{22}cm^{-3}$, $Z_{Ga} = 31$, $Z_{As} = 33$ for evaluation average value is as follows: $Z = 32$. In accordance with equation (3.11) we can get the following: $\lambda_{2\gamma,n_{ef}} \approx 10^{10}s^{-1}$. Hence positron lifetime resulting from its annihilation with electrons of lattice atoms is as follows: $1/\lambda_{2\gamma,n_{ef}} \approx 10^{-10}s$ (this value coincides in order of magnitude with values acquired experimentally). Therefore this annihilation mechanism can substantially affect positron lifetime. However it is worth at this point noting the following. For this evaluation equation $n_{ef} = Zn_A$was used. This resulted to $\lambda_{2\gamma,n_{ef}} \sim Z$. Meanwhile according to the measuring results positron lifetime is hardly dependent on chemical composition of the substance, in particular on Z [Wei64], [Are83]. Absence of visible dependence of lifetime on atomic number could be explained if we take into account that because of Coulomb repulsion of positron by atom nucleus not all electrons of atom are equally participating in positron annihilation. As a result of this $n_{ef} < Zn_A$. However this fact does not change the conclusion that the positron annihilation channel under consideration is of great importance.

Earlier during analysis of possible mechanisms of positron annihilation (annihilation of free positrons and positronium) thermalized positrons were examined. However source-emanating positrons possess energy $E_p \approx 0{,}51MeV$. In crystals positrons become slower returning energy for ionization of lattice atoms, activation of phonons, excitons [Per70]. To determine number $N(z)$ of non-thermalized positrons at depth of Z crystal the following damping model is used [Bra77]:

$$N(z) = N(0)\exp(-\alpha_+ z),\ \alpha_+ = 17\frac{\rho(g/\text{см}^3)}{E_p^{1{,}43}(MeV)}. \qquad (3.12)$$

At this point $\rho -$density of crystal material,$\alpha_+ -$linear damping coefficient. Given that $E_p \approx 0{,}51MeV$and $\rho \approx 5{,}4g/\text{см}^3$[Gri91] we can get the following: $1/\alpha_+ \approx 40$ micrometers. Therefore we can assume that for $z > 40$ micrometers all positrons are thermalized, i.e. practically in the whole crystal volume we have to do with thermalized positrons. At the same time positron thermalization time make up several picoseconds. Since positron thermalization time is far less than its annihilation time, thermalized positrons are mainly annihilated.

Therefore main mechanisms of positron annihilation in GaAs crystal without any defects are: two-photon annihilation of free thermalized positrons with electrons of lattice atoms (at the rate of $\lambda_{2\gamma,n_{ef}}$) and perhaps two-photon *pick-off annihilation* of positronium at low crystal temperatures (at the rate of λ_{pick}). Three-photon annihilation processes are not taken into account because they are essentially slower. Two-photon annihilation rate $\lambda_{2\gamma}$, consequently, is as follows:

$$\lambda_{2\gamma} = \lambda_{2\gamma,n_{ef}} + \lambda_{pick}. \tag{3.13}$$

3.4 Positron annihilation on defects

Above annihilation mechanisms of thermalized positrons in the crystal without any defects are examined. If there are defects in the crystal present one more annihilation channel of thermalized positrons can emerge: annihilation with electron of defect. Process of interaction of positron with defect can be conditionally divided into three phases: phase of approach of free (delocalized) positron to defect (*diffusion phase*), positron *trapping phase* by defect (after approach of positron to defect for a certain distance positron can be entrapped by defect and as a result of it positron transform to localized state), *annihilation phase* of localized positron with electrons of defects. Let’s discuss two phases of interaction of positron with defect.

If diffusive phase is slower than trapping phase, interaction reaction of positron with defect is *diffusion-limiting reaction*. If trapping phase of positron is slower reaction is limited by trapping phase. Rate of reaction between positron and defect can be figured as follows:

$$\frac{1}{\kappa_d} = \frac{1}{\tilde{\kappa}_d} + \frac{1}{\kappa_{tr}}. \tag{3.14}$$

where κ_d – trapping rate, $\tilde{\kappa}_d$ – rate of diffusion phase of the reaction, κ_{tr} – trapping phase rate. It appears from equation (3.14) that if $\tilde{\kappa}_d << \kappa_{tr}$, then $\kappa_d \approx \tilde{\kappa}_d$. At this point *diffusion-limiting reaction* takes place. If $\tilde{\kappa}_d >> \kappa_{tr}$, then $\kappa_d \approx \kappa_{tr}$ and reaction *limited by trapping* takes place. If $\tilde{k}_d \sim \kappa_{tr,}$ then the both phases of the reaction contribute to reaction rate. Usually $\tilde{\kappa}_d$ и κ_{tr} are represented as follows:

$$\tilde{\kappa}_d = \gamma_d n_d, \quad \kappa_{tr} = \gamma_{tr} n_d. \tag{3.15}$$

At this point n_d – concentration of defects interacting with positron, γ_d – specific trapping coefficient of *diffusion- limiting reaction*, γ_{tr} – specific trapping coefficient of positron by defect.

3.4.1 Diffusion - limited reaction

Let’s determine γ_d specific coefficient of diffusion-limited phase of reaction of positron with a defect. Let’s assume that:

1. Defects are point.
2. Defects in crystal are allocated uniformly.
3. Defects are isolated, i.e. their concentration is not enough to consider interaction between them.
4. $U(r)$ interaction energy of positron with a defect depends solely on r interval between them.

Figure 3.1 represents a diagram explaining further reasoning.

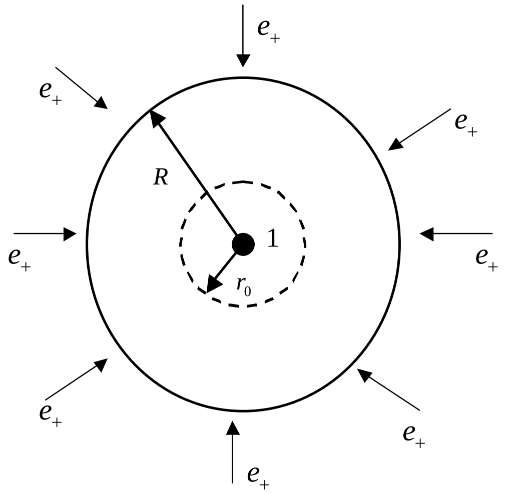

Fig. 3.1: Diagram of diffusion phase of reaction between positron (e_+) and defect (1). R - interval equal to half-interval between defects, r_0 – reaction radius.

On the surface of R radius sphere the following equation is taking place $\Phi = \gamma_d n_+(r = R)$ (n_+ – concentration of positrons in crystal volume, Φ – magnitude of positron flow in unit time trough spherical surface of R radius directed to the defect). This equation reflects the fact of retention of positron number: positron number disappeared in unit time in crystal volume (this number is equal to $\gamma_d n_+(R)$) is equal to positron number passed in unit time through the surface with R radius (this number is equal to Φ). Further $n_+(r = r_0) = 0$. This condition arises because during approach of positrons with a defect to the interval of r_0 reaction radius positrons are being captured by the defect and their concentration in delocalized condition under $r = r_0$ is equal to zero. Furthermore $\Phi(r_0 \le r \le R) = const$, because there are no other sources (apart from the defect given) of positron absorption in the spherical layer $r_0 \le r \le R$. Positron flow in unit time trough spherical surface with r radius is as follows:

$$\Phi = \left(D_+ \frac{dn_+}{dr} + \frac{n_+ D_+}{k_B T} \frac{dU}{dr} \right) 4\pi r^2 . \tag{3.16}$$

At this point D_+ – positron diffusion coefficient, first summand in the right part is conditional on diffusive part of the flow, the second one – drift part of the flow in the electrostatic field of defect (in the general case defects can be charged). Let's make the following change:

$$n_+(r) = \tilde{n}_+(r) \exp[-U(r)/k_B T]. \tag{3.17}$$

Then, given equations (3.16) and (3.17), we can get the following:

$$\Phi = 4\pi r^2 D_+ \exp[-U(r)/k_B T]\frac{d\tilde{n}_+}{dr}. \qquad (3.18)$$

Let's transfer two co-factors of the right part of the equation (3.18) into the left part and integrate. Then we get the following:

$$\frac{\Phi}{4\pi D_+}\int_{r_0}^{R}\frac{\exp[U(r)/k_B T]}{r^2}dr = \tilde{n}_+(R) - \tilde{n}_+(r_0). \qquad (3.19)$$

It is specified at this point that $\Phi = const$ (see above), $D_+ = const$. Since $n_+(r_0) = 0,$ then $\tilde{n}_+(r_0) = 0$ (see equation (3.17)). With the help of equation (3.19) and given that $\tilde{n}_+(R) = n_+(R)\exp[U(R)/k_B T]$ we can get the following:

$$\frac{\Phi}{n_+(R)}\exp[-U(R)/k_B T] = 4\pi D_+\left(\int_{r_0}^{R}\frac{\exp\left[U(r)/k_B T\right]}{r^2}dr\right)^{-1}.$$

Since $\Phi / n_+(R) = \gamma_d$ (see above) we get the following:

$$\gamma_d = 4\pi D_+ \exp[U(R)/k_B T]\left(\int_{r_0}^{R}\frac{\exp\left[U(r)/k_B T\right]}{r^2}dr\right)^{-1}.$$

Assuming that concentration of defects is small enough and $U(r = R) << k_B T,$ we finally get the following:

$$\gamma_d = 4\pi D_+\left(\int_{r_0}^{R}\frac{\exp\left[U(r)/k_B T\right]}{r^2}dr\right)^{-1}. \qquad (3.20)$$

If interaction between defect and positron does not exist $((U(r) = 0 -$ neutral defect), then with the help of equation (3.20) we can get the following:

$$\gamma_d = 4\pi D_+ (\frac{1}{r_0} - \frac{1}{R})^{-1}.$$

Given that $R >> r_0,$ we get the following:

$$\gamma_d = 4\pi D_+ r_0. \qquad (3.21)$$

Short conclusion from equation (3.20) for case mobile and charged point defects contains in the work [Ent73]. According to equation (3.20) attraction (U <0) between positron and defect leads to acceleration of diffusion-limited phase of the reaction (increase of γ_d) in comparison with neutral defect $(U=0)$. Repulsion (U >0) leads to deceleration of the reaction (decrease of γ_d).

It is worth noting that equation (3.20) can be used to determine γ_d and in case of interaction of positrons with defect clusters if we assume that cluster has a spherical and symmetric form. At this point $U(r)$ – interaction energy of cluster and positron, r_0 – reaction radius of positron and cluster.

Let's analyze dependence of γ_d on temperature of the crystal. Let's address Coulomb interaction between charged defect and positron:

$$U(r) = \pm \frac{Qe^2}{\varepsilon_0 r}. \tag{3.22}$$

Where Qe – defect charge. If we substitute equation (3.21) with equation (3.22) then we get the following:
a) in case of attraction

$$\gamma_d = 4\pi D_+ \frac{Qe^2}{\varepsilon_0 k_B T}\{\exp[-W_R / k_B T] - \exp[-W_{r_0} / k_B T]\}^{-1}.$$

b) in case of repulsion

$$\gamma_d = 4\pi D_+ \frac{Qe^2}{\varepsilon_0 k_B T}\{\exp[W_{r_0} / k_B T] - \exp[W_R / k_B T]\}^{-1}.$$

At this point

$$W_R = \frac{Qe^2}{\varepsilon_0 R}, \quad W_{r_0} = \frac{Qe^2}{\varepsilon_0 r_0}.$$

Let's perform the following evaluation:

$$\frac{W_{r_0}}{k_B T} = \frac{Qe^2}{\varepsilon_0 r_0 k_B T} = \frac{Qe^2}{\varepsilon_0 a_B k_B T}\left(\frac{a_B}{r_0}\right) \approx \frac{2.17(eV)Q}{k_B T(eV)}\left(\frac{a_B}{r_0}\right) >> 1.$$

It is considered at this point that $e^2 / a_B \approx 27.2 eV, \varepsilon_0 \approx 12.53, a_B \approx 0.53 \times 10^{-8} cm$ - *Bohr radius* of hydrogen atom, $k_B T \sim (10^{-2} \div 10^{-1}) eV$ (for example under $T = 300K$ $k_B T \approx 2{,}58 \times 10^{-2} eV$), $r_0 \sim a_m$ – interatomic interval.
Further,

$$\frac{W_R}{k_B T} \approx \frac{2.17(eV)Q}{k_B T(eV)}\left(\frac{a_B}{R}\right) << 1.$$

It is accepted at this point that $R >> 10^2 a_B \approx 0.53\times10^{-6} cm$ (since $R \sim n_d^{-1/3}$, this condition is applicable under $n_d << 10^{18} cm^{-3}$, n_d – defects concentration). Given the results of the evaluation we can get the following:

a) in case of attraction

$$\gamma_d \approx 4\pi D_+ \frac{Qe^2}{\varepsilon_0 k_B T}. \qquad (3.23)$$

b) in case of repulsion

$$\gamma_d \approx 4\pi D_+ \frac{Qe^2}{\varepsilon_0 k_B T} \exp[-Qe^2/(\varepsilon_0 k_B T r_0)]. \qquad (3.24)$$

D_+ coefficient of positron diffusion has the following dependence on temperature (taking into account that positrons are scattering only at acoustic phonons) [Saa89]:

$$D_+ \sim T^{-1/2}. \qquad (3.25)$$

With the help of equations (3.21), (3.23), (3.24) and (3.25) we can finally get the following:

a) in case of attraction

$$\gamma_d \sim T^{-3/2}. \qquad (3.26)$$

b) in case of lack of interaction

$$\gamma_d \sim T^{-1/2}. \qquad (3.27)$$

c) in case of repulsion

$$\gamma_d \sim T^{-3/2} \exp\left[-\frac{A}{T}\right]. \qquad (3.28)$$

Where

$$A = \frac{Qe^2}{\varepsilon_0 k_B r_0}.$$

According to equations (3.26), (3.27) and (3.28) sharper dependence of γ_d on T corresponds to repulsion, less sharper – to lack of interaction. At the same time in case of attraction $\gamma_d \sim Q$, dependence of γ_d on amount of charge in the defect in case of repulsion is essentially stronger: $\gamma_d \sim Q\exp(-BQ)$, where $B = e^2/(\varepsilon_0 k_B T r_0)$.

For defects clusters equations (3.21), (3.23), (3,24) can be used (and accordingly, equations (3.26), (3,27), (3,28)), if we assume that clusters have spherical and symmetric form and for them as well as for point defects the following conditions are applicable: $W_R / k_B T << 1$ and $W_{r_0} / k_B T >> 1$ (see above). For clusters r_0 – cluster radius, R – half-interval between clusters, Qe – cluster charge. In the general case defects can have a spectrum of charged states. If we change conditions of the experiment (concentration of dopant, crystal temperature) charge state (charge) of the defect can change and this can lead to substantial change of γ_d. One of the basics defects arising during deformation of GaAs are vacancies and their clusters. Figure 3.1 (a, b) shows levels of vacancy conversion into various charge states. Values of energy levels were calculated by different authors. Differentials of results received by different authors huge.

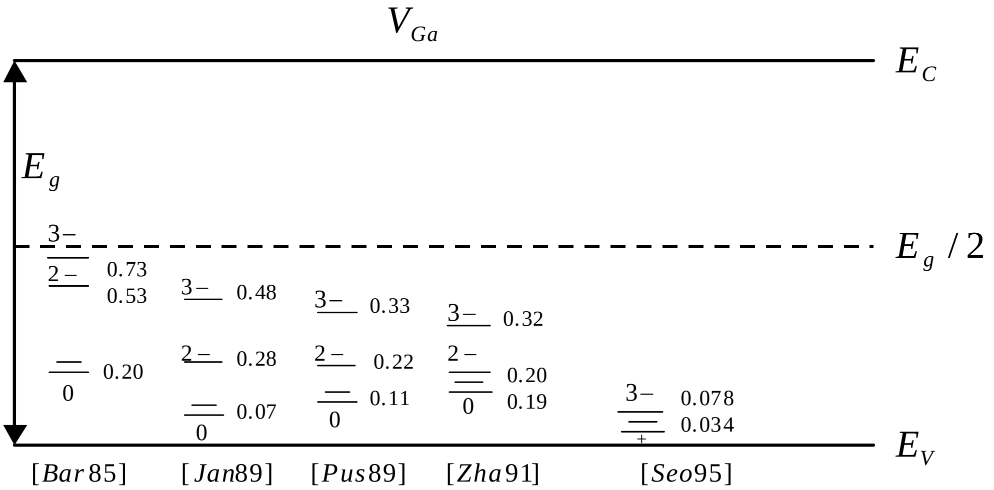

Fig. 3.2(a): Energy levels of gallium vacancies (V_{Ga}). E_υ – energy of valence band ceiling, E_C – energy of conduction band bottom, E_g – width of band gap ($E_g \approx 1.52eV$ [Gri91]). Values of energy levels of vacancy are given with regard to valence band ceiling (in eV).

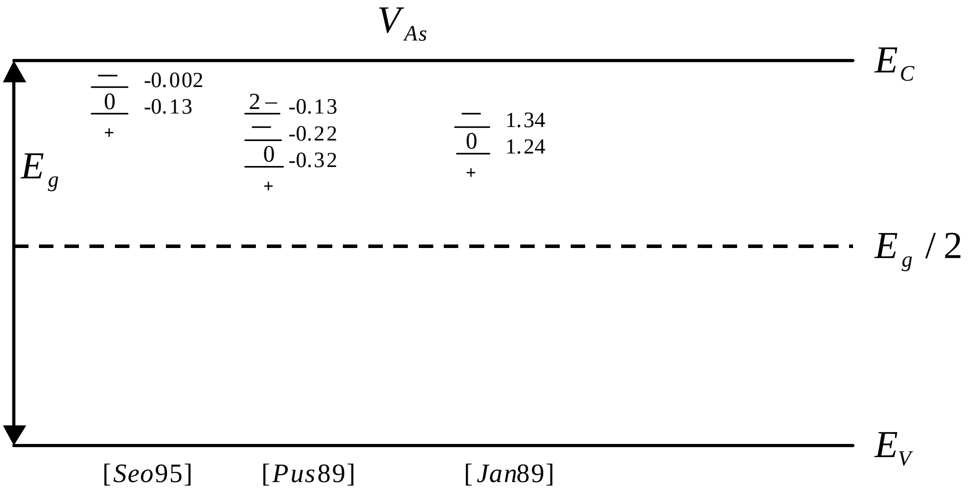

Fig. 3.2(b): Energy levels of arsenic vacancies (V_{As}). Values of energy levels of vacancy are given (in eV) with regard to valence band ceiling [Jan89] and conduction band bottom [Pus89], [Seo95].

This fact essentially complicates quantitative analysis of rate of diffusion phase of positron reaction with vacancies (V_{Ga}, V_{As}). However it is worth noting that this situation is quite definite for the reaction $e_+ + V_{Ga}$ in n-GaAs (according to the data presented in figure 3.2(a) V_{Ga} in n-GaAs has one charge state: thrice-repeated negative and, hence, attraction of positron and V_{Ga} is taking place in equation (3.23) $Q = 3$) and for reaction $e_+ + V_{As}$ in p-GaAs (according to the data presented in figure 3.2(b) V_{As} in p-GaAs has one charge state:

single positive and, hence, repulsion of positron and V_{As} is taking place in equation (3.24) $Q=1$).

3.4.2 Positron capture

There are shallow and deep positron traps. If binding energy is $E_b \leq k_B T$, there is a *shallow positron trap*. If binding energy is $E_b >> k_B T$, there is a *deep positron trap*. The same trap can be at one crystal temperature shallow and at another – deep. In case of a shallow trap not only positron trap can be observed but also thermal ejection of positron from the trap. For deep traps possibility of thermal ejection of positrons is rather low. Coupling between thermal ejection rate $\delta_S\,(s^{-1})$ of positron and specific trapping coefficient $\gamma_{tr}\ (cm^3 s^{-1})$, see equation (3.15)) of thermalized positrons of a shallow trap is follows [Man81]:

$$\frac{\delta_S}{\gamma_{tr}} = \left[\frac{m_+ k_B T}{2\pi\hbar^2}\right]^{3/2} \exp[-E_b / k_B T]. \tag{3.29}$$

Equation (3.29) is applicable if a shallow trap is a point center. If dislocation is a shallow trap, connection between thermal ejection rate $\delta_d\,(s^{-1})$ of positron and its specific trapping coefficient $\gamma_{trd}\,(cm^2 s^{-1})$ is as follows [Man81]:

$$\frac{\delta_d}{\gamma_{trd}} = \left(\frac{m_+ k_B T}{2\hbar^2}\right) \times \frac{\exp[-E_b / k_B T]}{erf(\sqrt{E_b / k_B T})}. \tag{3.30}$$

Where

$$erf(x) = \frac{2}{\sqrt{\pi}} \int_0^x e^{-y^2}\, dy.$$

In the general case calculation of specific trapping coefficient of a particle (in this case – of a thermalized positron) on a trap is a very intricate problem, particularly because calculation results are highly dependent on choice of interaction potential between a trap and a particle, which is as a rule unknown. However in some cases it is possible to determine by means of calculation temperature dependence of trapping coefficient of a particle on a trap. In particular one can manage to apply it for positron capture in a negatively charged vacancy. A vacancy does not have any positively charged nucleus (defect with an open volume). In this case Coulomb potential $Qe/\varepsilon_0 r$ ($r=0$ correspond to vacancy center, Qe – vacancy charge) is added to vacancy potential. This leads to potential shift near vacancy to $\approx 0.1Q(eV)$ [Pus90]. Figure 3.3 shows in diagram form interaction energy of a negatively charged vacancy with a positron. Because due to of Coulomb component *Rydberg states* in energy spectrum appear (three states are reflected in Figure 3.3: with energies E_1, E_2, E_3). At first free positron is captured into shallow state with E_1 energy (transition 1), further it goes into state with E_2 energy (transition 2), E_3 energy and so on until it comes to ground state with energy $E_0 = -0.1Q(eV)$. Difference between energy magnitudes of *Rydberg states* is comparable to phonon energy. That's why in the process of such cascaded transition of positron energy evolving is passed to phonon (at every phase: 1,2,3,4 energy is passed to one phonon). Another type of capture is possible. Free positron turns into ground state at once (direct transition 5). In this case energy evolving substantially exceeds phonon energy. At this point energy evolving is transferred not to phonon (multiphonon process is improbable), but to a free electron or one of the atoms electrons surrounding the vacancy.

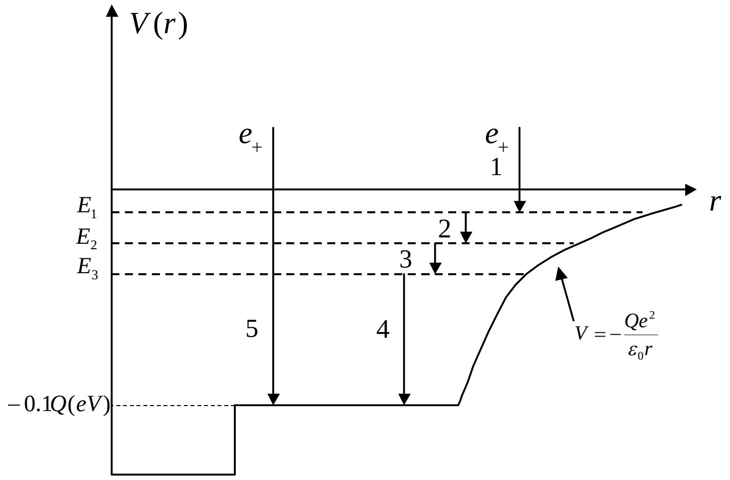

Fig. 3.3: Potential interaction energy V(r) of a negatively charged vacancy with a positron [Pus 94]. Explanations are given in the text.

In the work [Pus90] calculations of specific trapping coefficient for negatively charged vacancy were carried out. Connection between specific trapping coefficient γ_{tr} and temperature is as follows [Pus90]:

$$\gamma_{tr} \sim T^{-1/2}. \qquad (3.31)$$

Such dependence is applicable both for cascaded and direct capture mechanisms (Q magnitude does not influence nature of temperature dependence). To calculate transition probability ν (in unit time) of positron from free state into localized state we can use golden Fermi rule:

$$\nu_{if} = \frac{2\pi}{\hbar} P_i P_f \sum_{r,t} \left| M_{itrf} \right|^2 \delta(E_i - E_f - E_{if}). \qquad (3.32)$$

At this point ν_{if} – transition probability (in unit time) of positron from free state i into localized state f; P_i – probability of positron being in free state i; P_f – probability of final state f in the trap is free for positron; M_{itrf} – matrix element of transition from initial state i into final state f through intermediate states t,r (in figure 3.3 intermediate states are Rydberg states with energies E_1, E_2, E_3; intermediate transitions: $E_i \to E_1, E_1 \to E_2, E_2 \to E_3, E_3 \to E_f$). In δ – function reflects energy conservation law during transition: E_i – free positron energy in state i; E_f – positron energy in final localized state f; E_{if} – energy evolving during transition of positron from state i into state f. In case of direct transition (transition 5 in figure 3.3) intermediate transitions do not exist, as a result of it summation by indexes r,t disappears and indexes r,t disappear in matrix element.

Dependence of γ_{tr} from T (3.31) is also applicable for shallow acceptor traps (negatively charged ions), since in this case it is assumed that interaction energy of a shallow trap and positron has Coulomb aspect. If we compare equations (3.26) and (3.31) we can see that rate of diffusion phase of reaction of positron with negatively charged point defect depends more on T than specific trapping coefficient phase. Increase of T role of diffusive phase rise. In the work [Tru92] equation for positron trapping coefficient γ_{trc} with regard to vacancies accumulation was calculated:

$$\gamma_{trc} = \gamma_0 (1 + \alpha T). \tag{3.33}$$

where α and $\gamma_0 -$ constants independent on crystal temperature. According to equations (3.26) and (3.33) rate of diffusion phase of reaction of positron and capture phase ratio for vacancies accumulation have different temperature dependence. At the same time increase of temperature of role of diffusive phase is rise.

3.4.3 Kinetics of annihilation of positrons

If there are any defects in the crystal, positron annihilation can occur on these defects as well. Positron annihilation kinetics in crystals with defects was studied in a number of works (Brandt and Paulin [Bra72]; Frank and Seeger [Fra74]; Krause-Rehberg and Leipner [Kra99]). Further we will follow ideology proposed in the above-mentioned works.

Case of one type of deep traps

Let’s consider an easy case at first. Let’s assume that deep positron traps of one type are contained in the crystal. In this case number of $N_p(t)$ free positrons decreases due to two processes: capture of free positrons into deep traps at the rate $\kappa_d (s^{-1};$ see equation (3.14)) and annihilation of free positrons with electrons of lattice atoms and possibly *pick-off-annihilation* (see equation (3.13)) at the rate $\lambda_b (s^{-1}).$ Number of traps $N_d(t),$ containing positrons, increases due to capture at the trapping rate of k_d free positrons and decreases at the rate $\lambda_d (s^{-1})$ due to annihilation at the trap of positrons captured. We will ignore thermal ejection of positrons out of trap to the zone (where positrons are in free state), since traps are deep. Kinetics of these processes can be described trough the following combined equations:

$$\begin{aligned} \frac{dN_p(t)}{dt} &= -\lambda_b N_p - k_d N_p, \\ \frac{dN_d(t)}{dt} &= k_d N_p - \lambda_d N_d. \end{aligned} \tag{3.34}$$

Initial conditions for combined equations (3.34) are as follows: $N_p(t=0) = N_0, N_d(t=0) = 0.$ At this point kinetics of thermalized positron is considered. There are not concentrations of free positrons and traps containing positrons, but numbers of positrons $N_p(t)$ and traps with positrons $N_d(t)$ in combined equations (3.34). This can be explained due to the fact that during experiments such a positron source will be chosen that the sample does not contain more than one positron at any moment of time. When meeting this condition in the right part of combined equations (3.34) one should not take into account increase of N_d due to positron source. Role of positron source is reflected in the initial condition: $N_p(t=0)=N_0$.

During the experiments only acts of annihilation are to be registered (acts of positron capture into traps are not to be fixed). This process is characterized by frequency ratio of acts of annihilation $D(s^{-1})$:

$$D(t)=\lambda_b N_p+\lambda_d N_d. \qquad (3.35)$$

If we add both parts of equation (3.34), then we can get the following:

$$D(t)=-\frac{d(N_p+N_d)}{dt}. \qquad (3.36)$$

Therefore to evaluate $D(t),$ one should determine $N_p(t), N_d(t)$ and then use equation (3.36). Let's determine $N_p(t)$ and $N_d(t).$ Using the first equation of system (3.34) and given initial condition for N_p we can get the following:

$$N_p(t)=N_0 e^{-(\lambda_b+k_d)t}. \qquad (3.37)$$

Let's calculate $N_d(t)$ as follows:

$$N_d(t)=Ae^{-\lambda dt}+Be^{-(\lambda_b+k_d)t}. \qquad (3.38)$$

Let's set $N_d(t)$ from equation (3.38) into the second part of equation (3.34). Then given initial condition for N_d we get the following:

$$N_d(t)=\left(\frac{k_d N_0}{\lambda_b+k_d-\lambda_d}\right)\left[e^{-\lambda_d t}-e^{-(\lambda_b+k_d)t}\right] \qquad (3.39)$$

Using equations (3.36), (3.37) and (3.39) we can get the following:

$$D(t)=N_0\left[\frac{I_1}{\tau_1}e^{-\frac{t}{\tau_1}}+\frac{I_2}{\tau_2}e^{-\frac{t}{\tau_2}}\right], \qquad (3.40)$$

where

$$I_1=1-I_2,\ I_2=\frac{k_d}{\lambda_b+k_d-\lambda_d},\ \tau_1=\frac{1}{\lambda_b+k_d},\tau_2=\frac{1}{\lambda_d}.$$

Frequency ratio of annihilation can be characterized by the function $N(t) = D(t)/N_0$:

$$N(t) = \frac{I_1}{\tau_1} e^{-\frac{t}{\tau_1}} + \frac{I_2}{\tau_2} e^{-\frac{t}{\tau_2}}. \tag{3.41}$$

At this point $\tau_i -$ *lifetime for* $i-$*component of spectrum with intensity* I_i. According to equation (3.41) positron annihilation process is characterized by *lifetime spectrum with relevant intensity.* At the same time second component of spectrum (τ_2) is connected solely with positron annihilation in trap, first component of spectrum (τ_1) is not to be determined only by positron annihilation in zone. According to equations (3.40) τ_1, I_1, I_2 depend on positron trapping rate in defect as against to τ_2. Using equation (3.40) we can get the following:

$$k_d = \frac{I_2}{I_1}\left(\frac{1}{\tau_b} - \frac{1}{\tau_d}\right), \tag{3.42}$$

where $\tau_b, \tau_d -$ lifetime conditional on positron annihilation in zone and defect, accordingly ($\tau_b = 1/\lambda_b, \tau_d = 1/\lambda_d$; it is worth noting that $\tau_2 = \tau_d$).

From the experimental data and given equation (3.42) we can define defects concentration as follows. It follows from equations (3.14) and (3.15) that

$$k_d = \gamma n_d, \frac{1}{\gamma} = \frac{1}{\gamma_d} + \frac{1}{\gamma_{tr}}. \tag{3.43}$$

At this point $\gamma -$ coefficient of reaction rate, $n_d -$ defect concentration. Coefficient of diffusion phase of reaction γ_d can be calculated on the basis of equation (3.23) (cases of attraction of positron and defect are to be considered at this point). If we for example consider negatively charged vacancy as a defect, then according to equation (3.31) $\gamma_{tr} = AT^{-1/2}$ $(A -$unknown constant). If we from the experimental data and equation (3.42) define value of k_d at two different temperatures T_1 and T_2 (it is important to choose T_1 and T_2 so, that the value of defect concentration at these temperatures is equal). Then using equation

$$\frac{k_d(T_1)}{k_d(T_2)} = \frac{\dfrac{1}{\gamma_d(T_2)} + \dfrac{1}{\gamma_{tr}(T_2)}}{\dfrac{1}{\gamma_d(T_1)} + \dfrac{1}{\gamma_{tr}(T_1)}}.$$

we can evaluate A parameter, and hence $\gamma(T)$. Then we will determine concentration using equation $n_d = k_d(T)/\gamma(T)$.

Since τ_d does not depend on positron capture rate in defect (and hence on defect concentration), it can be characteristic for a defect with open volume. For example, for isolated vacancies in silicium $\tau_d/\tau_b \approx 1.25$. *Average lifetime* of τ_{aV} positrons is to be evaluated as follows:

$$\tau_{aV} = \sum_{i=1}^{N+1} I_i \tau_i, \tag{3.44}$$

where $N-$ number of defect types. In most cases value of average lifetime is less sensitive to numerical procedures during spectrum handling. In this connection it is worth determining trapping rate of positron by defect on the basis of the equation:

$$k_d = \frac{1}{\tau_b}\left(\frac{\tau_{aV} - \tau_b}{\tau_d - \tau_{aV}}\right), \tag{3.45}$$

which could be obtained from equations (3.40) and (3.41). For a very big defect concentration, when average interval L_d between defects is considerably smaller than diffusive positron length L_+ in zone (diffusive length conditional on positron annihilation in zone), positrons are not able to annihilate in zone, but are captured and annihilate in defects. In this case $I_1 = 0, I_2 = 1$ (see equation (3.40) for I_1 and I_2 given that $k_d >> \lambda_b$) and $\tau_{aV} = \tau_d$. This case is called saturated capture. Since in this situation spectrum consists of one component τ_d, that is independent on positron trapping rate (and therefore independent on defect concentration), it is impossible to determine value of defect concentration at this point. One can only evaluate low limit of defect concentration. Let's perform this evaluation. Since $L_+ \sim \sqrt{D_+ \tau_b}$ and $L_d \approx (2/n_d)^{1/3}$ (this equation can be obtained from the condition that $n_d (L_d/2)^3 4\pi/3 = 1$), then we get the following:

$$\left(\frac{2}{n_d}\right)^{1/3} << \sqrt{D_+ \tau_b}. \tag{3.46}$$

Given that $\tau_b \sim 10^{-10} s$, $D_+ \sim 1 cm^2 s^{-1}$ (in the work [Saa89] for GaAs the following value was obtained $D_+ \approx 1.3 cm^2 s^{-1}$), we get the following: $(2/n_d)^{1/3} << 10^{-5} cm$. It appears from this that under magnitudes of defect concentration approximately $10^{17} cm^{-3}$ and more effect of saturated capture can be observed. If magnitude of defect concentration is rather small to meet the condition $k_d << \lambda_b$, then defects cannot be detected (and therefore value of their concentration can not be determined) by means of evaluation of positron lifetime. In this case positrons are not able to be captured by defects and annihilate only in zone. In this situation $I_1 = 1, I_2 = 0$ (see equation (3.40) for I_1 and I_2 given that $k_d << \lambda_b$) and $\tau_{aV} = \tau_b$. Let's evaluate magnitude of defect concentration under which defects can not be detected. As an illustration let's consider a model situation: defects have single negative charge and reaction rate of positron and defect is diffusion-limited. Then $k_d = \gamma_d n_d$ ($\gamma_d -$specific trapping coefficient of diffusion-limited reaction). Using equation (3.23) (under $Q = 1$) and given that $k_d << \lambda_b$:

$$4\pi D_+ \frac{e^2 n_d}{\varepsilon_0 k_B T} << \lambda_b. \tag{3.47}$$

As a result of it we obtain that under values $n_d << 2\times10^{15} cm^{-3}$ defects cannot be detected. It was assumed in evaluation that $T = 300K$, $\lambda_b \sim 10^{10} s^{-1}$ ($\lambda_b = 1/\tau_b$, $\tau_b \sim 10^{-10} s$). If reaction of positron and defect is limited not by diffusion, but capture, then constant magnitude is less than assumed in evaluation. As a result of this values of n_d, under which defects cannot be detected, will be higher than values obtained during evaluation.

Case of several types of traps

Let's consider case of three traps: one shallow and two deep traps. Such a situation corresponds as a rule to general case for GaAs exposed to plastic deformation. At the same time deep traps mean single vacancies associated with dislocations (non-isolated vacancy) and vacancies clusters (second type of deep traps). Shallow traps means gallium ions in acceptor state or negatively charged dislocation. Figure 3.4 schematically presents processes of positron capture and annihilation for the case given.

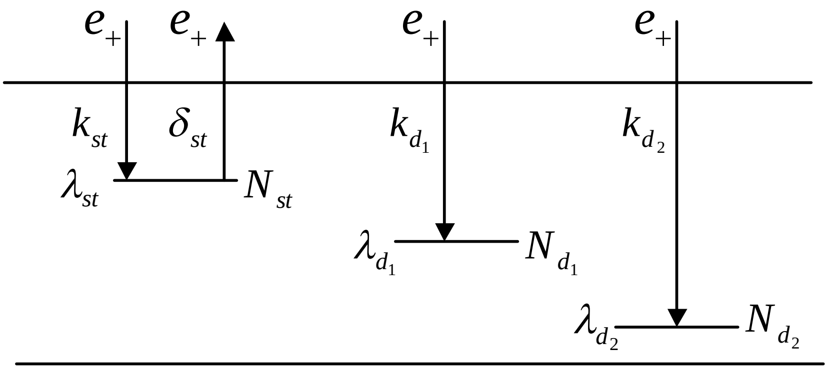

Fig. 3.4: Processes of positron capture and annihilation. Explanations are given in the text.

It is considered that positrons annihilate in zone (at the rate of λ_b), at shallow traps (at the rate of λ_{st}), at deep traps (at the rate of λ_{d_1} and λ_{d_2} at deep traps of first and second types, accordingly). Positrons are captured at shallow traps (at the rate of k_{st}), deep traps (at the rate of k_{d1} and k_{d2} at traps of first and second types, accordingly). Thermal ejection of positrons from shallow trap to zone is to be accounted (at the rate of δ_{st}). Thermal ejection of positrons from deep traps is not to be accounted. Thus number of positrons in zone $N_p(t)$ decreases due to annihilation in zone, capture at shallow and deep traps and increases due to thermal ejection of positrons to zone from shallow traps. Number of shallow traps containing positron $N_{st}(t)$ increases due to positron capture from zone and decreases due to annihilation at these traps of positrons captured and thermal ejection of positrons. Number of deep traps of first type containing positrons $N_{d_1}(t)$ increases due to positron capture at trap and decreases due to annihilation at these traps of positrons captured. The same case is for deep traps of second type. System kinetic equations explaining the above mentioned processes is as follows:

$$\frac{dN_p}{dt} = \delta_{st} N_{st} - (\lambda_b + k_{st} + k_{d_1} + k_{d_2}) N_p .$$

$$\frac{dN_{st}}{dt} = k_{st} N_p - (\lambda_{st} + \delta_{st}) N_{st} . \tag{3.48}$$

$$\frac{dN_{d_1}}{dt} = k_{d_1} N_p - \lambda_{d_1} N_{d_1} .$$

$$\frac{dN_{d_2}}{dt} = k_{d_2} N_p - \lambda_{d_2} N_{d_2} .$$

Initial conditions are as follows:

$$N_p(t=0) = N_0 ; N_{st}(t=0) = 0; N_{d_1}(t=0) = 0; N_{d_2}(t=0) = 0.$$

Since during the experiment acts of positron annihilation are registered (and not acts of capture), the following value is characteristic for the process:

$$D(t) = \lambda_b N_p + \lambda_{st} N_{st} + \lambda_{d_1} N_{d_1} + \lambda_{d_2} N_{d_2} . \tag{3.49}$$

If we sum all equations of combined equations (3.48), then we get for positron annihilation rate $D(t)$ the following equation:

$$D(t) = -\frac{d(N_p + N_{st} + N_{d_1} + N_{d_2})}{dt} . \tag{3.50}$$

Positron annihilation rate can be characterized by the following function $N(t) = D(t)/N_0$. Using set of equations (3.48) we can determine $D(t)$ trough equation (3.50) and hence we can define $N(t)$. Equation for $N(t)$ is as follows:

$$N(t) = \sum_{i=1}^{4} \frac{I_i}{\tau_i} \exp(-t/\tau_i), \tag{3.51}$$

where

$$\tau_1 = \frac{2}{\theta + \Gamma}, \tau_2 = \frac{2}{\theta - \Gamma}, \tau_3 = \frac{1}{\lambda_{d_1}}, \tau_4 = \frac{1}{\lambda_{d_2}} . \tag{3.52}$$

$$I_1 = 1 - (I_2 + I_3 + I_4). \tag{3.53}$$

$$I_2 = \frac{\delta_{st} + \lambda_{st} - \frac{1}{2}(\theta - \Gamma)}{\Gamma} \left(1 + \frac{\kappa_{st}}{\delta_{st} + \lambda_{st} - 1/2 \times (\theta - \Gamma} + \frac{\kappa_{d_1}}{\lambda_{d_1} - 1/2 \times (\theta - \Gamma)} + \frac{\kappa_{d_2}}{\lambda_{d_2} - 1/2(\theta - \Gamma)} \right). \tag{3.54}$$

$$I_3 = \frac{k_{d_1}(\delta_{st} + \lambda_{st} - \lambda_{d_1})}{(\lambda_{d_1} - 1/2 \times (\theta + \Gamma))(\lambda_{d_1} - 1/2 \times (\theta - \Gamma))}. \qquad (3.55)$$

$$I_4 = \frac{k_{d_2}(\delta_{st} + \lambda_{st} - \lambda_{d_2})}{(\lambda_{d_2} - 1/2(\theta + \Gamma))(\lambda_{d_2} - 1/2(\theta - \Gamma))}. \qquad (3.56)$$

$$\theta = \lambda_b + \lambda_{st} + k_{st} + k_{d_1} + k_{d_2} + \delta_{st}. \qquad (3.57)$$

$$\Gamma = \sqrt{(\lambda_b - \lambda_{st} + k_{st} + k_{d_1} + k_{d_2} - \delta_{st})^2 + 4\delta_{st}k_{st}}. \qquad (3.58)$$

According to equation (3.51) *spectrum components* τ_3 and τ_4 are solely connected with positron annihilation at deep traps of first and second types, accordingly. At that $\tau_3 = \tau_{d_1} = 1/\lambda_{d_1}$, $\tau_4 = \tau_{d_2} = 1/\lambda_{d_2}$ (τ_{d_1}, τ_{d_2} – *positron lifetime* conditional on annihilation at deep traps of first and second types, accordingly). *Spectrum component* τ_2 is not determined solely by positron annihilation rate at shallow trap. That's why τ_2 can not be interpreted as positron lifetime conditional on annihilation at shallow traps τ_{st} ($\tau_2 \neq \tau_{st} = 1/\lambda_{st}$). *Spectrum component* τ_1 can not be interpreted as positrons lifetime conditional on their annihilation in zone τ_b ($\tau_1 \neq \tau_b = 1/\lambda_b$). *Average positron lifetime* is determined in the following way:

$$\tau_{av} = \sum_{i=1}^{4} I_i \tau_i. \qquad (3.59)$$

Let's consider the case of low temperature, when we could assume that $\delta_{st} \to 0$. Then it follows from equations (3.57) and (3.58) that:
$\Gamma = \lambda_b - \lambda_{st} + k_{st} + k_{d_1} + k_{d_2}$, $\theta = \lambda_b + \lambda_{st} + k_{st} + k_{d_1} + k_{d_2}$. Thus $\theta - \Gamma = 2\lambda_{st}$ and $\theta + \Gamma = 2\theta - 2\lambda_{st}$. Then using equations (3.55) and (3.56) we get the following:

$$I_3 = \frac{k_{d_1}}{\lambda_b + k_{st} + k_{d_1} + k_{d_2} - \lambda_{d_1}}. \qquad (3.60)$$

$$I_4 = \frac{k_{d_2}}{\lambda_b + k_{st} + k_{d_1} + k_{d_2} - \lambda_{d_2}}. \qquad (3.61)$$

From the equations (3.60) and (3.61) we can define k_{d_1} and k_{d_2}, using joint system of equations (3.60) and (3.61):

$$k_{d_1} = \frac{I_3[(\lambda_b + k_{st} - \lambda_{d_1}) + I_4(\lambda_{d_1} - \lambda_{d_2})]}{(1 - I_3 - I_4)}. \qquad (3.62)$$

$$k_{d_2} = \frac{I_4[(\lambda_b + k_{st} - \lambda_{d_2}) + I_3(\lambda_{d_2} - \lambda_{d_1})]}{(1 - I_3 - I_4)}. \qquad (3.63)$$

In these equations k_{st} trapping rate of positron at shallow trap is unknown. Additional connection between k_{st} and k_{d_1}, k_{d_2} can be ascertained in the following way. Using equation (3.54) we can get the following (on the assumption that $\delta_{st} \to 0)$:

$$I_2 = \frac{\delta_{st}}{\theta - 2\lambda_{st}}\left(1 + \frac{k_{st}}{\delta_{st}} + \frac{k_{d_1}}{\lambda_{d_1} - \lambda_{st}} + \frac{\kappa_{d_2}}{\lambda_{d_2} - \lambda_{st}}\right).$$

It follows that:

$$I_2 = \frac{\delta_{st}}{\theta - 2\lambda_{st}}\frac{k_{st}}{\delta_{st}}\left[1 + \frac{\delta_{st}}{k_{st}}\left(1 + \frac{k_{d_1}}{\lambda_{d_1} - \lambda_{st}} + \frac{k_{d_2}}{\lambda_{d_2} - \lambda_{st}}\right)\right].$$

Since (δ_{st} / k_{st}) tends to zero, we get the following:

$$I_2 \approx \frac{k_{st}}{\theta - 2\lambda_{st}} = \frac{k_{st}}{\lambda_b + k_{st} + k_{d_1} + k_{d_2} - \lambda_{st}}.$$

From the equation we can determine k_{st} :

$$k_{st} = \frac{I_2}{1 - I_2}(\lambda_b - \lambda_{st} + k_{d_1} + k_{d_2}). \qquad (3.64)$$

Using equations (3.62), (3.63), (3.64) we get the following:

$$k_{st} = \frac{I_2}{I_1}\{\lambda_b + \lambda_{d_2}(I_3 - 2I_4) + \lambda_{d_1}(I_4 - 2I_3) - \lambda_{st}(1 - I_3 - I_4)\}. \qquad (3.65)$$

Therefore from the equations (3.62), (3.63), (3.65) we can determine k_{st}, k_{d_1} and k_{d_2} at low crystal temperature. At this point $\lambda_b = 1/\tau_b, \lambda_{st} = 1/\tau_{st}, \lambda_{d_1} = 1/\tau_{d_1}, \lambda_{d_2} = 1/\tau_{d_2}$. At that $\tau_{st} = \tau_2$ (which follows from equation for τ_2 (3.52) under $\delta_{st} = 0$). If we consider the situation of one type of deep traps (where $N_{st} = 0, N_{d_2} = 0, k_{d_2} = 0, k_{st} = 0, \lambda_{d_2} = 0, \lambda_{st} = 0$), then it follows from equation (3.62) that:

$$\kappa_{d_1} = \frac{I_3}{1 - I_3 - I_4}\left(\frac{1}{\tau_b} - \frac{1}{\tau_{d_1}}\right).$$

Further it is necessary to identify $I_4 = 0, I_3$ with $I_2, 1 - I_3 = I_1$. Then we get the following:

$$k_{d_1}=\frac{I_2}{I_1}(\frac{1}{\tau_b}-\frac{1}{\tau_{d_1}}),$$

which is coincide with equation (3.42) obtained for positron trapping rate by deep trap within the framework of model of one type of deep traps. Thus equations describing positron annihilation kinetics in case of three types of traps explain more easy situations as well.

Conditions (3.46) and (3.47) restricting limit of trap concentration (where measurement method of positron lifetime is effective to determine value of trap concentration) are applicable for each type of traps in the case in question. Estimation method for trap concentration on the basis of fixed magnitudes of positron trapping rate at traps is given below.

3.5 Trap concentration

Magnitude of trap concentration can be determined if trapping rate and specific trapping coefficient are known: k_d and γ (see equation (3.43))

$$n_d=k_d/\gamma\ ,\ \frac{1}{\gamma}=\frac{1}{\gamma_d}+\frac{1}{\gamma_{tr}}.$$

Further we will consider the case of three traps: one type of shallow point traps with n_{st}, concentration, one type of deep traps with n_{d_1} concentration and one type of deep traps with n_{d_2} concentration representing accumulations of defects (clusters). First we will obtain equations for n_{d_1}, then for n_{st} and further for n_{d_2}. In case of attraction of positron to point trap coefficients of diffusive phase of reaction γ_d and capture phase γ_{tr} are as follows (see equations (3.23) and (3.31)):

$$\gamma_{d_1}=4\pi D_+(T)\frac{Qe^2}{\varepsilon_0 k_B T},\ \gamma_{tr}=\frac{A_{d_1}}{T^{1/2}}.$$

At this point A_{d_1} – constant independent from temperature. For γ_{d_1} we get the following: $\gamma_{d_1}\approx 1.68\times 10^{-3}QD_+(T)/T$, where $\gamma_{d_1}(cm^3/s), D_+(cm^2/s), T$ is specified in Kelvin degree. Then we obtain for γ the following equation:

$$\frac{1}{\gamma}=\frac{0.6\times 10^3 T}{QD_+}+\frac{T^{1/2}}{A_{d_1}}. \tag{3.66}$$

Let's evaluate A_{d_1}. For this purpose let's take up equation $k_{d_1}(T_2)/k_{d_1}(T_1)$ for trapping rates at two measurement temperatures (values of T_1 and T_2 are to be chosen from T interval where defect concentration is constant, i.e. $n_{d_1}(T_1)=n_{d_1}(T_2)$):

$$\frac{k_{d_1}(T_2)}{k_{d_1}(T_1)}=\frac{\gamma(T_2)}{\gamma(T_1)}. \tag{3.67}$$

It follows from equation (3.66) that:

$$\frac{\gamma(T_2)}{\gamma(T_1)} = \frac{\left(\dfrac{0.6\times10^3 T_1}{Q(T_1)D_+(T_1)} + \dfrac{T_1^{1/2}}{A_{d_1}}\right)}{\left(\dfrac{0.6\times10^3 T_2}{Q(T_2)D_+(T_2)} + \dfrac{T_2^{1/2}}{A_{d_1}}\right)}. \tag{3.68}$$

Let's choose T_1 and T_2 from T interval where not only value of defect concentration does not change, but also number of electrons localized at defect, i.e. $Q(T_1) = Q(T_2)$. Using equations (3.67) and (3.68) we can determine value of A_{d_1} :

$$A_{d_1} = \frac{1.67\times10^{-3} Q(T_1^{1/2} - aT_2^{1/2})}{\left[\dfrac{aT_2}{D_+(T_2)} - \dfrac{T_1}{D_+(T_1)}\right]}. \tag{3.69}$$

At this point

$$a = \frac{k_{d_1}(T_2)}{k_{d_1}(T_1)}.$$

From the equations (3.66) and (3.69) we get the following:

$$\frac{1}{\gamma} = \frac{0.6\times10^3\times T}{QD_+(T)}\left\{1 + \frac{D_+(T)\left[\dfrac{aT_2}{D_+(T_2)} - \dfrac{T_1}{D_+(T_1)}\right]}{T^{1/2}\left(T_1^{1/2} - aT_2^{1/2}\right)}\right\}. \tag{3.70}$$

Since $D_+(T) \sim T^{-1/2}$ [Saa89], we can get the following:

$$\frac{D_+(T)}{D_+(T_2)} = \left(\frac{T_2}{T}\right)^{1/2},\ \frac{D_+(T)}{D_+(T_1)} = \left(\frac{T_1}{T}\right)^{1/2}.$$

Given these equations and equation (3.70) we get the following:

$$\frac{1}{\gamma} = \frac{0.6\times10^3 T}{QD_+(T)}\left\{1 + \frac{\left(aT_2^{3/2} - T_1^{3/2}\right)}{T\left(T_1^{1/2} - aT_2^{1/2}\right)}\right\}. \tag{3.71}$$

From the equations (3.71) and $n_{d_1} = k_{d_1}/\gamma$ we can obtain equation for product of trap concentration and number of electrons localized at trap:

$$Q_{d_1} n_{d_1} = \frac{0.6\times10^3 T k_{d_1}(T)}{D_+(T)} \left\{ 1 + \frac{\left(aT_2^{3/2} - T_1^{3/2} \right)}{T\left(T_1^{1/2} - aT_2^{1/2} \right)} \right\}. \qquad (3.72)$$

Similarly we can get for shallow traps the following:

$$Q_{st} n_{st} = \frac{0.6\times10^3 T k_{st}(T)}{D_+(T)} \left\{ 1 + \frac{\left(bT_2^{3/2} - T_1^{3/2} \right)}{T\left(T_1^{1/2} - bT_2^{1/2} \right)} \right\}. \qquad (3.73)$$

At this point

$$b = \frac{k_{st}(T_2)}{k_{st}(T_1)}.$$

To evaluate cluster concentration let's do the following. Let's determine relation between coefficient diffusive phase of positron reaction with cluster and capture phase: $\gamma_{d_2} / \gamma_{trc}$. In case of attraction of positron to cluster γ_{d_2} can be determined from the equation (3.23) where Q – number of electrons localized at one cluster. As to capture phase coefficient γ_{trc}, it can be determined on the basis of equation (3.33) where γ_0 and α - unknown constants. However it is worth noting the following: results of calculations of particle capture ratio (in this case - positron) to attractive center (in this case – vacancy accumulation) are very sensitive to choice of type of interaction potential between particle and trapping center. In case of cluster this type of potential is characterized by several factors: in particular by size of cluster and number of charged vacancies containing in cluster (these characteristics influence charge density in cluster and hence determine electrostatic potential of cluster), geometric shape of cluster (usually cluster is assumed to be spherically symmetric). As a rule size of cluster and number of charged vacancies containing in cluster is unknown. Assumption of spherically symmetric shape of cluster is an idealization. In such situation it is impossible to evaluate correctly interaction potential between charged cluster and positron. Therefore it is difficult to obtain reliable results on γ_{trc} magnitudes from quantum-mechanical calculations of transition probability of positron from free state into localized state in cluster (equation (3.33) was obtained of such calculations [Tru92]. At this point to evaluate γ_{trc} let's do the following. Let's show γ_{trc} in form of $\gamma_{trc} = \sigma \upsilon_+$, where σ – capture cross-section of positron by cluster, υ_+ – velocity of free thermalized positron. We can determine magnitude of capture cross-section as follows: $\sigma \approx \pi r_c^2$, where r_c – capture radius of positron by cluster ($r = 0$ corresponds to center of spherically symmetric cluster). Magnitude of r_c can be evaluated as follows: let's consider positron to be captured when it approaches at such distance r_c to center of cluster at which absolute value of electrostatic interaction energy is equal to kinetic energy of free positron. If we assume that probability of different values of free positron impulse is specified by Maxwellian distribution, then kinetic energy of free positron is equal to $3k_B T/2$. Then we get the following:

$$\frac{Q_{d_2} e^2}{\varepsilon_0 r_c} = \frac{3}{2} k_B T.$$

Therefore

$$r_c = \frac{2Q_{d_2}e^2}{3\varepsilon_0 k_B T}.$$

At this point Q_{d_2} – number of electrons localized at one cluster. Magnitude of υ_+ can be evaluated on the basis of the following equation:

$$\upsilon_+ = \left(\frac{8k_B T}{\pi m_+}\right)^{1/2}.$$

As a result of it we get the following:

$$\frac{\gamma_{d_2}}{\gamma_{trc}} \approx \frac{1{,}88 D_+(T)}{Q_{d_2}}\left(\frac{T}{300K}\right)^{1/2}. \qquad (3.74)$$

If we assume that $D_+ \sim 1cm^2/s$ [Saa89] and given that $Q_{d_2} >> 1,$ then we can get the following: at measurement temperature $T \le 300K$ relation is $(\gamma_{d_2}/\gamma_{trc}) << 1.$ Hence interaction reaction between positron and cluster is most likely limited by diffusion phase of reaction. Accordingly, in this case reaction rate is determined by diffusion phase: $k_{d_2} = \gamma_{d_2} n_{d_2}$. Given this equation and equation (3.23) we can get the following:

$$Q_{d_2} n_{d_2} = \frac{k_{d_2}(T)}{4\pi D_+(T)\left(\dfrac{e^2}{\varepsilon_0 k_B T}\right)}.$$

On the basis of this equation we can finally get the following:

$$Q_{d_2} n_{d_2} \approx \frac{0.18\times 10^6 k_{d_2}(T)}{D_+(T)}\left(\frac{T}{300K}\right). \qquad (3.75)$$

It follows from equations (3.72), (3.73) and (3.75) that for evaluation of magnitudes of trap concentration it is necessary to determine values of rate $(k_{st}, k_{d_1}, k_{d_2})$ and number of electrons localized at traps $(Q_{st}, Q_{d_1}, Q_{d_2})$. Let's address these two tasks one after another.

Using experimental data values of trapping rate can be determined on the basis of equations (3.62), (3.63) and (3.65). These equations were obtained under condition that $\delta_{st} \to 0$ (practically – under condition that $(\delta_{st}/k_{st}) << 1$). Let's evaluate limit of temperature at which this condition is met. Given equation (3.29) we get the following:

$$\frac{\delta_{st}}{\gamma_{st} n_{st}} = \frac{1}{n_{st}}\left[\frac{m_+ k_B T}{2\pi\hbar^2}\right]^{3/2} \exp(-E_{st}/k_B T).$$

At this point E_{st} – positron binding energy in shallow trap. It follows from literary data that: $E_{st} \approx 4\times 10^{-2} eV$ [Dan91], $E_{st} \approx (6.3\pm 1.0)10^{-2} eV$ [Saa90], $E_{st} \approx 4.3\times 10^{-2} eV$ [Kra94]. For evaluation let's take on value of $E_{st} \approx 4\times 10^{-2} eV$.

Then we can get the following:

$$\frac{\delta_{st}}{\gamma_{st} n_{st}} \approx \frac{1}{n_{st}} 2.2\times 10^{17} \left(\frac{T}{20K}\right)^{3/2} \exp[-23.2(20K/T)]. \qquad (3.76)$$

Minimum value of trap concentration (when they can be detected by method of positron annihilation yet) is approximately equal to $10^{15}\,cm^{-3}$(see section 3.4.3). Therefore it makes sense to analyze the situation when $n_{st} \geq 10^{15}\,cm^{-3}$. If we place value of $n_{st} \approx 10^{15}\,cm^{-3}$ into equation (3.76), we can get the following:

$$\frac{\delta_{st}}{\gamma_{st} n_{st}} \leq 2.2\times 10^{2} \left(\frac{T}{20K}\right)^{3/2} \exp[-23.2(20K/T)].$$

It follows from this condition that $T \leq 50K$

$$\frac{\delta_{st}}{\gamma_{st} n_{st}} << 1.$$

Thus equations (3.62), (3.63) and (3.65) are applicable at measurement temperature $T \leq 50K$ (values of T_1 and T_2 in equations (3.72) and (3.73) should meet this condition). If spectrum of charge states of point defect and position of Fermi level in band gap of semiconductor are known, then it is possible to determine number of electrons localized at defect using the following equation [Ash79]:

$$Q = \frac{\sum_j j \exp[-(E^{(j)} - jE_F)/k_B T]}{\sum_j \exp[-(E^{(j)} - jE_F)/k_B T]}. \qquad (3.77)$$

At this point $E_F -$ value of *Fermi level* in band gap of semiconductor; $E^{(j)}$ and $j-$energy and number of electrons in $j-$charge state of point defect. All charge states of defect are summed up. Relation between energy $E^{(j)}$ in $j-$charge state and energy $E^{(j-1)}$ in $j-1-$charge state is as follows:

$$E^{(j)} = E^{(j-1)} + E_j. \qquad (3.78)$$

At this point $E_j -$energy level of defect transition from $j-1-$charge state into $j-$charge state. If spectrum of charge states of defect are known, then magnitudes in equation (3.78) are known. Therefore for evaluation of magnitude of Q on the basis of equation (3.77) it is necessary to determine E_F. Position of Fermi level can be determined as follows.

Let's consider the case of *nondegenerated* semiconductor when the following conditions are met:

$$E_c - E_F >> k_B T \quad \text{for } n\text{-type} \qquad (3.79)$$
$$E_F - E_\upsilon >> k_B T \quad \text{for } p\text{-type}$$

At this point $E_{c,}E_{\upsilon}$ – energy for conduction band valence band ceiling, accordingly. When conditions (3.79) are met, value of n electron concentration in semiconductor of n-type and P holes in semiconductor of p-type are connected with Fermi level by the following equations [Ash79]:

$$n(T) = N_c(T)\exp[-(E_c - E_F)/k_B T] \text{ for } n\text{-type} \qquad (3.80)$$
$$p(T) = N_{\upsilon}(T)\exp[-(E_F - E_{\upsilon})/k_B T] \text{ for } p\text{-type}$$

At this point

$$N_c(T) = 2.5\left(\frac{m_c}{m_e}\right)^{3/2}\left(\frac{T}{300K}\right)^{3/2}\times 10^{19}cm^{-3},$$
$$N_{\upsilon}(T) = 2.5\left(\frac{m_{\upsilon}}{m_e}\right)^{3/2}\left(\frac{T}{300K}\right)^{3/2}\times 10^{19}cm^{-3},$$

m_c, m_{υ}, m_e – *density mass of electron states* in conduction band, holes in valence band and electron mass, accordingly. For GaAs $m_{\upsilon} \approx 0.5 m_e, m_c \approx 0.065 m_e$ [Gri91]. According to equations (3.80) conditions (3.79) are met if $n(T) << N_c(T)$ and $p(T) << N_{\upsilon}(T)$. If concentration of electrons and holes is known (for example from Hall measurement), then on the basis of equations (3.80) we can evaluate magnitudes of E_F. If experimental data are not available, we can do the following. In the general case value of Fermi level is determined on the basis of electroneutrality equation:

$$N_{d_z}(E_F) + p(E_F) + \sum_k Q_k(E_F)n_{d_k} = n(E_F) + N_{az}(E_F) + \sum_m Q_m(E_F)n_{ak}. \quad (3.81)$$

At this point $N_{dz}, N_{az}, n_{d_k}, n_{ak}$ – concentration of charged donors, charged acceptors, defects of donor κ-type and defects of acceptor m-type, accordingly; Q_k, Q_m – number of holes localized at donor defect of κ-type and number of electrons localized at acceptor defect of m-type, accordingly. All k- and m-types of defect are summed up. Let' s consider several situations.

Intrinsic semiconducting material

In intrinsic semiconducting material (undoped or low-doped) concentration of electrons and holes substantially exceeds magnitudes of N_{d_z} and N_{d_a}. Before crystal deformation defect concentration was far less than magnitudes of n and p. After deformation of intrinsic semiconducting material there are defects in the sample (of donor and acceptor types), which have appear in the process of deformation. Generally the following condition is met:

$$\left|\sum_k Q_k n_{d_k} - \sum_m Q_m n_{d_m}\right| << n, p. \qquad (3.82)$$

As a result of it electroneutrality equation (3.81) is as follows:

$$n(E_F) = p(E_F). \qquad (3.83)$$

Using equations (3.80) and (3.83) we can get the following:

$$E_F = E_\upsilon + \frac{1}{2}E_g + \frac{3}{4}k_B T \ln\left(\frac{m_\upsilon}{m_c}\right). \qquad (3.84)$$

At this point E_g – value of band gap width. According to equation (3.84) in undoped semiconductor Fermi level is situated before and after crystal deformation near midgap (a little bit higher than midgap since $(m_\upsilon / m_c) > 1$).

N-type semiconducting material

The following conditions are met in n-type material: $N_{d_z} >> N_{a_z}$ and $n >> p$. Before deformation defect concentration can be ignored in comparison with concentration of donor dopant. In the process of deformation in crystal defects are arising, but in actual practice concentration of these defects is low as compared to concentration of charged donor dopants. As a result of it using equation (3.81) we can obtain a more simple equation:

$$N_{d_z}(E_F) = n(E_F). \qquad (3.85)$$

For concentration of charged donor dopant N_{d_z} the following equation is applicable [Ash 79]:

$$N_d - N_{d_z} = \frac{N_d}{\frac{1}{2}\exp[(E_d - E_F)/k_B T] + 1}. \qquad (3.86)$$

At this point N_d – full concentration of donor dopant, E_d – energy level of donor dopant. It follows from equations (3.80), (3.86) and (3.85) that:

$$E_F = E_c - k_B T \ln\left[\frac{N_d}{N_c} - \frac{1}{2}\exp\left[-\left(E_c - E_d\right)/k_B T\right]\right]^{-1}. \qquad (3.87)$$

Therefore value of Fermi level for n-type semiconducting material can be determined on the basis of equation (3.87) for both cases: before and after crystal deformation.

P-type semiconducting material

The following conditions are met in p-type material: $N_{d_z} << N_{a_z}$ and $n << p$. As to defect concentration all that, what was set out with regard to n-type material, is applicable. In this case electoneutrality equation is as follows:

$$N_{a_z}(E_F) = p(E_F). \qquad (3.88)$$

For concentration of charged acceptor dopant N_{a_z} the following equation is applicable [Ash 79]:

$$N_a - N_{a_z} = \frac{N_a}{\frac{1}{2}\exp[(E_F - E_a)/k_B T] + 1}. \qquad (3.89)$$

At this point N_a – full concentration of acceptor dopant, E_a – energy level of acceptor dopant. Using equations (3.80), (3.89) and (3.88) we can get the following:

$$E_F = E_\upsilon + k_B T \ln\left[\frac{N_a}{N_\upsilon} - \frac{1}{2}\exp\left[-(E_a - E_\upsilon)/k_B T\right]\right]^{-1}. \qquad (3.90)$$

Accordingly, value of Fermi level for semiconducting p-type material can be determined with help of equation (3.90) for both cases: before and after crystal deformation. Let's consider Q values for point traps: for gallium vacancies (V_{Ga}) and gallium ions substituting arsenic atoms (Ga_{As}). It follows from literary data for V_{Ga} that (see figure 3.2(a)):

1. In n-type semiconductor gallium vacancy is in one charge state – triple negative. Therefore at this point for V_{Ga} $Q = 3$ and there is no need to make calculations by formula (3.77).
2. Since for GaAs relation is $(m_\upsilon / m_c) > 1,$ in undoped (intrinsic) semiconductor Fermi level is situated a little bit higher than midgap (see equation (3.84)). Hence in undoped semiconductor V_{Ga} is in one charge state – triple negative. Therefore at this point $Q = 3$ and there is no need to make calculations by formula (3.77).
3. In p-type semiconductor V_{Ga} can be in different charge states and at this point for determination of Q value we should use formula (3.77), but beforehand it is necessary to determine value of Fermi level on the basis of equation (3.90). However it follows from literary data (see figure 3.2(a)) that results of different authors on values of V_{Ga} energy levels in different charge states strongly differ. Calculation results by formula (3.77) strongly depend on values of V_{Ga} energy levels taken on in different charge states. In such situation it does not make sense to carry out calculations by formula (3.77) and we should admit that in p-type semiconductor it is impossible to uniquely determine Q value for V_{Ga} at different measurement temperatures and doping levels. Therefore in p-GaAs on the basis of measurement of positron lifetime it is possible to evaluate not V_{Ga} concentration, but concentration product per number of electrons localized at gallium vacancy: nQ. It follows from literary data for Ga_{As} [Bar85], [Jan89], [Zha91] that:

1. In undoped semiconductor and n-type semiconductor Ga_{As} ions are in one charge state - double negative. Therefore at this point for Ga_{As} $Q = 2$ and there is no need to make calculations by formula (3.77).
2. In p-type semiconductor Ga_{As} ions can be in different charge states. However literary data on values of Ga_{As} energy levels in different charge states are conflicting. That's why in p-GaAs on the basis of measurement of positron lifetime it is possible to evaluate Ga_{As} ions concentration product per number of electrons localized at Ga_{As} ion. As to V_{As} arsenic vacancies and arsenic ions As_{Ga}, substituting gallium atoms, then it follows from literary data that:

1. Ions As_{Ga}, in GaAs can be in donor and neutral charge states [Bar85], [Jan89], [Zha91]. Therefore ratio of trapping rate of positron with ions As_{Ga}, is far less than ratio of trapping rate of positron with Ga_{As} ions. In this connection Ga_{As} ions most likely have more influence on value of positron lifetime than ions As_{Ga}.
2. In undoped semiconductor and p-type semiconductor V_{As} is in donor charge state (see figure 3.2(b)). Therefore at this point ratio of trapping rate of positron and V_{As} is far less than trapping rate of positron with V_{Ga}. In this connection at this point gallium vacancies most likely have more influence on value of positron lifetime than arsenic vacancies.
3. In n-type semiconductor V_{As} can be under certain conditions (at relevant values of doping levels and measurement temperature) in single negative or double negative charge state [Pus89] (see figure 3.2(b)). That's why at this point trapping rate of positron and V_{As} can be compared with trapping rate of V_{Ga}. But according to calculations [Jan89] in n-GaAs arsenic vacancy formation energy E_{As} ($E_{As} \approx 4.0 eV$) is considerably higher than gallium vacancy formation energy $E_{Ga} (E_{Ga} \approx (0.5-2) eV)$. As a result of it concentration of gallium vacancies V_{Ga},. formed by crystal deformation of n-GaAs can be substantially higher than arsenic vacancy concentration V_{As}. In this regard gallium vacancies have more influence on value of positron lifetime than arsenic vacancies.

Therefore on the basis of the above mentioned analysis we can draw the following conclusion: using measurement of positron lifetime in undoped GaAs and n-GaAs it is possible to determine values of trap concentration. In p-type GaAs it is possible to determine not value of concentrations, but values of trap concentration product per number of electrons localized at trap: nQ.

Equations (3.72) and (3.73) for concentration of point traps were obtained using two assumptions (see above): at measurement temperatures T_1 and T_2 $n(T_1) = n(T_2)$ and $Q(T_1) = Q(T_2)$. Condition $n(T_1) = n(T_2)$ is usually met (during limit of measurement temperature of positron lifetime trap concentration do not change). As to the second condition in undoped GaAs and n-GaAs point traps are in fixed charge states remaining constant during change of measurement temperature (see above). Hence condition $Q(T_1) = Q(T_2)$ is satisfiability. In p-GaAs condition $Q(T_1) = Q(T_2)$ can be disturbed. However at this point on the basis of measurement not trap concentration is to be evaluated but Qn product, that's why formulas (3.72) and (3.73) can be applied. Formulas (3.72) and (3.73) contain trapping rates k_{st} and k_{d_1}. If these rates are to be evaluated on the basis of equations (3.62) and (3.65), which are applicable at measurement temperatures $T \le 50K$, then T_1 and T_2 should be chosen taking into account this temperature constraints.

In literature [Pus90] values for positron trapping rate at vacancy at different temperatures were obtained. However the above-mentioned method of evaluation of point trap concentration does not use values of γ_{tr}, obtained in the work [Pus90], but take into account dependence of γ_{tr} on T : $\gamma_{tr} \sim T^{-1/2}$ [Pus90]. At that A constant is to be determined taking into consideration experimental data. Such approach can be explained for several reasons:

1. In the work [Pus90] values of γ_{tr} were obtained for isolated vacancy. However in deformed sample vacancies are as a rule not isolated and are situated in electrostatic

and deformative fields of dislocations. These fields can have influence on positron capture process by vacancy (i.e. they can influence value of γ_{tr}).

2. There are other point defects as well, for example gallium ions Ga_{As} in acceptor state. In this case dependence of γ_{tr} on T is similar to dependence for charged vacancy, but absolute values can differ.
3. Reaction of positron and trap consists of two phases: diffusion phase and positron capture phase and not only positron capture phase.

In this regard for evaluation of γ_{tr} one should better rely on experimental data. At that dependence of γ_{tr} on T is assumed in accordance with results of the work [Pus90].

In vacancy cluster value of number of electrons localized in Q cluster is unknown since number of vacancies in cluster is unknown as well. In this connection on the basis of measurement of positron lifetime for vacancy cluster and equation (3.75) we can determine value of $Q_{d_2}n_{d_2}$. At the same time if we evaluate rate of k_{d_2}, which is part of equation (3.75), on the basis of equation (3.63) applicable under $T \leq 50K$, then we should determine value of $Q_{d_2}n_{d_2}$ under $T \leq 50K$.

Conclusions

1. Main positron annihilation channels in crystal GaAs without defects are the following: annihilation of free thermalized positrons with electrons of lattice atoms and possibly (at low crystal temperatures) annihilation of parapositronium with electrons of lattice atoms (*pick-off*-annihilation).
2. In crystals GaAs exposed to plastic deformation additional positron annihilation channels appear. In literature annihilation at three trap types is considered (as a most general case): shallow traps of one type and two types of deep traps. At that vacancies associated with dislocations and vacancy clusters are considered to be deep traps for positrons. Negatively charged dislocations or (and) negatively charged gallium ions are considered to be shallow traps.
3. Measurement method of positron lifetime is effective to determine value of n_d trap concentration in certain concentration limit (it follows from estimation that: $n_d \approx 10^{15} cm^{-3} \div 10^{17} cm^{-3}$). Low bound of n_d value (see condition (3.47)) is conditional on the following: at low values of trap concentration when positron annihilation rate in zone considerably exceeds their trapping rate (trapping rate is proportional to trap concentration) at traps only one component in spectrum appears connected solely with positron annihilation in zone. In this case experimental data is lacking information on traps. Upper bound of n_d value (see condition (3.46)) is conditional on the following: at high values of trap concentration when positron trapping rate by traps considerably exceeds positron annihilation rate in zone and at traps components in spectrum appear connected solely with positron annihilation (case of saturated positron capture). Experimental data will be lacking information on positron trapping rate by traps. It not enables evaluating value of trap concentration.
4. Rates of diffusive phase and positron capture phase at negatively charged traps have different temperature dependence (see equations (3.26), (3.31), (3.33)). In this regard on the basis of experimental data on dependence of reaction rate of positron and trap on measurement temperature (subject to constant value of trap

concentration) it is possible to determine the phase limiting reaction rate of positron and trap.

5. Reaction of positron and vacancy cluster is most likely limited by diffusive phase.
6. On the basis of positron lifetime it is possible to determine values of point trap concentration in undoped GaAs and in n-GaAs. In p-GaAs it is possible to determine point trap concentration product per number of electrons localized at trap: Qn_d (number of electrons localized at trap means exceeding of number of electrons at charged trap in comparison with number of electrons at neutral trap).
7. On the basis of positron lifetime in GaAs it is possible to evaluate for vacancy cluster product of cluster concentration per number of electrons localized in cluster.

4. Materials and Methods

4.1 Test material

The tested gallium arsenide was given from “Freiberger Compound Materials GmbH”. The n-type GaAs is a tellurium-doped material with electron concentration of $5.0\times10^{17}cm^{-3}$, and dislocation density $N_d = 10^4 cm^{-2}$.

4.2 Samples preparation for experiments

First, 4mm-6mm-thickness semiconductor washers have been used to saw out rectangular parallelepipeds with approximate dimensions of 4x4x12 (mm x mm x mm) and [110] crystallographic orientation using a diamond thread milling machine. The surfaces of the samples have not been polished up as B_2O_3 is chemically active: at $800^0 C$ the sample may be destroyed due to chemical reaction between the boron oxide and the polished surface of the sample. Lateral sides have been rounded off to avoid fractures.

For experiments which determine average positron lifetime by means of positron annihilation spectroscopy method two discs of about 0,7mm thickness have been obtained from the middle of the parallelepiped. To eliminate imperfections that appeared after sawing the discs have been etched out in a 3% solution of bromide methanol for some time.

4.3 Deformation experiments

The apparatus produced by “Material Testing System” has been applied for deformations over quite wide range of the velocity of extension. The machine is monitored with the computer recording the readings. Figure 4.1 represents the deformation machine.

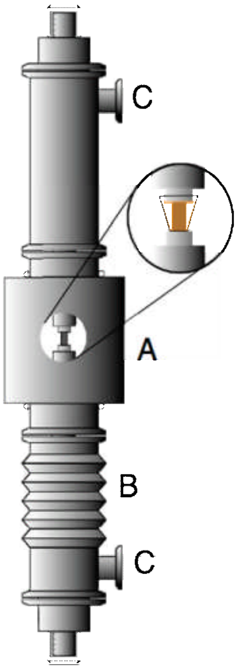

Fig. 4.1: Deformation equipment. A combustion chamber, *B* vacuum diaphragm, *C* flange for connect a pump. The smaller figure shows the sample between quartz plates.

Equipment must meet specific requirements. As deformation temperature can amount to 1000C, diffusion of impurity may occur and chemical reactions may run on surface of the samples. Thus, deformation process should be made possible in vacuum or under action of protective gas. Moreover, a rapid cooling of samples should be provided after deformation in order to detect their actual configuration at the end of deformation. Cooling speed of samples reaches $100^0 C/\min$.The vacuum diaphragm helps to part the combustion chamber from the sample very rapidly. So it’s possible to cool the sample down within a couple of minutes. The cooling process can run at applied loads and that helps to prevent the relaxation of samples. The achievable cooling speed is sufficient to freeze configuration of dislocations but, however, there’s little hope that partial annealing of defects during the cooling process can be totally avoided.

The value of deformation has been obtained by measurement of piston way. In order to measure deformation of samples more precisely the sample-free toughness of all equipment has been determined. It can be determined during measurement by control program. Temperature is regulated by a thermoelement, which is placed inside the combustion chamber.

Pressure bars consist of aluminoxide ceramics and are able to withstand required force. Silica glass discs are found between the puncheon and the sample. They are placed there to avoid contamination of the sample and to protect the ceramics discs. Measurement schedule is the following. First, the press puncheon approaches the sample until dynamometer detects a weak force (40N). At such a force the sample can be placed precisely in superposition. Attainment thermal equilibrium can be traced in course of thermal stretching. If changes in length of the sample are not registered anymore (i.e. there’s thermal equilibrium), we can proceed directly to the deformation. Experiments have been conducted in dynamic regime, i.e. the deformation of the sample runs at a constant speed during the whole process. Once the specified value of final deformation has been achieved, the combustion chamber turns off and the sample is cooled. After the cooling is completed, the sample is taken out of the mount.

4.4 Positron annihilation spectroscopy method

In positron annihilation spectroscopy experiments NaCl mineral salt is used as a source of positrons. The source is wrapped in a $1.5\mu m.$-thick aluminium foil. As a result of β^+ disintegration of ^{22}Na isotope a positron and a $\gamma-$quantum with 1.28MeV are born. The positron penetrating into the sample annihilates. The result is a new $\gamma-$quantum with the energy of 0.51MeV is born.

The main idea of the positron lifetime determining method is to measure the speed of delayed $\gamma-\gamma$ coincidences between of $\gamma-$quanta with the energy of 1.28MeV (nuclear $\gamma-$quanta) and annihilation $\gamma-$quanta with the energy of 0.51MeV. To register $\gamma-$quanta two detectors are used. One is designed to register the moment of positron birth in the source (this is achieved by registering nuclear $\gamma-$quantum), the other – to register the moment of positron annihilation (this is achieved by registering annihilation $\gamma-$quantum). Birth and annihilation of positrons are identified by the energy of $\gamma-$quanta with help of a discriminator of equal parts. Time interval between the beginning and the end of signals (between birth and annihilation of a positron) is time of delay which is converted by means of “time-amplitude” converter to a impulse with voltage amplitude proportionate to time of delay. Spectrum of impulse is registered by a multichannel analyzer.

Positron annihilation processes occur not only into the tested GaAs sample but also in the proper source of positrons and in the foil. It had been found out [Sta96] that there are three positron lifetime components for annihilation of positrons in the source and the foil. The first component ((365 ± 15)ps) forms due to annihilation in the salt, the second ((165 ± 3)ps) – due to annihilation in the foil. The third component $((2 \pm 0.5) ns)$ due to annihilation of positronium that formed in the salt [Mog95]. This components must be delete from the positron lifetime spectrum as they have nothing to do with the GaAs sample positron annihilation processes. That’s why an experiment with a non-deformed sample should be conducted.

Positron lifetime in a reference sample (non-deformed and without defects) is 230ps [Geb 2000] – that is so because positrons annihilate with electrons of the lattice (bulk life time). The power of source is chosen so that at any moment of time there’s only one positron in the sample. As the value τ_p of positron lifetime in the sample has the order of $10^2 \, ps$, radioactivity A of the source must meet this criterion: $A\tau_p < 1$. Hence, $A < 10^{10}$ acts per second that is $A < 10^{10} Bq$. In experiments radioactivity of the source has been $(1 \div 1.5) \times 10^6 Bq$.

From 3×10^6 to 3.6×10^6 acts of annihilation have been registered in every experiment for more or less precise decomposition of spectra. Computer program “Lifspecfit” has been used to analyze spectra [Pus78]. We should dwell on one problem connected with decomposition of spectra. To ensure splitting of two components it is necessary that they differ in lifetime at least by 30ps [Som96]. Otherwise they both blend.

5. Results of Deformation Experiments

Two important things have been considered when conducting experiments. On the one hand, it has been necessary to get samples deformed in a specific way in order to put them to the test of positron lifetime spectroscopy later. On the other hand, deformation experiments have been aimed at determining such values as rate of stress indicator, activation energy of plastic deformation, hardening coefficient, which are used to characterize deformation mechanism. The first requirement places certain restrictions on parameters of deformation. We tried to choose them to identify defects with concentration within area of sensitivity of the positron lifetime spectroscopy method. Defects can form only then when dislocations become active on more than one slip plane (see chapter 2). That's why the present paper treated samples that have been subject to deformation in the [110] direction (complex dislocation glide orientation). Dislocations glide there in four slip systems (see appendix A).

5.1 Doped gallium arsenide

Fig. 5.1 shows deformation curves of tellurium-doped GaAs samples with electrons concentration of $n = 5.0 \times 10^{17} cm^{-3}$. Samples have been deformed in [110] direction at different deformation temperature T and different strain rate $\dot{\varepsilon}$.
Fig. 5.1 information lets us think that in all cases there's no overt liquidity area (except the experiment with $T = 950^0 C$ and $\dot{\varepsilon} = 2.27 \times 10^{-5} s^{-1}$, where liquidity stage is seen in the area of $\varepsilon \approx (0.1 \div 0.5)\%$). For $T = 800^0 C$ (at every $\dot{\varepsilon}$ value), $T = 900^0 C$ (at $\dot{\varepsilon} = 2.28 \times 10^{-4} s^{-1}$, and $\dot{\varepsilon} = 1.08 \times 10^{-4} s^{-1}$) and $T = 950^0 C$ (at $\dot{\varepsilon} = 2.3 \times 10^{-4} s^{-1}$) deformation curves have a convex bend.

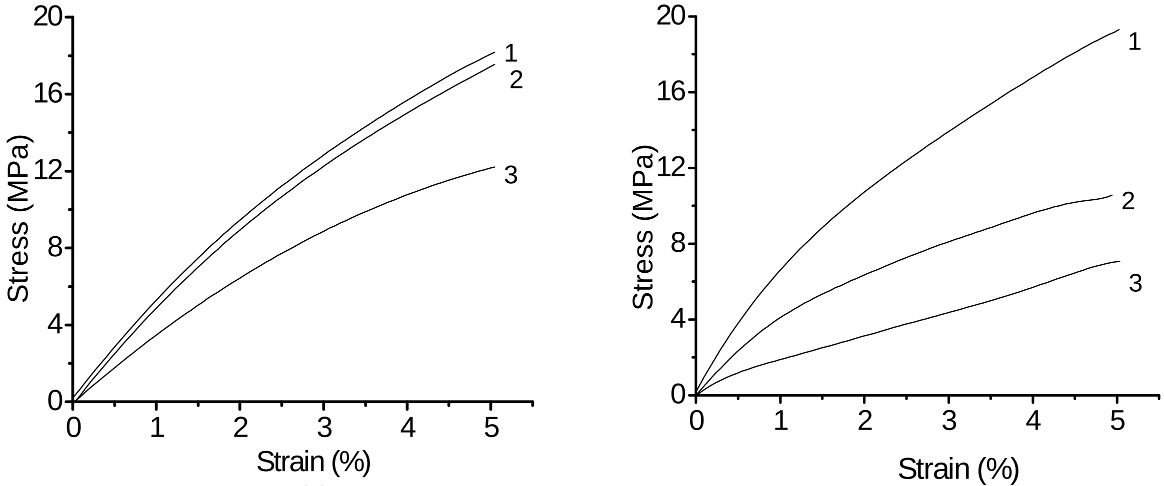

(a)

(b)

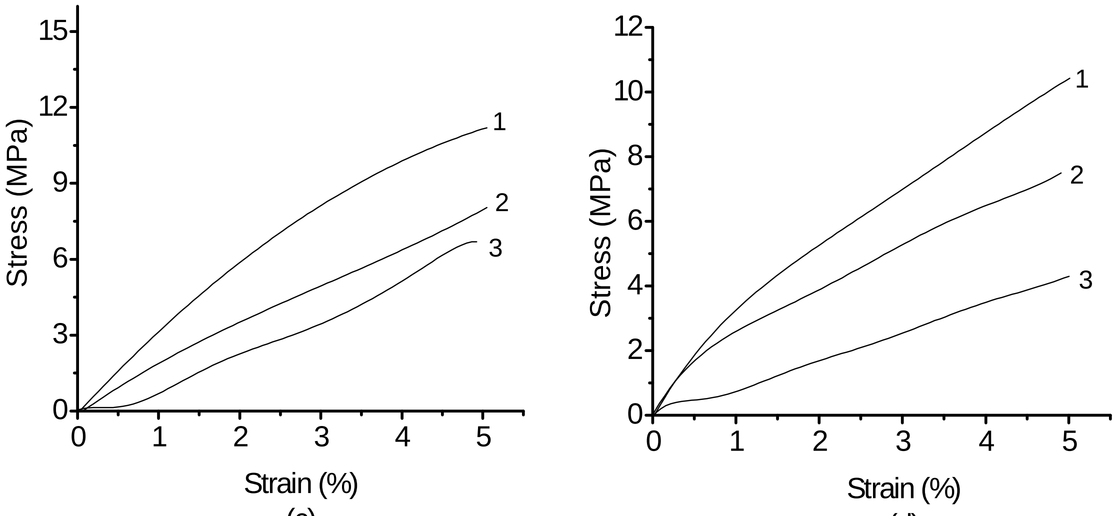

(c) (d)

Fig. 5.1:GaAs:Te deformation curves in [110] direction at different values of T and $\dot{\varepsilon}$.

(a) $T = 800^0 C$ 1) $\dot{\varepsilon} = 2.23\times10^{-4} s^{-1}$, 2) $\dot{\varepsilon} = 1.06\times10^{-4} s^{-1}$, 3) $\dot{\varepsilon} = 2.27\times10^{-5} s^{-1}$.

(b) $T = 900^0 C$ 1) $\dot{\varepsilon} = 2.28\times10^{-4} s^{-1}$ 2) $\dot{\varepsilon} = 1.08\times10^{-4} s^{-1}$, 3) $\dot{\varepsilon} = 2.26\times10^{-5} s^{-1}$.

(c) $T = 950^0 C$ 1) $\dot{\varepsilon} = 2.3\times10^{-4} s^{-1}$, 2) $\dot{\varepsilon} = 1.0\times10^{-4} s^{-1}$, 3) $\dot{\varepsilon} = 2.27\times10^{-5} s^{-1}$.

(d) $T = 1000^0 C$ 1) $\dot{\varepsilon} = 2.3\times10^{-4} s^{-1}$, 2) $\dot{\varepsilon} = 1.0\times10^{-4} s^{-1}$, 3) $\dot{\varepsilon} = 2.27\times10^{-5} s^{-1}$.

The explanation is that these samples experience initiation of cross slip processes very early due to high stress. This leads, on the one hand, to increase in concentration of mobile dislocations, and, on the other hand, to increase in concentration of tree-like dislocations. The first factor leads to reduction in the hardening coefficient, the latter – to its increase. These factors' impact on each other leads to dependence of the hardening coefficient on the value of ε. For these cases there's no phase of glide (phase I).

Tables 5.1, 5.2, 5.3 contain values of ε at which this or that phase of plastic deformation could be observed.

Table 5.1: values of ε for GaAs samples have been deformed in the [110] direction.

$T_{def} = 900^0 C$	I	II	III	IV	V
$\dot{\varepsilon} \approx 2{,}3\times10^{-4} s^{-1}$	—	—	—	—	—
$\dot{\varepsilon} \approx 1{,}0\times10^{-4} s^{-1}$	—	—	—	—	—
$\dot{\varepsilon} \approx 2{,}3\times10^{-5} s^{-1}$	$\varepsilon \approx 1\% \div 4\%$	$\varepsilon \geq 4\%$	—	—	—

Table 5.2

$T_{def} = 950^0 C$	I	II	III	IV	V
$\dot{\varepsilon} \approx 2{,}3 \times 10^{-4} s^{-1}$	—	—	—	—	—
$\dot{\varepsilon} \approx 1{,}0 \times 10^{-4} s^{-1}$	$\varepsilon \approx 1{,}7\% \div 4{,}5\%$	$\varepsilon \geq 4{,}5\%$	—	—	—
$\dot{\varepsilon} \approx 2{,}3 \times 10^{-5} s^{-1}$	$\varepsilon \approx 0{,}5\% \div 0{,}8\%$	$\varepsilon \approx 1\% \div 2\%$	$\varepsilon \approx 2\% \div 3{,}5\%$	$\varepsilon \geq 3{,}5\%$	—

Table 5.3

$T_{def} = 1000^0 C$	I	II	III	IV	V
$\dot{\varepsilon} \approx 2{,}3 \times 10^{-4} s^{-1}$	$\varepsilon \geq 1{,}5\%$	—	—	—	—
$\dot{\varepsilon} \approx 1{,}0 \times 10^{-4} s^{-1}$	$\varepsilon \approx 1\% \div 2{,}5\%$	$\varepsilon \approx 2{,}5\% \div 4\%$	$\varepsilon \geq 4\%$	—	—
$\dot{\varepsilon} \approx 2{,}3 \times 10^{-5} s^{-1}$	$\varepsilon \approx 0{,}5\% \div 1\%$	$\varepsilon \approx 1\% \div 1{,}7\%$	$\varepsilon \approx 2\% \div 2{,}5\%$	$\varepsilon \geq 2{,}5\%$	—

It's clear from the above analysis of experimental data that in the considered value intervals of T and $\dot{\varepsilon}$:

1. Number of regions of plastic deformation increases with increasing of T_{def} and (or) with decreasing of $\dot{\varepsilon}$.
2. The value of ε at which this or that phase begins decreases with increase of T_{def} and (or) with decrease of $\dot{\varepsilon}$.

In [Hub98] for [110] direction deformed GaAs it was observed that:

1. Number of phases of a plastic deformation increases with decreases of $\dot{\varepsilon}$ $(T = 600^0 C)$ when undoped GaAs is being deformed.
2. The value of ε at which the glide phase begins decreases if $\dot{\varepsilon}$ is decreased for undoped GaAs $(T = 400^0 C)$, for zinc-doped GaAs $(T = 400^0 C)$, for tellurium-doped GaAs $(T = 500^0 C)$. The value of ε decreases if there's increase of T_{def} $T = 400^0 C \div 600^0 C)$ for undoped GaAs.

Increase of plastic deformation phases viewed in experiments as a result of increase of a sample's temperature is because if we increase T, processes that run on this or that phase will reveal themselves at lower stresses in samples.

Processes responsible for origination of this or that phase run at certain velocities. Let, for instance, a process run in the strain interval $\varepsilon_1 \div \varepsilon_2$. If, under experimental conditions, the value of $\dot{\varepsilon}$ is chosen so that the time interval during which the deformation of the sample changes from ε_1 to ε_2, is significantly lower than the usual required time on this phase, then at this $\dot{\varepsilon}$ the phase is not be seen. That means that reduction of $\dot{\varepsilon}$ leads to increase in number of plastic deformation phases viewed in the experiment.

The observed dependence of ε value (at which this or that plastic deformation phase begins) on T and $\dot{\varepsilon}$ can be qualitatively explained for the case of the glide phase (phase I) the following way. In the glide phase dislocations moves relatively free passing the Peierls potential (see chapter 2.2). Movement of dislocations velocity can be obtained from (2.15) where activation energy U of movement of dislocations should be taken as the Peierls potential (2.3). This is, however, true for the case of phase of glide only because on other phases of plastic deformation activation energy of movement of dislocations is of a different nature and isn't directly connected with the Peierls potential. The Peierls potential value is determined by the crystal condition before deformation and doesn't change during the glide phase. If we assume that all samples are identical before deformation then we may think that the Peierls potential value is the same for all the samples of a single ingot and is constant during the glide phase. It results from (2.15) that the value of dislocation velocity is determined by crystal temperature and stress in the slip plane of a dislocation. Increase of T gives the same value of dislocation velocity at lower σ and, hence, at lower τ (as $\sigma = \tau m_s$). Hence, if we increase T dislocations will move more rapidly on an earlier phase of deformation. The $\dot{\varepsilon}$ value is not apparent in (2.15). From the Orowan equation (2.11) and $\dot{\gamma} = \dot{\varepsilon}/m_s$ results that $\upsilon = \dot{\varepsilon}/(m_s b N_{d_m})$. Hence if we reduce $\dot{\varepsilon}$ the velocity υ will also reduce. However, concentration of mobile dislocations N_{d_m} on glide phase slightly changes. According to (2.15) lower movement of dislocations velocity is due to reduction of σ (T=const) and, hence, reduction of τ. So at lower $\dot{\varepsilon}$ shear will occur on an earlier deformation phase.

Experimental results shown on fig. 5.1 prove that in studied value intervals of T and $\dot{\varepsilon}$ hardening coefficients on the glide phase θ_I and on the hardening phases θ_{II}, θ_{IV} reduce with increase in temperature of the sample and (or) with decrease of $\dot{\varepsilon}(\theta = \partial\tau/\partial\varepsilon)$. Table 5.4 contain values of hardening coefficient θ at different deformation temperatures and strain rate $\dot{\varepsilon}$.

The values of θ have been obtained from:

$$\theta = \frac{\tau(\varepsilon_2)-\tau(\varepsilon_1)}{\varepsilon_2-\varepsilon_1}\left\{1 \pm \left[\left(\frac{\varepsilon_2+\varepsilon_1}{\varepsilon_2-\varepsilon_1}\right)\left(\frac{\delta\Delta l}{\Delta l}\right)+\left(\frac{\delta\tau(\varepsilon_2)+\delta\tau(\varepsilon_1)}{\tau(\varepsilon_2)-\tau(\varepsilon_1)}\right)\right]\right\}. \quad (5.1)$$

Here $\delta\Delta l/\Delta l -$ is the relative error when measuring change in length of the sample during deformation; $\delta\tau(\varepsilon_2)$ and $\delta\tau(\varepsilon_1) -$ are absolute errors for τ at $\varepsilon = \varepsilon_2$ and $\varepsilon = \varepsilon_1$ respectively.

Table 5.4: values of hardening coefficient θ.

T_{def}	$\dot{\varepsilon} \approx 2,3\times10^{-4}s^{-1}$	$\dot{\varepsilon} \approx 1,0\times10^{-4}s^{-1}$	$\dot{\varepsilon} \approx 2,3\times10^{-5}s^{-1}$
800^0C	—	—	—
900^0C	—	—	$\theta_I = 127 \pm 1,5 MPa$ $\theta_{II} = 200 \pm 3 MPa$
950^0C	—	$\theta_I = 141 \pm 1,7 MPa$ $\theta_{II} = 180 \pm 2,8 MPa$	$\theta_I = 52 \pm 0,5 MPa$ $\theta_{II} = 174 \pm 2,2 MPa$ $\theta_{VI} = 215 \pm 5,2 MPa$
1000^0C	$\theta_I = 171 \pm 2,6 MPa$	$\theta_I = 120 \pm 3,6 MPa$ $\theta_{II} = 151 \pm 4,5 MPa$	$\theta_I = 30 \pm 0,6 MPa$ $\theta_{II} = 96 \pm 1,6 MPa$ $\theta_{VI} = 110 \pm 1,8 MPa$

[Hub98] came to the following conclusions:

1. There's no systematic dependence of θ_I on $\dot{\varepsilon}$ in the interval $\dot{\varepsilon} = 1.6\times10^{-4}s^{-1} \div 1.6\times10^{-5}s^{-1}$ in an undoped GaAs at $T = 400^0C$. The author of [Hub98] explains strong variations of values of θ_I for samples on the glide phase by dependence of θ_I on hard controllable parameters such as value of dislocations density before deformation and plane-parallelism of edge surfaces of samples.
2. There is decrease of θ_I with decrease of $\dot{\varepsilon}$ in the interval of $\dot{\varepsilon} = 2.7\times10^{-4}s^{-1} \div 1.7\times10^{-5}s^{-1}$ in a zinc-doped GaAs at $T = 400^0C$ ($p = 2.5\times10^{18}cm^{-3}$).
3. The value of θ_I is constant in the interval of $\dot{\varepsilon} = 3\times10^{-5}s^{-1} \div 8\times10^{-6}s^{-1}$ in a tellurium-doped GaAs at $T = 500^0C$ ($n = 2.5\times10^{18}cm^{-3}$).

However, there's no information about the dependence of θ_I on T at a constant $\dot{\varepsilon}$ in [Hub 98]. Still, the experimental data obtained in the paper help us to get the following for an undoped GaAs: at $T = 400^0C$ and $\dot{\varepsilon} = 1.6\times10^{-5}s^{-1}\theta_I \approx 840MPa$, at $\mathrm{T} = 600^0\mathrm{C}$ and $\dot{\varepsilon} = 1.2\times10^{-5}s^{-1}\theta_I \approx 360MPa$. So θ_I reduces with increase in temperature.

Using the above mentioned experimental data for values of θ_I obtained in the present paper and in [Hub98] it's hard to say for sure whether there is systematic dependence of θ_I on T and $\dot{\varepsilon}$. Let us show that, most likely, there is systematic dependence of θ_I on T and

$\dot{\varepsilon}$ for identical samples: the hardening coefficient on the glide phase reduces with increase in T and (or) with decrease of $\dot{\varepsilon}$. Taking into consideration (2.10) we get:

$$\theta = \frac{\partial \tau}{\partial \varepsilon} = \frac{\alpha \mu b}{2N_d^{1/2}} \frac{\partial N_d}{\partial \varepsilon} = \frac{\alpha \mu b N_d^{1/2}}{2}\left(\frac{1}{N_d}\frac{\partial N_d}{\partial \varepsilon}\right) = \frac{\alpha \mu b N_d^{1/2}}{2}\left(\frac{\partial \ln N_d}{\partial \varepsilon}\right).$$

Hence,

$$\theta \sim N_d^{1/2}\left(\frac{\partial \ln N_d}{\partial \varepsilon}\right). \qquad (5.2)$$

Dislocation density changes slightly on the phase of glide. That's why in (5.2) the value of N_d can be determined on the initial period of the slip phase at $\varepsilon = \varepsilon_{ly}$ (ε_{ly} – is the value of ε, at which $\tau = \tau_{ly}$). Then we get:

$$\theta_I \sim N_d^{1/2}(\varepsilon = \varepsilon_{ly})\left(\frac{\partial \ln N_d}{\partial \varepsilon}\right)_{\varepsilon=\varepsilon_{ly}}.$$

As at $\varepsilon = \varepsilon_{ly}$ $N_d^{1/2} \sim \tau_{ly}$ (according to (2.10)), then

$$\theta_I \sim \tau_{ly}\left(\frac{\partial \ln N_d}{\partial \varepsilon}\right)_{\varepsilon=\varepsilon_{ly}}. \qquad (5.3)$$

Taking into account (2.19) and (5.3) we arrive at:

$$\theta_I \sim (\dot{\varepsilon})^{\frac{1}{2+m}} \exp\left[\frac{U}{(2+m)k_B T}\right]\left(\frac{\partial \ln N_d}{\partial \varepsilon}\right)_{\varepsilon=\varepsilon_{ly}}. \qquad (5.4)$$

Change of dislocation density on the glide phase is small at any $\dot{\varepsilon}$ and T. Hence, we may suppose that here on this phase $\partial \ln N_d / \partial \varepsilon$ depend little not only on ε, but also on $\dot{\varepsilon}$ and T (still, the dependence of N_d on $\dot{\varepsilon}$ and T can be strong). Then from (5.4) we get:

$$\theta_I \sim (\dot{\varepsilon})^{\frac{1}{2+m}} \exp\left[\frac{U}{(2+m)k_B T}\right]. \qquad (5.5)$$

It results from (5.5) that θ_I reduces with increase of T and (or) decrease of $\dot{\varepsilon}$. This statement agrees with experimental data obtained in the present paper. What is to findings of [Hub98] stated above, they do not contradict the conclusion about the dependence of θ_I

on $\dot{\varepsilon}$ and T with the exception of data for dependence of θ_I on $\dot{\varepsilon}$ for an undoped GaAs at deformation temperature of samples $T = 400^0 C$ (there's no systematic dependence of θ_I from $\dot{\varepsilon}$ here). It has been said above that the author of [Hub98] relates the absence of systematic dependence of θ_I on $\dot{\varepsilon},$ in particular, to unequal dislocation density in samples before deformation. Under the experimental conditions [Hub98] values of τ_{ly} (values of $\tau,$ at which the region of easy glide begins) are in the interval of $(40 \div 70) MPa.$ It results from (2.10) that at these τ dislocation density is $N_d \sim (10^8 \div 10^9) cm^{-2} (\alpha \sim 1, \mu \approx 5.0 \times 10^{10} Pa$ [Sch82], $b = \left(\sqrt{2}/2\right)a$, where the constant of the GaAs lattice is $a \approx 5.69 \times 10^{-8} cm$ [Gri91]). To ensure that the initial dislocation density N_{d_0} (dislocation density before deformation) influences the value of N_d on the glide phase the following must be true: $N_{d_o} \sim (10^8 \div 10^9) cm^{-2}$.Typical values of the average dislocation density before deformation take, as a rule, these values: $< N_{d_0} > \sim (10^4 \div 10^5) cm^{-2}$. To ensure that the initial dislocation density in the sample is comparable to the dislocation density on the glide phase, the relative fluctuation of dislocation density $\delta N_{d_0} / < N_{d_0} >$ in a ingot should reach to almost 10^4. If this is done then fluctuations in values of the initial dislocation density in samples prepared from a single ingot may result in random dependence of θ_I on T and $\dot{\varepsilon}$ (see (5.2)).

The experimental data shown on fig. 5.1 prove that in the value interval of T and $\dot{\varepsilon}$ studied the value of τ_{ly} decreases with decrease of $\dot{\varepsilon}$ (in cases when the liquidity area cannot be clearly seen during the experiment, the value of τ_{ly} is determined the following way: a tangent is drawn from the coordinated origin to the deformation curve; then from the point where $\varepsilon = 0.2\%$ another line is drawn parallel to the tangent; the value of projection of point of intersection of this line with the deformation curve on τ axis is taken as the value of τ_{ly}). Table 5.5 contain values of τ_{ly} at different deformation temperatures and strain rate $\dot{\varepsilon}$.

Table 5.5: values of lower yield stress τ_{ly}.

T_{def}	$\dot{\varepsilon} \approx 2{,}3 \times 10^{-4} s^{-1}$	$\dot{\varepsilon} \approx 1{,}0 \times 10^{-4} s^{-1}$	$\dot{\varepsilon} \approx 2{,}3 \times 10^{-5} s^{-1}$
$800^0 C$	$\tau_{ly} \approx 11 MPa$	$\tau_{ly} \approx 8{,}2 MPa$	$\tau_{ly} \approx 5{,}6 MPa$
$900^0 C$	$\tau_{ly} \approx 8 MPa$	$\tau_{ly} \approx 4{,}3 MPa$	$\tau_{ly} \approx 1{,}5 MPa$
$950^0 C$	$\tau_{ly} \approx 7 MPa$	$\tau_{ly} \approx 3 MPa$	$\tau_{ly} \approx 0{,}15 MPa$
$1000^0 C$	$\tau_{ly} \approx 3{,}4 MPa$	$\tau_{ly} \approx 2{,}2 MPa$	$\tau_{ly} \approx 0{,}5 MPa$

Such a dependence of τ_{ly} from $\dot{\varepsilon}$ results from (2.19), too. According to (2.19), the value of τ_{ly} decreases with increase of T (if $\dot{\varepsilon}$ is constant). The information given above confirms that this very dependence of τ_{ly} on T is observed for $\dot{\varepsilon} = 1.0 \times 10^{-4} s^{-1}$ and $\dot{\varepsilon} = 2.2 \times 10^{-4} s^{-1}$. For $\dot{\varepsilon} = 2.3 \times 10^{-5} s^{-1}$, τ_{ly} decreases with increase of T in temperature interval $800^0\mathrm{C} \div 950^0\mathrm{C}$ and increases with increase of T in temperature interval $950^0\mathrm{C} \div 1000^0\mathrm{C}$. The growth of τ_{ly} if T is increased can be qualitatively explained the following way. For $950^0\mathrm{C} \div 1000^0\mathrm{C}$ and $\dot{\varepsilon} = 2.3 \times 10^{-5} s^{-1}$ $\tau_{ly} \approx (0.15 \div 0.5) MPa$. This τ_{ly} value agrees with values of dislocation density $N_d \sim (10^4 \div 10^5) cm^{-2}$ (according to (2.10)). These values of dislocation density are comparable to the dislocation density in the sample before deformation. Hence, insignificant fluctuations in values of dislocation density in samples before deformation may lead to ruining of systematic dependence of τ_{ly} on T (see (2.10)). It should be noted here that at bigger values of T and lower values of $\dot{\varepsilon}$, when $\tau_{ly} \sim 1.0 MPa$ (and lower), it’s possible that not only systematic dependence of τ_{ly} on T will be ruined, but also that from $\dot{\varepsilon}$ because of great influence of the initial dislocation density (dislocation density before deformation) on values of τ_{ly}.

Let’s mention that systematic dependence of τ_{ly} on T and $\dot{\varepsilon}$ was obtained in [Hub98] as well: τ_{ly} reduces with increase of T and (or) with decrease of $\dot{\varepsilon}$. Tables 5.6 and 5.7 contain values of $(2+m)$ and $U/2+m$ calculated using:

$$2+m = \frac{\ln(\dot{\varepsilon}_2/\dot{\varepsilon}_1)}{\ln(\tau_{ly2}/\tau_{ly1})} \left\{ 1 \pm \left[\frac{2\left(\frac{\delta \Delta l}{\Delta l} + \frac{\delta l}{l}\right) + \frac{\delta t_1}{t_1} + \frac{\delta t_2}{t_2}}{\ln(\dot{\varepsilon}_2/\dot{\varepsilon}_1)} + \frac{\frac{\delta \tau_{ly2}}{\tau_{ly2}} + \frac{\delta \tau_{ly1}}{\tau_{ly1}}}{\ln(\tau_{ly2}/\tau_{ly1})} \right] \right\}. \tag{5.6}$$

$$\frac{U}{2+m} = \frac{\ln(\tau_{ly1}/\tau_{ly2})}{\left(\frac{1}{k_B T_1} - \frac{1}{k_B T_2}\right)} \left\{ 1 \pm \frac{\frac{\delta \tau_{ly1}}{\tau_{ly1}} + \frac{\delta \tau_{ly2}}{\tau_{ly2}}}{\ln(\tau_{ly1}/\tau_{ly2})} + \frac{\delta T_1 + \delta T_2}{T_2 - T_1} + \frac{\delta T_2}{T_2} + \frac{\delta T_1}{T_1} \right\}. \tag{5.7}$$

Here $\delta t -$ is the absolute error time of experiment; $t_1, t_2 -$ are experiment duration times for $\dot{\varepsilon}_1, \dot{\varepsilon}_2$ accordingly; $\delta \tau_{ly} -$ is the absolute error of τ_{ly}; $\delta T -$ is the absolute error of T.

Table 5.6: values of (2+m).

T_{def}, $\dot{\varepsilon}(s^{-1})$.	$2.3 \times 10^{-5} \div 1.0 \times 10^{-4}$	$1.0 \times 10^{-4} \div 2.3 \times 10^{-4}$
$800^0 C$	3.9 ± 0.1	2.9 ± 0.1
$900^0 C$	1.4 ± 0.03	1.3 ± 0.05
$950^0 C$	0.5 ± 0.01	1.0 ± 0.03
$1000^0 C$	1.0 ± 0.02	2.0 ± 0.07

Table 5.7: Values of U/(2+m),eV.

$T_{def}, \dot{\varepsilon}(s^{-1})$.	2.3×10^{-5}	1.0×10^{-4}	2.3×10^{-4}
$800^0C\div900^0C$	1.43 ± 0.03	0.69 ± 0.02	0.35 ± 0.01
$900^0C\div950^0C$	5.4 ± 0.16	0.87 ± 0.04	0.32 ± 0.02
$950^0C\div1000^0C$	—	0.83 ± 0.04	1.87 ± 0.09

For dislocations moving in the fracture regime the rate of stress indicator for semiconductor materials takes values $m=1.0\div1.5$ [Ale68a]. Table 5.6 data prove that at the temperature of $T=800^0C$ rate of stress indicator values do not fluctuate too much from the above figure. At different deformation temperature rate of stress indicator values fluctuate significantly from the expected $m=1.0\div1.5$. So, (2.19) does not quantitatively describe the dependence of τ_{ly} on $\dot{\varepsilon}$ and T (the case when $T=800^0C$ and $\dot{\varepsilon}\approx2.3\times10^{-5}s^{-1}\div2.3\times10^{-4}s^{-1}$ is an exception). We should mention that by means of expression (2.19) we can qualitative description of the dependence of τ_{ly} on $\dot{\varepsilon}$ and T. Tables 5.6 and 5.7 show that at $T=800^0C$ the plastic deformation activation energy U value is highly dependable on the value of $\dot{\varepsilon}$:

$U\approx(1.0\pm0.07)eV$ for $\dot{\varepsilon}\approx2.3\times10^{-4}s^{-1}$,

$U\approx(5.57\pm0.26)eV$ for $\dot{\varepsilon}\approx2.3\times10^{-5}s^{-1}$.

We do not include the value of U for $T>800^0C$ here as for other T the expression (2.19) does not give a qualitative description of the dependence of τ_{ly} on T and $\dot{\varepsilon}$. Table 5.7 doesn't include the value of $U/2+m$ for $T=950^0C\div1000^0C$ and $\dot{\varepsilon}\approx2.3\times10^{-5}s^{-1}$, because at this $\dot{\varepsilon}$ in the interval of $T=950^0\div1000^0C$ there's increase of τ_{ly} with increase of T. This leads to $U/2+m$ obtaining negative value.

In [Hub98] for GaAs with tellurium impurity $(n=2.5\times10^{18}cm^{-3})$ at $T=500^0C$ and $\dot{\varepsilon}=3\times10^{-5}s^{-1}\div8\times10^{-6}s^{-1}: m+2=2.0$. As a result, the author concluded that the expression relating τ_{ly} to T and $\dot{\varepsilon}$ cannot be used to quantitative interpretation experimental data. The following conclusions can be made using the above mentioned analysis of experimental data obtained at $T=800^0C\div1000^0C$ and $\dot{\varepsilon}\approx2.3\times10^{-5}s^{-1}\div2.3\times10^{-4}s^{-1}$:

1. (2.10), (2.11), (2.19) allow us to qualitatively describe certain regularities observed in experiments:

a) the increase in number of plastic deformation phases at increase deformation temperature T and (or) after reduction of $\dot{\varepsilon}$;

b) decrease in the value of ε, at which the beginning of this or that plastic deformation phase is seen, if T is increased and (or) $\dot{\varepsilon}$ is decreased;

c) reduction of the hardening coefficient θ_I on the glide phase if T is increased and (or) $\dot{\varepsilon}$ is decreased;

d) reduction of τ_{ly} if T is increased and (or) $\dot{\varepsilon}$ is decreased;

2. (2.19) can be applied to measure the rate of stress indicator value and the value of the activation energy at deformation temperature of $T = 800^0 C$ and can’t be applied when $T > 800^0 C$.

The no-best plane-parallelism of side surfaces of samples explains inclinations of deformation curves one away from the other in the elasticity area at different experimental conditions (at different T and $\dot{\varepsilon}$). Too divergent deformation curves let us assume that corresponding mechanisms of deformation differ one from another and that dislocation movement mechanisms are different, too. Studies of dislocation movement have shown [Yon89], that doping of GaAs samples has a significant impact over movement of dislocations velocity. At the same time, doping process influences different dislocation types in a different manner. This means that change in concentration of doping impurity may result in rise of the activation energy and the rate of stress indicator of dislocation movement in a particular dislocation type, and may reduce the activation energy and the rate of stress indicator for other dislocations. As concentration of dislocations of this or that dislocation type may change at different experimental conditions (if changing T and $\dot{\varepsilon}$), values of the activation energy and the rate of stress indicator of dislocation movement may also change. This results, in particular, from the experimental data shown in tables 5.6 and 5.7. This serves to qualitatively explain that deformation curves are not parallel at different experimental conditions (beginning from the first phase).

It has been said above, that (2.19) can be used to determine the rate of stress indicator and the activation energy of dislocation movement for samples subject to deformation at $T = 800^0 C$. Using U and m (see Tables 5.6 and 5.7) we can quantitative determine by (2.15) the dependence of the movement of dislocations velocity on parameters that specify experimental conditions. Speaking about the movement of dislocations velocity we mean an averaged value because there are different types of dislocations with different velocities in a crystal. But there is a problem. As velocity is exponentially dependable on the activation energy, then the slightest error when determining U and (or) insignificant change of U when experimental conditions change will lead to grave errors for calculating velocity. There’s no such a problem, if U does not depend on the experimental conditions and may be precisely evaluated. So it’s better to have such an expression for velocity that doesn’t include exponential dependence of υ on U. For this purpose we may proceed as follows. From (2.19) we get:

$$(\tau_{ly})^{m+2} = C^{(m+2)}\,\dot{\varepsilon}\exp(\frac{U}{k_B T}).$$

Using this and (2.15) we arrive at:

$$\upsilon \cdot (\tau_{ly})^{m+2} = C^{(m+2)} \cdot B \cdot \dot{\varepsilon} \cdot \sigma^{m} . \tag{5.8}$$

Using $\sigma = \tau m_s$ and (5.8) we have:

$$\upsilon \cdot (\tau_{ly})^{m+2} = C^{(m+2)} m_s^m \cdot B \cdot \dot{\varepsilon} \cdot \tau^{m} . \tag{5.9}$$

Let analyze the dependence of υ on $\dot{\varepsilon}$ and T at such values of τ that correspond to the end of the liquidity phase, that is at $\tau \approx \tau_{ly}$. In case there is the glide phase in the experiment, $\tau \approx \tau_{ly}$ corresponds to the very beginning of the glide phase. From (5.9) we get (taking into consideration $\tau \approx \tau_{ly}$):

$$\upsilon = \frac{\dot{\varepsilon}}{\tau_{ly}^{2}} B \cdot C^{(m+2)} \cdot m_s^m .$$

If the rate of stress indicator changes insignificantly at altering experimental conditions (table 5.6 data prove that at $T = 800^0 C$ and $\dot{\varepsilon} \approx 2.3 \times 10^{-5} s^{-1} \div 2.3 \times 10^{-4} s^{-1}$ the value of $m + 2$ changes from 3.9 to 2.9), we may roughly assume:

$$\upsilon \sim \frac{\dot{\varepsilon}}{\tau_{ly}^{2}} . \tag{5.10}$$

Fig. 5.2 represents the dependence of the movement of dislocations relative velocity at the end of the liquidity area on $\dot{\varepsilon}$ for GaAs: Te samples ($n = 5 \times 10^{17} cm^{-3}$), deformed in the [110] direction at $T = 800^0 C$. It has been calculated using (5.10) (the experimental values of τ_{ly} have been shown earlier in this paper). This proves that increase of $\dot{\varepsilon}$ gives an increase in velocity. At the same time, increase of $\dot{\varepsilon}$ results in slower increase in the dislocations velocity.

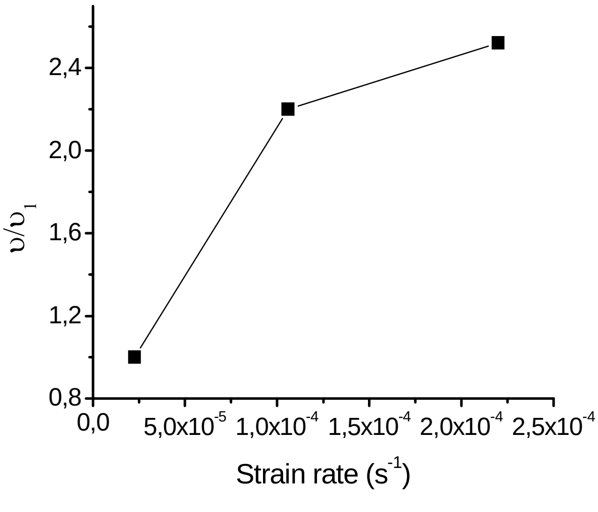

Fig. 5.2:calculated dependence of movement of dislocations relative velocity at the end of the liquidity area on $\dot{\varepsilon}$ for GaAs: Te samples deformed in the [110] direction at $T = 800^0 C$ (υ_1 – is the velocity of dislocations at $\dot{\varepsilon} = 2.27 \times 10^{-5} s^{-1}$).

Fig. 5.3 represents calculated dependence of movement of dislocations relative velocity at the end of the liquidity area on $\dot{\varepsilon}$ for undoped GaAs samples deformed in the [110] direction at $T = 500^0 C$. To effect calculations experimental data have been taken from [Hub98]: $\tau_{ly} = 18 MPa$ at $\dot{\varepsilon} = 3.26 \times 10^{-3} s^{-1}$, $\tau_{ly} = 13 MPa$ at $\dot{\varepsilon} = 1.5 \times 10^{-3} s^{-1}$, $\tau_{ly} = 8.0 MPa$ at $\dot{\varepsilon} = 3.0 \times 10^{-4} s^{-1}$, $\tau_{ly} = 5.0 MPa$ at $\dot{\varepsilon} = 7.4 \times 10^{-5} s^{-1}$, $\tau_{ly} = 2.5 MPa$ at $\dot{\varepsilon} = 2.88 \times 10^{-5} s^{-1}$. Using the findings of the experiments the [Hub98] author have found out that $m + 2 = 3{,}8$. This allows us to consider that for these experiments the expression (2.19) may be used to determine the rate of stress indicator and the movement of dislocations activation energy. Hence, (5.10) can be used to analyze the dependence of movement of dislocations velocity on $\dot{\varepsilon}$.

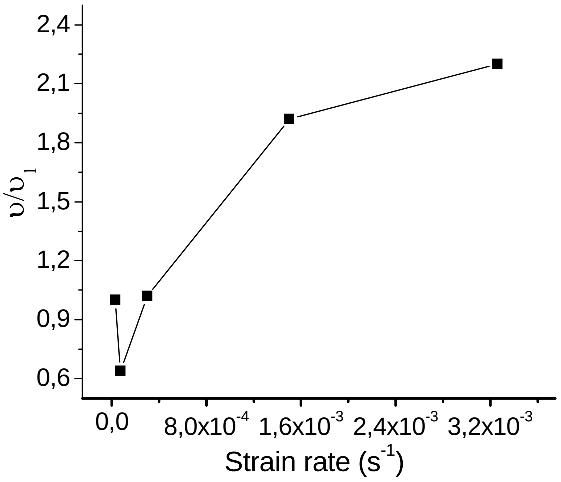

Fig. 5.3:calculated dependence of movement of dislocations relative velocity at the end of the liquidity area on $\dot{\varepsilon}$ for undoped GaAs samples. The samples have been deformed in the [110] direction at $T = 500^0 C$ (υ_1 – is the velocity of dislocations at $\dot{\varepsilon} = 2.88 \times 10^{-5} s^{-1}$).

Here we observe non-monotonous dependence of movement of dislocations velocity on $\dot{\varepsilon}$. Fig. 5.4 depicts calculated dependence of movement of dislocations relative velocity at the end of the liquidity area on $\dot{\varepsilon}$ for undoped GaAs samples deformed in the [110] direction at $T = 400^0 C$. To effect calculations experimental data have been taken from [Hub98]: $\tau_{ly} = 65 MPa$ at $\dot{\varepsilon} = 1.6 \times 10^{-4} s^{-1}$, $\tau_{ly} = 48 MPa$ at $\dot{\varepsilon} = 3.3 \times 10^{-5} s^{-1}$, $\tau_{ly} = 39 MPa$ at $\dot{\varepsilon} = 1.6 \times 10^{-5} s^{-1}$. Here, as well, (2.19) may be used to determine the rate of stress indicator and the movement of dislocations activation energy and, hence, (5.10) may be used to analyze the dependence of movement of dislocations velocity on $\dot{\varepsilon}$. Here we have a monotonous increase in velocity if $\dot{\varepsilon}$ is increased.

Fig. $5.2 \div 5.4$ results prove that the movement of dislocations velocity at the end of the liquidity area (or in the beginning of the glide phase in case it can be clearly seen) is a non-monotonous $\dot{\varepsilon}$ function that has its minimum. However, change of $\dot{\varepsilon}$ in a large spectrum gives a slight change in velocity.

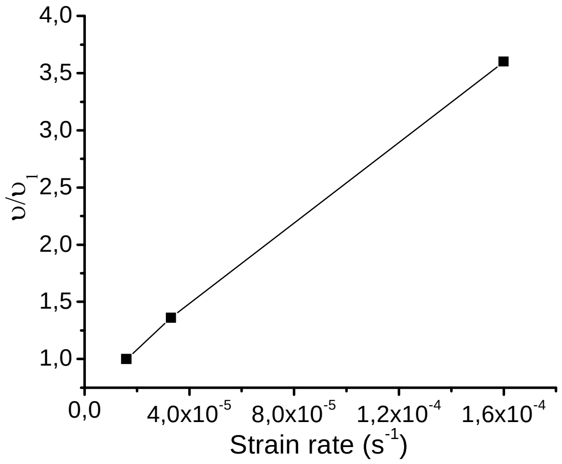

Fig. 5.4: Calculated dependence of movement of dislocations relative velocity at the end of the liquidity area on $\dot{\varepsilon}$ for undoped GaAs samples. Samples have been deformed in the [110] direction at $T = 400^0 C$ ($\upsilon_1 -$is the velocity of dislocations at $\dot{\varepsilon} = 1.6 \times 10^{-5} s^{-1}$).

From (5.10) it is clear that the velocity of dislocations at the end of the liquidity area increases monotonously with increase of deformation temperature T (it has been said that τ_{ly} goes down if T rises at $\dot{\varepsilon} = const$ $\upsilon \sim 1/\tau_{ly}^2,$). As there is exponential dependence of τ_{ly} on T (see (2.19)), we may expect a very strong dependence of velocity of dislocations on T. Experimental data provided by [Hub98] and discussed above when analyzing the dependence of υ on $\dot{\varepsilon}$ (fig. 5.3, 5.4), and (5.10) (at $\dot{\varepsilon} = const$) testify that increase in deformation temperature T from 400^0C to 500^0C in an undoped GaAs sample results in a 370-time rise of the velocity of dislocations at the end of the liquidity area ($\tau_{ly} \approx 2.5MPa$ at $T = 500^0 C,$ $\tau_{ly} \approx 48MPa$ at $T = 400^0 C,$ and in both cases $\dot{\varepsilon} \approx 3 \times 10^{-5} s^{-1}$).

Using $\dot{\gamma} = \dot{\varepsilon}/m_s$ and (2.11), (5.10) for density N_{dm} of mobile dislocations at the end of the liquidity area we get:

$$N_{dm} \sim \tau_{ly}^2. \qquad (5.11)$$

From (5.11) results that the concentration of mobile dislocations at the end of the liquidity area decreases monotonously when there's increase in deformation temperature and (or) decrease of $\dot{\varepsilon}$ (for the case of complete density of dislocations N_d this results from (2.10)).

It should be said, that conclusions with respect to the dependence of υ and N_{dm} on $\dot{\varepsilon}$ and T at the end of the liquidity area refer to cases when (2.19) quantitative describes the dependence of τ_{ly} from T and $\dot{\varepsilon}$. These conclusions require an experimental examination further on.

Fig. 5.5 shows deformation curves of a tellurium-doped GaAs samples ($n = 5 \times 10^{17} cm^{-3}$), at different values of T and at different total values of ε_f. These data, together with the experimental data shown on fig. 5.1(a) and on fig. 5.1(b) (curves 1), will be used later on to analyze the impact that the values of ε_f have over concentration of defects.

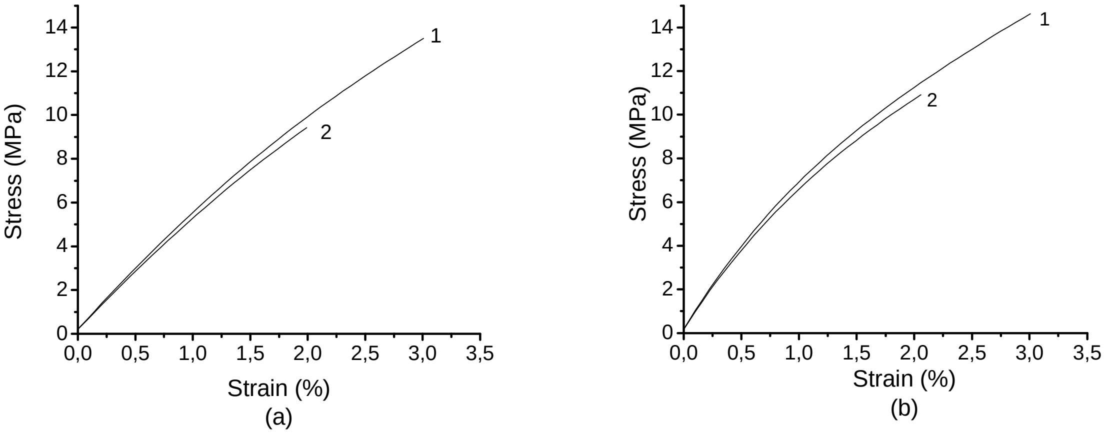

Fig. 5.5: GaAs: Te deformation curves in the [110] direction at different values of temperature T ($\dot{\varepsilon} = 2.3\times10^{-4}s^{-1}$). The samples have been deformed until two different total values (ε_f) were achieved: ε_f = 3% (curves 1) and ε_f = 2% (curves 2). (a) $T = 800^0 C$. (b) $T = 900^0 C$.

It has been said that when deforming GaAs samples in the interval of $T = (800 \div 1000)^0 C$, certain regularities can be seen in the experimental data. The same regularities are evident, too, when deforming GaAs samples at significantly lower deformation temperature. Fig. 5.6 and fig. 5.7 represent deformation curves of tellurium-doped GaAs samples ($n = 5\times10^{17} cm^{-3}$), at deformation temperatures $T = 20^0 C, 300^0 C, 600^0 C$. At $T = 20^0 C$ and $300^0 C$ we can see the liquidity and the glide phases (at $T = 20^0 C$ we see only the beginning of the glide phase). At $T = 600^0 C$ we can see the glide and the hardening phases. In case then $\dot{\varepsilon} = 2.23\times10^{-6}s^{-1}$, the liquidity phase is observed.

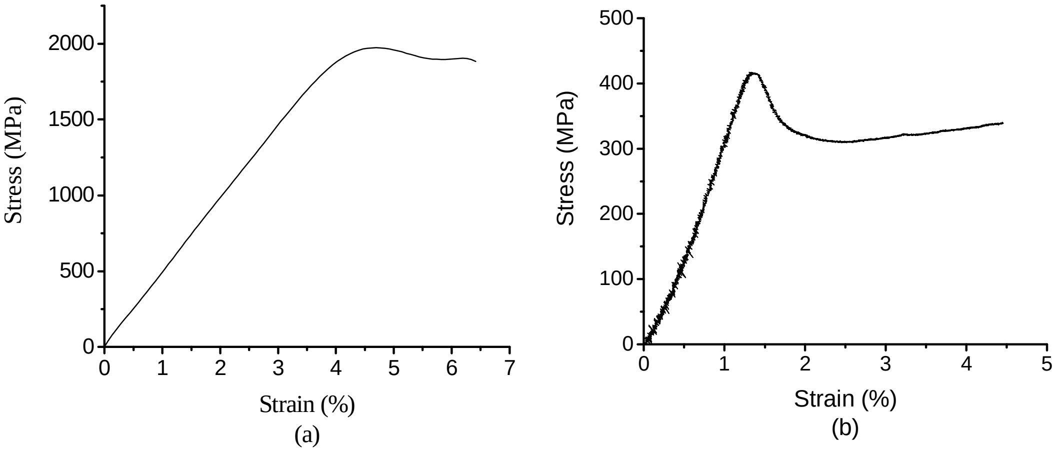

Fig. 5.6: Deformation curves of GaAs: Te in the [110] direction at different values of temperature T ($\dot{\varepsilon} = 2.23\times10^{-5}s^{-1}$). $(a) T = 20^0 C$. (b) $T = 300^0 C$.

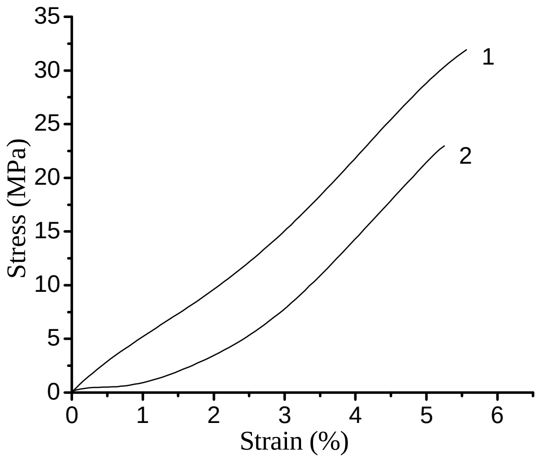

Fig. 5.7: Deformation curves of GaAs: Te in the [110] direction at different values of $\dot{\varepsilon}$ $(T = 600^0 C)$

1) $\dot{\varepsilon} = 2.23\times10^{-5}s^{-1}$ 2) $\dot{\varepsilon} = 2.23\times10^{-6}s^{-1}$.

Experimental data shown on figures 5.6(a), 5.6(b), 5.7 prove that:

1. The number of phases observed is growing with increase of T and (or) with decrease of $\dot{\varepsilon}$.
2. The values of ε, at which the glide phase (stage I) and the hardening phase (stage II) begin, reduce with increase of T and (or) with decrease of $\dot{\varepsilon}$ (stage I can be seen for $T = 20^0 C$ and $\dot{\varepsilon} = 2.23\times10^{-5}s^{-1}$ (in the value area of $\varepsilon \geq 6\%$), for $T = 300^0 C$ and $\dot{\varepsilon} = 2.23\times10^{-5}s^{-1}$ (in the value area of $\varepsilon \geq 2{,}5\%$), for $T = 600^0 C$ at two values of $\dot{\varepsilon}$: $\dot{\varepsilon} = 2.23\times10^{-5}s^{-1}$ (in the area $\varepsilon = (1.5\div2.5)\%$) and $\dot{\varepsilon} = 2.23\times10^{-6}s^{-1}$ (in the area $\varepsilon = (1\div2)\%$; stage II can be seen at $T = 600^0 C$ for two values of $\dot{\varepsilon}$: $\dot{\varepsilon} = 2.23\times10^{-5}s^{-1}$ (in the area $\varepsilon \geq 2{,}5\%$) and $\dot{\varepsilon} = 2.23\times10^{-6}s^{-1}$ (in the area $\varepsilon \geq 2\%$)).
3. The values of hardening coefficients θ_I and θ_{II} reduce with increase of T and (or) with decrease of $\dot{\varepsilon}$ (for $\dot{\varepsilon} = 2.23\times10^{-5}s^{-1}$ at $T = 300^0 C$ $\theta_I \approx (2000\pm65)MPa$, at $T = 600^0 C$ $\theta_I \approx (430\pm11)MPa$ and $\theta_{II} \approx (510\pm15)MPa$; for $\dot{\varepsilon} = 2.23\times10^{-6}s^{-1}$ at $T = 600^0 C$ $\theta_I \approx (230\pm7.0)MPa$ and $\theta_{II} \approx (320\pm9.0)MPa$).
4. The values of τ_{ly} reduce with increase of T and (or) with decrease of $\dot{\varepsilon}$ (for $\dot{\varepsilon} = 2.23\times10^{-5}s^{-1}$at $T = 20^0 C$ $\tau_{ly} \approx 1850MPa$, at $T = 300^0 C$ $\tau_{ly} \approx 320MPa$, at $T = 600^0 C$ $\tau_{ly} \approx 6.5MPa$; for $\dot{\varepsilon} = 2.23\times10^{-6}s^{-1}$ at $T = 600^0 C$ $\tau_{ly} \approx 2.0MPa$).

   For $T = 600^0 C$ in the interval $\dot{\varepsilon} = (2.23\times10^{-6}\div2.23\times10^{-5})s^{-1}$ $2+m \approx 1.9\pm0.03$.

   For $\dot{\varepsilon} = 2.23\times10^{-5}s^{-1}$ in the interval $T = (20\div300)^0 C$ $U/2+m \approx (0.1\pm0.01)eV$ and in the interval $T = (300\div600)^0 C$ $U/(2+m) \approx (0.53\pm0.04)eV$.

Here rate of stress indicator values differ a lot from expected values. This signifies that in doped GaAs movement of dislocations is considerably influenced by doping impurity atoms (and their accumulations). [Yon89] shows that doping of a GaAs has its impact on the movement of dislocations velocity, i.e. has its impact on the value of rate of stress indicator and the movement of dislocations activation energy. This may be caused by doping impurity atoms interaction with the nucleus of dislocations (as has been proposed in [Sie93b] for a GaAs with impurity of indium). The author of [Hub98] also found out that the rate of stress indicator value differs a lot form the expected values for a tellurium-doped GaAs ($n = 2.5\times10^{18} cm^{-3}$) and a zinc-doped GaAs ($p = 2.5\times10^{18} cm^{-3}$),. In case of tellurium we have $2 + m = 2$, in case of zinc $m + 2 = 1.8 \pm 0.2$. Experimental data for doped GaAs have been obtained in [Hub98] for two values of deformation temperature: $T = 400^0 C$ (a zinc-doped GaAs), $T = 500^0 C$ (a tellurium-doped GaAs). The experiments of the present paper gave results for a wide range of temperatures.

Conclusions

Experimental data for deformation of tellurium-doped GaAs samples ($n = 5\times10^{17} cm^{-3}$), deformed in the [110] direction at temperatures $T = 20^0 C, 300^0 C, 600^0 C, 800^0 C, 900^0 C, 950^0 C, 1000^0 C$ and with strain rate $\dot{\varepsilon} \approx 2.2\times10^{-6} s^{-1}$, $2.2\times10^{-5} s^{-1}, 1.0\times10^{-4} s^{-1}, 2.2\times10^{-4} s^{-1}$, prove that:

1.When increasing T and (or) decreasing $\dot{\varepsilon}$ we observe:

a) more phases of plastic deformation (when these phases can be clearly viewed);

b) lower stretching (deformation) values (ε) at which this or that plastic deformation phase begins;

c) lower values of hardening coefficients θ_I on the glide phase and lower values of hardening coefficients θ_{II} and θ_{IV} on hardening phases;

d) decreasing values of lower yield stress τ_{ly}.

2. Equations (2.10),(2.11),(2.15) and (2.19) serve to qualitatively explain the above considered regularities (except dependencies of θ_{II} and θ_{IV} on T and $\dot{\varepsilon}$).

3. The rate of stress indicator value is highly dependable on T and $\dot{\varepsilon}$ (there's no regularity) and is a lot different from the values of $m = 1.0 \div 1.5$ (that are usual for movement of dislocations in the fracture regime on the glide phase). The case for $T = 800^0 C$, where $m + 2 = 2.9 \div 3.9$, is an exception.

4. Equation (2.19) cannot be applied to determine the values of rate of stress indicator and of movement of dislocations activation energy (excluding the case when $T = 800^0 C$), but can be applied to qualitatively describe the dependence of τ_{ly} from T and $\dot{\varepsilon}$.

6. Experimental Data for Lifetime of Positrons

The chapter deals with experimental data for values of lifetime of positron of the tellurium-doped GaAs being previously subject to deformation (one can find deformation experiments results in the previous chapter). The data were collected after studying the dependence of temperature and stretching (deformation) velocity on positron lifetime, as well as the dependence of total value of deformation on it.

6.1Influence of deformation temperature

Fig. **6**.1 represents data on the dependence of positron lifetime in the GaAs: Te ($n = 5\times10^{17} cm^{-3}$) on measurement temperature. Samples had been previously subject to deformation at 800^0C,$900^0 C$,$1000^0 C$. Positron lifetime has been measured according to the method described in chapter 3 (see (3.44), (3.52 $\div$ 3.58) expressions).
Results of the three-component adaptation of positron lifetime spectrum are given for 800^0C and 1000^0C . The two-component adaptation results are given for 900^0C .

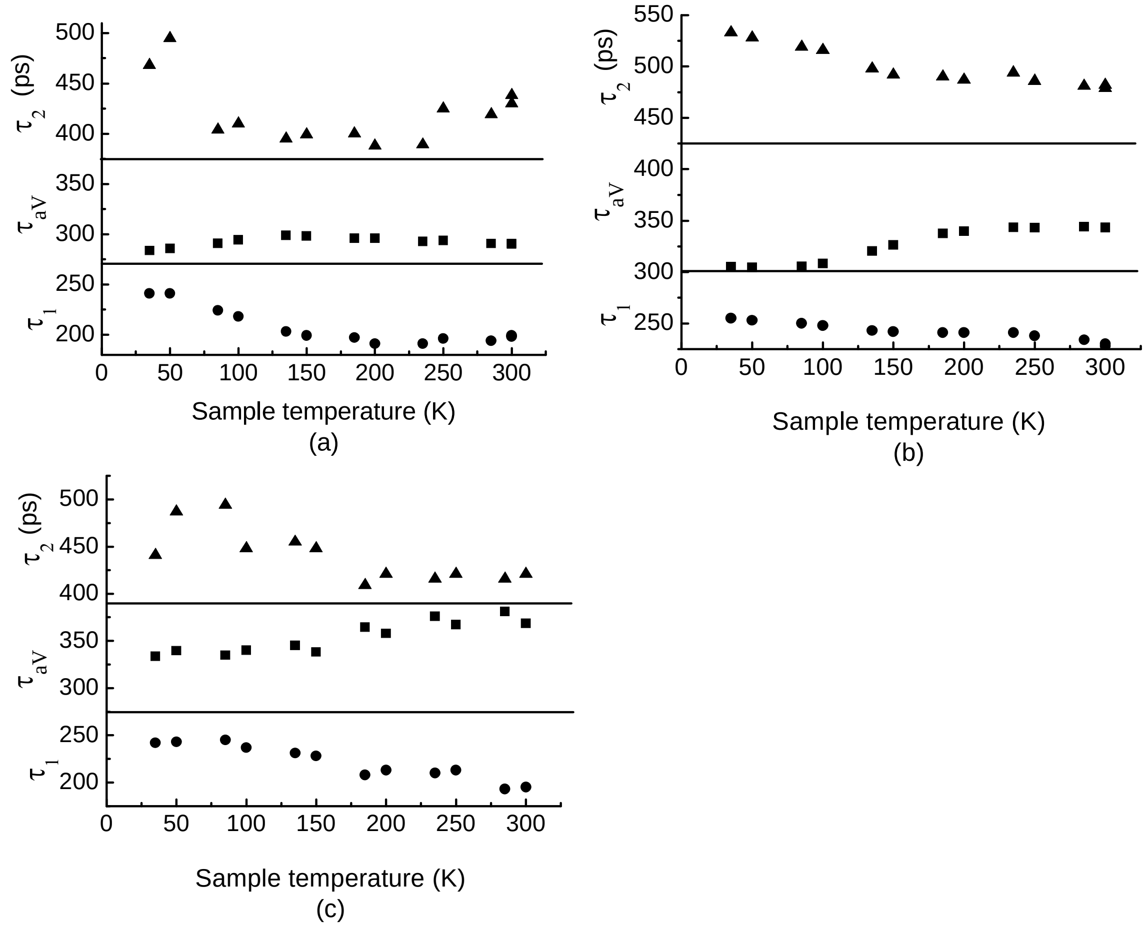

(a)

(b)

(c)

Fig. 6.1: Dependence of positron lifetime in the GaAs: Te on temperature of measurement. Samples have been deformed in the [110] direction. a) deformation temperature is $800^0\mathrm{C}$, strain rate – $2.23\times10^{-4}s^{-1}$, total stretching value – 5%. (b) deformation temperature is $900^0\mathrm{C}$, strain rate – $2.28\times10^{-4}s^{-1}$, total stretching value – 5%. (c) deformation temperature is $1000^0\mathrm{C}$, strain rate – $2.3\times10^{-4}s^{-1}$, total stretching value – 5%. The upper part – lifetime due to annihilation of positron with electron of defects (τ_2).

The middle part of figures represents average lifetime (τ_{aV}); the lower – inner positron lifetime (τ_1) (inner lifetime is 230ps in the basic sample).

For $800^0\mathrm{C},900^0C,1000^0C$ spectra adaptation is firm in temperature intervals of $85K \le T \le 300K$, $285K < T \le 300K$, $135K \le T \le 300K$ accordingly, as at these temperatures $\tau_1 \le 230ps$. Here we'll analyse to changes in positron lifetime within these very intervals of measurement temperature where spectra adaptation is firm.

It results from the information on the fig. 6.1 that the avarage positron lifetime is more than in the basic material (230ps). Samples deformed at 800^0C, have $\tau_{aV} \approx (291\div299)ps$ (increase of T from $85K$ to $135K$ gives increase of τ_{aV} which decreases later if we continue to increase T), if deformation temperature is 900^0C, $\tau_{aV} \approx 343ps$ (in the interval of $285K \le T \le 300K$), if temperature is 1000^0C, $\tau_{aV} \approx (338\div384)ps$ (measurement temperature increase from $135K$ to $300K$ results in fluctuations of τ_{aV} values and, however, τ_{aV} does up). This testifies that open volume defects are formed during deformation.

The first lifetime component τ_1 (τ_1, which reduces with increase of measurement temperature for all three cases) is connected with the process of positron annihilation with lattice electrons and with processes of capture of positrons on defects (see expressions (3.52)) but has no connection with positron annihilation with electrons of defects. That's why information on τ_1 values does not allow us to draw conclusions about the nature of defects.

The second lifetime component (τ_2) is fully connected with processes of positron annihilation on defects (see (3.52) expressions). At temperature of deformation equal to $900^0\mathrm{C}$ τ_2 changes from $(479\pm3)ps$ to $(481\pm3)ps$.

At $1000^0\mathrm{C}$ τ_2 decreases (taking into consideration errors occurring when calculating the magnitude) with increase of measurement temperature from $(455\pm17)ps$ to $(412\pm6)ps$. Taking temperature equal to 800^0C, we note that τ_2 largely fluctuates. However, if we take into account the error when calculating the magnitude, we'll have an approximately constant τ_2 of $(403\pm22)ps$, in the interval $85K \le T \le 285K$, and at $T = 300K$ $\tau_2 \approx (438\pm9)ps$.

From the literature data we know that lifetime of positrons in the GaAs influenced by annihilation on accumulations of vacancies is 460ps [Kra94], $(500\div600)ps$ [Pog84]. Most likely, at deformation temperatures of $800^0C,900^0C,1000^0C$ τ_2 is connected with positrons annihilation on accumulations of vacancies. Decreases τ_1 with increase of measurement temperature because the trapping rate of positron by accumulations of vacancies increases (in this case defects do not totally absorb positrons when $\lambda_b << k_d$, and, hence, the value of concentration of defects can be measured here). Decrease of τ_2

with increase of measurement temperature when deformation temperature is 1000^0C (when deformation temperature is 800^0C or 900^0C τ_2 slightly depends on measurement temperature within the limits of error) can be qualitatively explained if assumed that there are accumulations with a different number of vacancies in a sample. In accumulations with different number of vacancies lifetime of positron is also different. Reading [Hub98], one will find calculated dependence of lifetime of positrons at annihilation on accumulation of vacancies on the number of such vacancies (according to a method explained in [Pus83]). Hence, increase of number of vacancies in an accumulation results is increase lifetime of positrons which comes closer to the saturation value (approximately 500ps). If higher measurement temperature produces more annihilation acts on accumulations with a smaller amount of vacancies (with shorter lifetime), the τ_2 parameter will decrease.

When deformation temperature is 1000^0C decrease of τ_1 and τ_2 with increase of measurement temperature does not result in lower τ_{aV}, as intensity of the second component rises (from 0.302 to 0.598). This is the reason why the product of $I_2\tau_2$, grows increasing τ_{aV}.

When deformation temperature is 800^0C I_2 increases (from 0.273 to 0.384) if measuring temperature is increased from $85K$ to $200K$, and decreases (from 0.384 to 0.349) if we continue to increase temperature. This leads to initial increase of τ_{aV} and then to its decrease (with increase of measurement temperature).

The data shown on fig. 6.1 prove that:

1. Higher deformation temperature average positron lifetime increases, and results in initial increase of τ_1 and τ_2 (in the value interval of deformation temperature from 800^0C to 900^0C), and in subsequent decrease of their values (in the interval of $900^0C \div 1000^0C$).
2. There is one type of deep positron traps – accumulation of vacancies. Most likely, value of concentration of monovacancies (of monovacancy complex) in these samples doesn’t reach the sensitivity limits of the positron annihilation spectroscopy method.
3. Higher deformation temperature gives rise to the number of vacancies contained into an accumulation (in the temperature interval from $800^0\mathrm{C}$ to $900^0\mathrm{C}$), but then decrease (in the interval from $900^0\mathrm{C}$ to $1000^0\mathrm{C}$).

[Hub98] showed that not only accumulations of vacancies could be seen in an undoped GaAs samples deformed in the [110] direction at $400^0\mathrm{C}$ $(\dot{\varepsilon} \approx 1.6\times10^{-5}s^{-1})$, $600^0\mathrm{C}(\dot{\varepsilon} \approx 6.9\times10^{-5}s^{-1})$ and $800^0C(\dot{\varepsilon} \approx 3.3\times10^{-3}s^{-1}$ and $\dot{\varepsilon} \approx 4.8\times10^{-5}s^{-1})$, but also monovacancies (or monovacancy complexes). The situation is the same in the GaAs: Te $(n \approx 2.5\times10^{18}cm^{-3})$, deformed in the [110] direction at $500^0\mathrm{C}(\dot{\varepsilon} \approx 2.5\times10^{-5}s^{-1})$ [Hub 98].

The experimental data of the present paper and findings of [Hub98] prove that if we change deformation temperature and strain rate the set of deep traps types also changes. Further explanations also serve to prove this fact.

Fig. 6.2 represents how lifetime of positrons in GaAs:Te samples depends on measurement temperature. Samples have been subjected to deformation in the [110] direction at $200^0\mathrm{C}, 300^0C$. Results of the three-component adaptation spectrum are given for samples deformed at $200^0\mathrm{C}$ and $300^0\mathrm{C}$. At 200^0C and 300^0C adaptation of spectra is firm for every measurement temperature (here $\tau_1 < 230ps$). Fig. 6.2 data prove that average positron lifetime is higher in the basic material: in samples deformed at 200^0C, τ_{aV} slightly decreases (from 239ps to 235ps) if measurement temperature is increased, and in samples deformed at 300^0C, τ_{aV} slightly increases (from 239ps to 243ps).

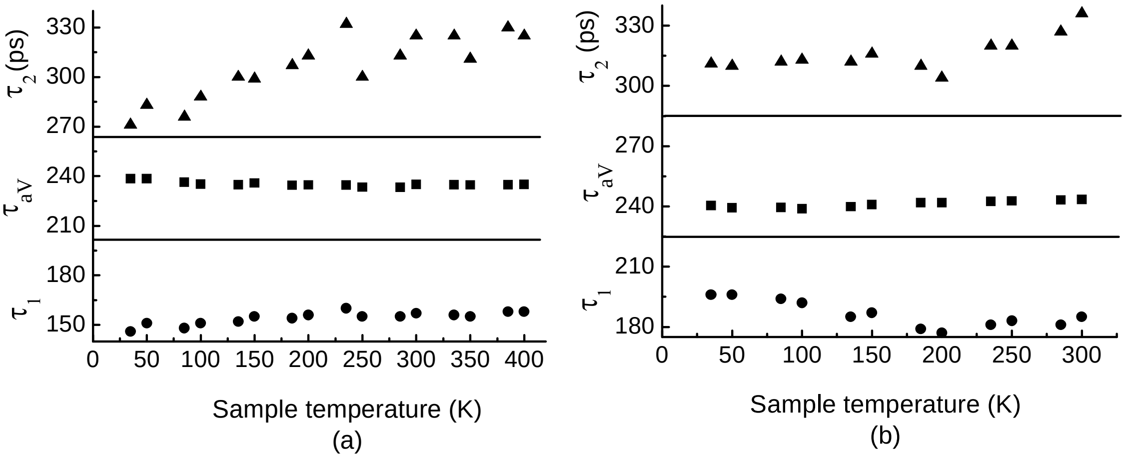

Fig. 6.2: Dependence of positron lifetime in GaAs: Te on measurement temperature strain rate $2.23 \times 10^{-5} s^{-1}$. (a) deformation temperature is $200^0 C$; total stretching value is 5%. (b) deformation temperature is 300^0C; total stretching value is 4.5%.

When the temperature is 200^0C τ_1 is almost independable on measurement temparature within error. When it is 300^0C τ_1 decreases with increase of measurement temperature from $35K$ to $150K$, but then goes up.

At deformation temperature equal to 300^0C τ_2 is within error and is slightly depend on measurement temparature. The average τ_2 in the temperature interval amount 318ps. At deformation temperature equal to 200^0C a wide range of τ_2 values is viewed (even if we take into account the error when determining the magnitude as $\pm(8 \div 12)ps$). Here τ_2 changes within $(276 \div 339)ps$.

Other papers studied argue that positron lifetime in the GaAs conditional by the annihilation on monovacancies or on complexes containing a monovacancy (e.g. on acceptor complex Te_{As} V_{Ga}), lies within the interval from 255ps [Kra94] to 297ps [Cor 90]. Lifetime determined by annihilation on divacancies is 332ps [Geb99] (calculated value). At deformation temperature equal to 300^0C the value of τ_2 (318ps – see above) is notably higher than the values of τ_2 typical for annihilation on monovacancies and(or) complexes containing a monovacancy ($255ps \div 297ps$). At the same time τ_2 is significantly lower than the lifetime connected with annihilation on divacancies. It's natural to suppose that τ_2 is a mixed component connected with the positron annihilation on divacancies and monovacancies (or on complexes containing a monovacancy). At a deformation temperature of 200^0C τ_2, supposedly, is a mixed component as well connected with annihilation of positrons on divacancies and monovacancies (complexes containing a monovacancy).Unlike deformation at 800^0C,$900^0 C$ and $1000^0 C$, here in this case (at temperatures running at $200^0 C$ and $300^0 C$) deep positron traps are represented by monovacancies (monovacancy complexes) and divacancies but not accumulations of vacancies.

6.2 Influence of stretching velocity

Fig. 6.3 shows data for dependence of positron lifetime in the GaAs: Te on measurement temperature. Samples have been deformed at $800^0 C$ and $900^0 C$ at lower stretching velocities in comparison with the cases treated in the previous chapter. Fig. 6.3(a) represents results for the three-component adaptation spectrum, and fig. 6.3 (b) – results for the two-component adaptation spectrum.

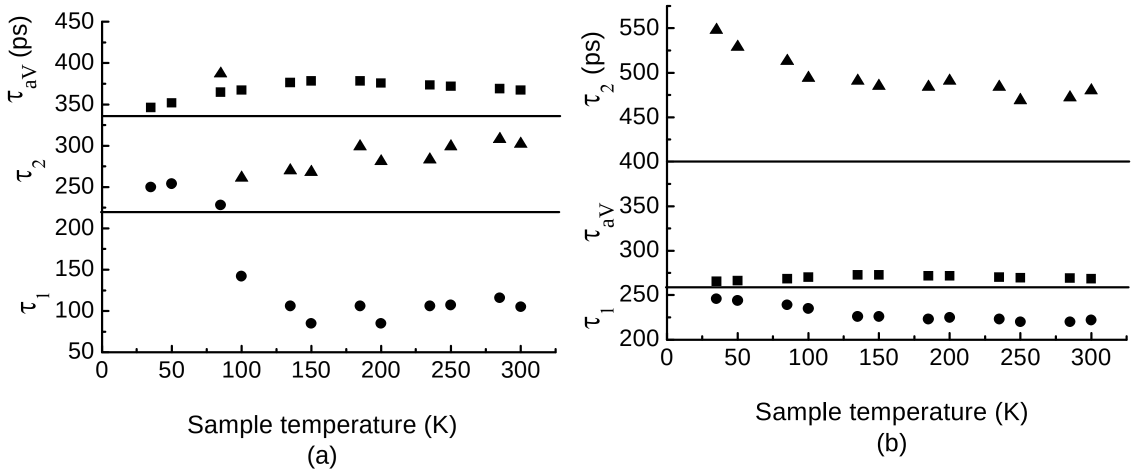

Fig. 6.3: Dependence of lifetime of positrons in the GaAs:Te on measurement temperature. Samples have been deformed in the [110] direction. (a) Deformation temperature – $800^0 C$, strain rate – $1.06\times10^{-4} s^{-1}$, total stretching value – 5%. (b) Deformation temperature – $900^0 C$, strain rate – $1.08\times10^{-4} s^{-1}$, total deformation value – 5%.

It results from the data on fig. 6.3(a) that if we increase measurement temperature (the interval of temperature values from $100K$ to $300K$ is considered as $\tau_1 < 230 ps$) τ_2 will also increase (taking into account the error when determining τ_2). It's natural to suppose that $\tau_2 -$ is a mixed component connected with positron annihilation on divacancies and monovacancies (or on complexes containing a monovacancy). So different positron traps can be seen in samples deformed at 800^0C,: if strain rate is $2.23\times10^{-4} s^{-1}$ then accumulations of vacancies are traps (see data on fig. 6.1(a)), if strain rate is $1.06\times10^{-4} s^{-1}$ then point defects – monovacancies are traps (or complexes containing a monovacancy) and a divacancy). This weights in favour of the conclusion (see chapter 6.1) that changes in deformation temperature and stretching velocity produce changes in sets of deep traps of positrons.

The data on the fig. 6.3(b) let us believe that in the value interval of measurement temperature from $135K$ to $300K$ (where $\tau_1 < 230 ps$) τ_{aV} and τ_1 change only a little. Values of τ_2 mean that accumulations of vacancies are traps for positrons in this case. Comparing data on fig. 6.1(b) and fig. 6.3(b) (comparison can only be made in the value interval of measurement temperature from $285K$ to $300K$ because that which is shown on fig. 6.1(b) is true in this very interval) we have: changes in strain rate from $2.28\times10^{-4} s^{-1}$ to $1.08\times10^{-4} s^{-1}$ do not alter type of positron traps; the number of vacancies in an accumulation is always the same because in both cases the values of τ_2 are very close taking into account errors occurring when determining them.

6.3 Influence of total stretching value

Fig. 6.4 represents data for dependence of positron lifetime on measurement temperature in GaAs:Te samples deformed at $800^0 C$.

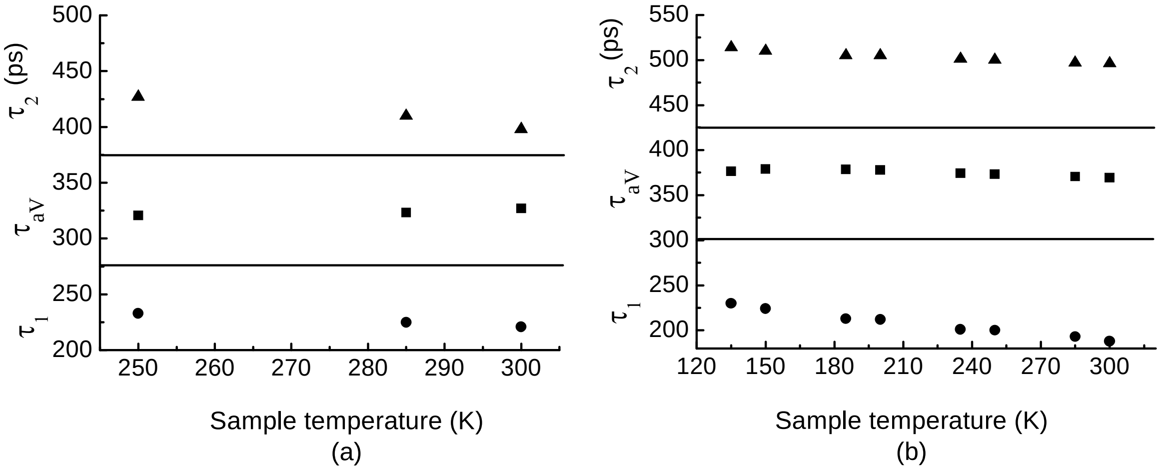

Fig. 6.4: Dependence of positron lifetime on measurement temperature in the GaAs:Te. Samples have been deformed in the [110] direction at $800^0 C$, strain rate being equal to $2.23 \times 10^{-4} s^{-1}$. (a) Total stretching value is 2%.(b) Total stretching value is 3%.

Total stretching values have been taken as 2% and 3%. Fig. 6.4(a) shows results for the three-component adaptation spectrum, fig. 6.4(b) shows results for the two-component adaptation spectrum. Experimental data prove that in both cases accumulations of vacancies are traps for positrons. Comparing results on fig. 6.1(a) and on fig. 6.4 we conclude that increase in the rate of stretching (from 2% to 3%) gives initial incrementation to the number of vacancies in accumulations which, subsequently, decreases (if we continue to change stretching value from 3% to 5%).

Fig. 6.5 represents data for dependence of positron lifetime on measurement temperature in GaAs: Te samples deformed at 900^0C. The adaptation is the three-component. Total stretching value is 3%. The experimental data prove that accumulations of vacancies are traps for positrons in this case. Experimental data for total stretching value of 2% are also evidence of the fact that accumulations of vacancies are traps as here, for example, at measurement temperature is equal to $300K$ $\tau_2 = (481 \pm 7) ps$). If deformation temperature is $900^0 C$ the number of vacancies in an accumulation, first, reduces when stretching value is increased from 2% to 3%, and then rises (when stretching value is increased from 3% to 5%).

If we compare dependence of number of vacancies in accumulations on rate of stretching for deformation temperatures 800^0C and $900^0 C$ we'll see that these dependencies are quite different. As the stretching process progresses, not only changes of defect concentration occur but also restructuring of defects takes place, i.e. number of vacancies in accumulations changes.

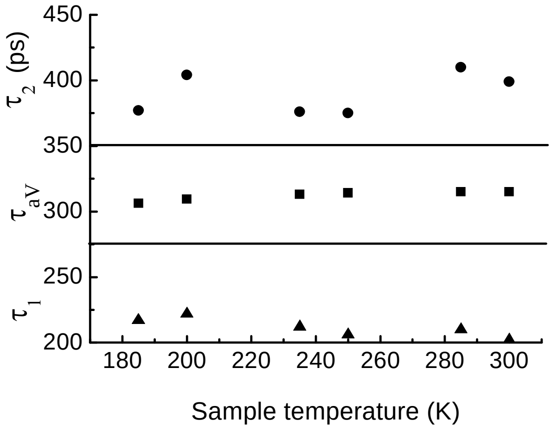

Fig. 6.5: Dependence of positron lifetime on measurement temperature in the GaAs: Te.The sample has been deformed in the [110] direction at $900^0 C$ and strain rate being equal to $2.28\times10^{-4}s^{-1}$. Total stretching value is 3%.

Fig.6.6 represents data for dependence of positron lifetime on measurement temperature in undeformed GaAs:Te. Here τ_1 and τ_2 highly different then the values of τ_1 and τ_2 in deformed samples.Therefore in deformed samples we can observe a defects that appear during the deformation process.
The error of $\tau_{1,2}$ for all experiments is $\le 5\%$.

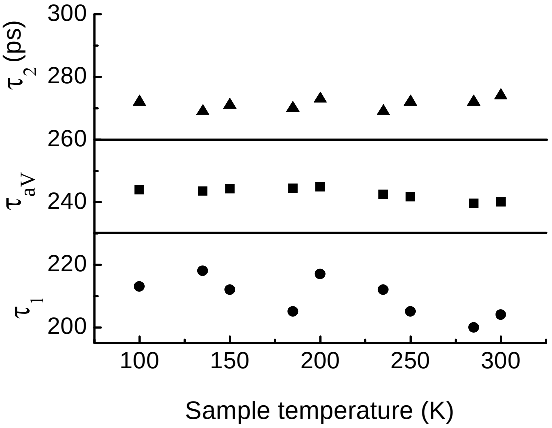

Fig. 6.6: Dependence of positron lifetime on measurement temperature in undeformed GaAs.

Mechanisms of formation of defects are treated in the next chapter.

Conclusions

1. In all samples either accumulations of vacancies or point defects – monovacancies (or complexes containing a monovacancy) or divacancies – have been detected. Both point defects and accumulations of vacancies have not been seen at the same time.
2. Changes in deformation temperature and stretching velocity produce changes in type of traps of positrons. If deformation temperature and stretching velocity reduce then formation of point defects is more preferential.
3. Changes in deformation temperature and stretching velocity produce changes in the number of vacancies that are contained in defects.
4. Higher stretching rate restructures accumulations of vacancies: the number of vacancies in accumulations changes. At this the nature of dependence of the number of vacancies in an accumulation on rate of stretching is not the same for different deformation temperatures.

7. Analysis of Results for Positrons Lifetime

This chapter relying upon experimental data for positrons lifetime analyzes the influence that deformation conditions (deformation temperature, stretching velocity, total value of deformation) exert on concentration of defects introduced in GaAs samples during deformation. Dependencies of concentration of defects on deformation experiments parameters obtained have been compared with results arising from existing models(see chapter 2.5.2).

7.1 Specific trapping coefficient of positron by defect

To determine concentration of defects one sould resort to this equation (arising from (3.43)):

$$n_d = \frac{k_d}{\gamma}, \tag{7.1}$$

where

$$\frac{1}{\gamma} = \frac{1}{\gamma_d} + \frac{1}{\gamma_{tr}}.$$

Here $n_d -$ concentration of defects; $k_d -$trapping rate of a positron by a defect; $\gamma, \gamma_d, \gamma_{tr} -$ specific trapping coefficient, coefficient of the diffusion phase of the reaction and capture phase accordingly. The value of trapping rate k_d is obtained from experimental data for positrons lifetime. Thus, to determine the value of concentration of defects n_d one must know the value of specific trapping coefficient γ, that is values γ_d and γ_{tr}.

Expressions for γ_d one can find in chapter (3.4.1): (3.21) applies when a positron interacts with a neutral point defect or with an accumulation of neutral defects with different reactions radius r_0 for point defect and accumulation of defects; (3.23) applies when a positron and a defect (a point charged defect) or an accumulation of charged defects attract; (3.24) applies when a positron and a charged defect (a point defect) or an accumulation of defects repulse.

The following cases are of practical importance:

(a) interaction between a positron and a negatively charged point defect (γ_d can be found from (3.23));

(b) interaction between a positron and a negatively charged accumulation of defects (γ_d can be found from (3.23));

(c) interaction between a positron and a neutral accumulation of defects (γ_d can be found from(3.21)). Here saying ‘point defect’ we mean a monovacancy, a divacancy or a complexes containing a monovacancy. For the case of attraction between a positron and a negatively charged vacancy γ_{tr} can be present as (see chapter 3.5): $\gamma_{tr} = A_d T^{-1/2}$, as $\gamma_{tr} \sim T^{-1/2}$ [Pus90].

Value of A_d can be defined with help of (3.69). If we assume that for any other point defects γ_{tr} can be expressed similarly A_d, in this case, is also determined by (3.69) (at this A_d values for various types of point defects are not the same). As a result, if we view the case of attraction between a positron and a point defect γ can be determined by (3.70). For the case of attraction between a positron and an accumulation of charged defects it has been shown (see (3.74)) that the reaction of interaction between the positron and the accumulation is limited, most likely, by the diffusion phase of the reaction and $\gamma \approx \gamma_d$ (γ_d is determined by (3.23)). Unfortunately, scientific papers lack evaluations for γ_{tr} for the case of interaction between a positron and a neutral accumulation, so let's take $\gamma = \gamma_d$ (γ_d is determined by (3.21)). Thus, for practically important cases the value of γ can be determined.

However, the expression (3.23) for γ_d in case of attraction between a positron and a charged defect (a point defect or an accumulation of defects) has been obtained given that the interaction energy between the positron and the defect is expressed by the Coulomb type (see (3.22), attraction is noted by the minus sign). Strictly speaking, this is true for a slightly doped or an undoped semiconductor. In the present paper experiments have been conducted with heavy doped GaAs samples. For results for values of γ_d to be used in this case as well the expression (3.23) should be modified a little which, in fact, will be done further.

If we have an doped sample in the interaction energy $U(r)$ between a positron and a charged defect we must take into account screening by free charge carriers (by electrons in this case as the n-GaAs is treated here):

$$U(r) = -\frac{Qe^2}{\varepsilon_0 r}\exp(-r/r_d), \tag{7.2}$$

where r_d – is the Debye screening radius. The expression for r_d is given by [Ans78]:

$$r_d = \left(\frac{\varepsilon_0 k_B T}{4\pi e^2 n}\right)^{1/2}, \tag{7.3}$$

where n is concentration of electrons in the conduction band. Then the equation for γ_d can be obtained by substituting (7.2) in (3.20). The integral in the right part of (3.20) cannot be calculated analytically in case $U(r)$ is determined by (7.2). Let's write down $U(r)$ as:

$$U(r) \approx -\frac{Qe^2}{\varepsilon_0 r} \text{ for } r_0 \le r < r_d$$

and (7.4)

$$U(r) \approx 0 \text{ for } R \ge r \ge r_d.$$

Then form (3.20) taking into account (7.4) we get:

$$\gamma_d = 4\pi D_+ R_{ef}, \tag{7.5}$$

where

$$R_{ef} = \left[\frac{1}{r_d} - \frac{1}{R} + \frac{\varepsilon_0 k_B T}{Qe^2} \left\{ \exp\left[\frac{U(r_d)}{k_B T} \right] - \exp\left[\frac{U(r_0)}{k_B T} \right] \right\} \right]^{-1} .$$

Taking into account that $U(r_d) = 0$ (see (7.4)) and $|U(r_0)| / k_B T >> 1$ (see chapter (3.4.1)), we get:

$$R_{ef} = \left[\frac{1}{r_d} - \frac{1}{R} + \frac{\varepsilon_0 k_B T}{Qe^2} \right]^{-1} . \qquad (7.6)$$

From (7.5) and (7.6) we have:

$$\gamma_d = 4\pi D_+ \frac{Qe^2}{\varepsilon_0 k_B T} \left[\frac{1}{1 + \frac{Qe^2}{\varepsilon_0 k_B T} (\frac{1}{r_d} - \frac{1}{R})} \right] . \qquad (7.7)$$

(7.7) and (3.23) are coincide if the expression below holds:

$$\frac{Qe^2}{\varepsilon_0 k_B T} \left| \frac{1}{r_d} - \frac{1}{R} \right| << 1. \qquad (7.8)$$

Taking into account (7.3) from (7.8) we get (for values interval of measurement temperature of $(30 \div 300)K)$:

$$n << 10^{15} cm^{-3}. \qquad (7.9)$$

We have considered that, Q ~1, and concentration of defects is $N_d << 10^{17} cm^{-3}$ and

$$R = \left(\frac{3}{4\pi N_d} \right)^{1/3} .$$

Thus, if (7.9) holds (for instance, in undoped sample) we should take (3.23) to determine γ_d , otherwise (7.3) and (7.7) apply. For further analysis it's necessary to know the exact value of electrons concentration $n = 5 \times 10^{17} cm^{-3}$. Then $r_d \approx 0.6 \times 10^{-6} (T / 300K)^{1/2} cm$ and $R >> 10^{-6} cm.$ As a result for γ_d we have:

$$\gamma_d (cm^3 / c) \approx 5.6 \times 10^{-6} Q D_+ \times \left(\frac{300K}{T} \right) \left[\frac{1}{1 + 0.74 \times Q \times \left(\frac{300K}{T} \right)^{3/2}} \right] . \qquad (7.10)$$

The expression for γ_{tr} in case of point defects is: $\gamma_{tr} = A_d T^{-1/2}$. Using (7.10) and the expression for γ_{tr}, we are able to calculate the value of A_d by the method explained in chapter (3.5).

Chapter (3.5) (see (3.74)) showed that the reaction of interaction between a positron and a charged accumulation of defects is limited, in all probability, by the diffusion phase of the reaction and $\gamma \approx \gamma_d$. At that to evaluate γ_d we used (3.23), and for γ_{tr} we took $r_c \approx 2Qe^2/(3\varepsilon_0 k_B T)$, where $r_c -$ is the capture radius of a positron by an accumulation of defects. Having $n = 5\times10^{17} cm^{-3}$ for γ_d we should use (7.10), and for $\gamma_{tr} = \pi r_c^2 \upsilon_+$ (see chapter (3.5)) $r_c = r_d$. Then for γ_{tr} we get:

$$\gamma_{tr}(cm^3/s) \approx 1.2\times10^{-5}\left(\frac{T}{300K}\right)^{3/2}. \tag{7.11}$$

Using (7.10) and (7.11) for charged accumulations of defects we get:

$$\frac{\gamma_d}{\gamma_{tr}} \approx 0.5QD_+\left(\frac{300K}{T}\right)^{5/2}\left[\frac{1}{1+0.74Q\left(\frac{300K}{T}\right)^{3/2}}\right]. \tag{7.12}$$

Findings of [Saa89] prove that for $T \le 400K$ $D_+ = D_0(300K/T)^{1/2}$, where $D_0 -$ is the diffusion of positron coefficient value at $T = 300^0 K$ $(D_0 \approx 1cm^2/s)$. At that we assumed that positrons are scattering on acoustic phonons. It's true for undoped and slightly doped samples when we can disregard the scattering of a thermalised positron on charged doping admixtures. When concentration of doping impurity is $5\times10^{17} cm^{-3}$ scattering of electrons on acoustic phonons prevails over scattering on charged impurities at $T \ge 200K$ [Bon77]. Supposing that mechanisms of scattering of positrons and electrons are the same we get: the expression for D_+ [Saa89] is true in this case if $200K \le T \le 400K$. Using the expression for D_+ obtained in [Saa89] and (7.12) for values interval of measurement temperature $(200 \div 300)K$: we get: $\gamma_d/\gamma_{tr} \sim 1$ for any $Q(Q \ge 1)$. Thus, in this case $(n = 5\times10^{17} cm^{-3})$ when determining the value of γ for the reaction of interaction between a positron and a charged accumulation of defects we should take into consideration both coefficients (γ_d and γ_{tr}) while in case of undoped and slightly doped samples (when (7.9) is true) we should take into consideration only γ_d. Thereby it must be noted that the fifth conclusion made in the third chapter is true for those GaAs samples for which (7.9) holds. Later on, from (7.10) and (7.11) it results that in the values interval of measurement temperature of $(200 \div 300)K$ $\gamma_d(Q=\infty)/\gamma_d(Q=1) \le 2.4$ and $\gamma(Q=\infty)/\gamma(Q=1) \le 1.9$ (maximum is at $T = 300K$). Hence, in case of strongly doped GaAs samples the dependence of γ_d and γ on Q is rather weak unlike that for the case of undoped or slightly doped samples where the dependence (in case accumulation of defects $\gamma = \gamma_d$) is linear (see 3.23). Thus, the seventh conclusion made in the third chapter is true for the case of undoped and slightly doped GaAs samples.

7.2 Comparison with experimental data

As the trapping rate of positrons by defects is closely connected with the specific trapping coefficient by $\kappa_d = \gamma n_d$, the natures of dependence of k_d and γ on measurement temperature coincide (measurement temperature has such values that the concentration of defects stays the same).

[Hub98] lists results for dependence of k_d on temperature. The results have been obtained on the basis of experimental data. It follows that for undoped GaAs samples deformed in the [110] direction k_d monotonously decreases with increase of measurement temperature both of monovacancies (point defects) and of accumulations of vacancies. Analysis of those results gives:

1. For samples deformed at $800^0\mathrm{C}$ with strain rate equal to $4.8 \times 10^{-5} s^{-1}$ $k_d \sim T^{-1}$ for accumulations and $k_d \sim T^{-1.2}$ for monovacancies (in the values interval of measurement temparature of $(100 \div 400)K$).
2. For samples deformed at $800^0\mathrm{C}$ with strain rate equal to $3.3 \times 10^{-3} s^{-1}$ $k_d \sim T^{-0.8}$ for accumulations and $k_d \sim T^{-1.5}$ for monovacancies (in the values interval of measurement temperature of $(200 \div 400)K$).
3. For samples deformed at $600^0 C$ with strain rate equal to $6.9 \times 10^{-5} s^{-1}$ $k_d \sim T^{-1.2}$ for monovacancies (in the values interval of measurement temperature of $(300 \div 500)K$). The dependence of κ_d on T for accumulations cannot be measured here due to large fluctuation values of k_d.

As appears from above:

1. For the case of interaction of positrons with point defects $\gamma \sim T^{-\alpha}$, where $\alpha \approx 1.2 \div 1.5$. If when calculating γ we take into consideration both γ_d (according to (3.26) $\gamma_d \sim T^{-3/2}$), and γ_{tr} (according to (3.31) $\gamma_{tr} \sim T^{-1/2}$), we'll manage to explain such a dependence of γ from T.
2. For the case of interaction of positrons with accumulations of vacancies $\gamma \sim T^{-\alpha}$, where $\alpha \approx 1$. If we suppose that there are charged accumulations of vacancies (for which, according to (3.26), $\gamma \sim T^{-3/2}$) and accumulations of neutral vacancies (for which, according to (3.21), $\gamma \sim T^{-1/2}$), in samples we'll manage to explain such a dependence of γ on T.

Let's consider strongly doped GaAs:Te samples. Fig. 7.1 shows data for dependence of the trapping rate k_d of positrons by accumulations of vacancies on measurement temperature.Values of k_d have been determined according to the model $(3.52) \div (3.58)$ taking into consideration experimental data for I_i and τ_i. Only the most typical dependencies of k_d on measurement temperature are shown. For any other cases of interaction between positrons and accumulations of vacancies the dependence of k_d on measurement temperature is very mush the same as the one portrayed either on fig. 7.1(a), or on fig. 7.1(b). Data represented on fig. 7.1 let us consider that the nature of dependence of k_d on measurement temperature for the case of strongly doped and undoped GaAs samples is quite different.

If to determine the specific trapping coefficient γ of positrons in accumulations of vacancies we use (3.23) (negatively charged accumulations) or (3.21) (neutral accumulations) we'll get a monotonous decrease of γ with increase of measurement temperature. This contradicts data shown on fig. 7.1. Hence, (3.21) and (3.23) correct for undoped GaAs samples and are wrong for a strongly doped GaAs.

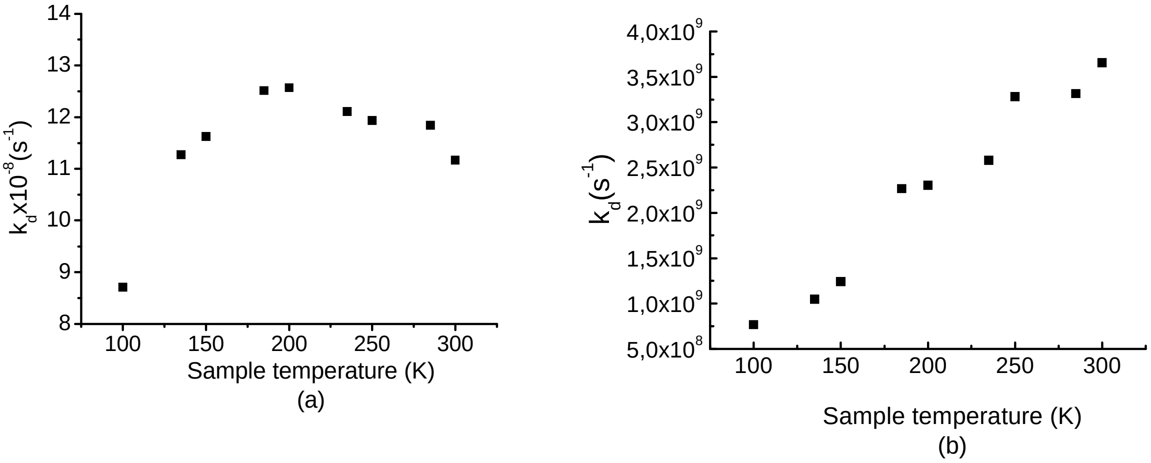

Fig. 7.1: Dependence of the trapping rate k_d of positrons in accumulations of vacancies on measurement temperature in GaAs:Te. Samples have been deformed in the [110] direction. (a). Deformation temperature is 800^0C, strain rate is $2.23\times10^{-4}s^{-1}$, total stretching value is 5.0%. (b). Deformation temperature is $1000^0 C$, strain rate is $2.3\times10^{-4}s^{-1}$, total stretching value is 5.0%. The error of trapping rate is $\pm(8-12)\%$.

Fig. 7.2 represents calculated dependencies of trapping coefficient of the diffusion phase of the reaction γ_d (according to (7.10)) and specific trapping coefficient γ (according to (7.1), (7.10) and (7.11)) of positrons with negatively charged accumulations of vacancies on measurement temperature for GaAs:Te. For the specific trapping coefficient for the capture phase of positrons by negatively charged accumulations of vacancies holds: $\gamma_{tr} \sim T^{3/2}$ (according to (7.11)).

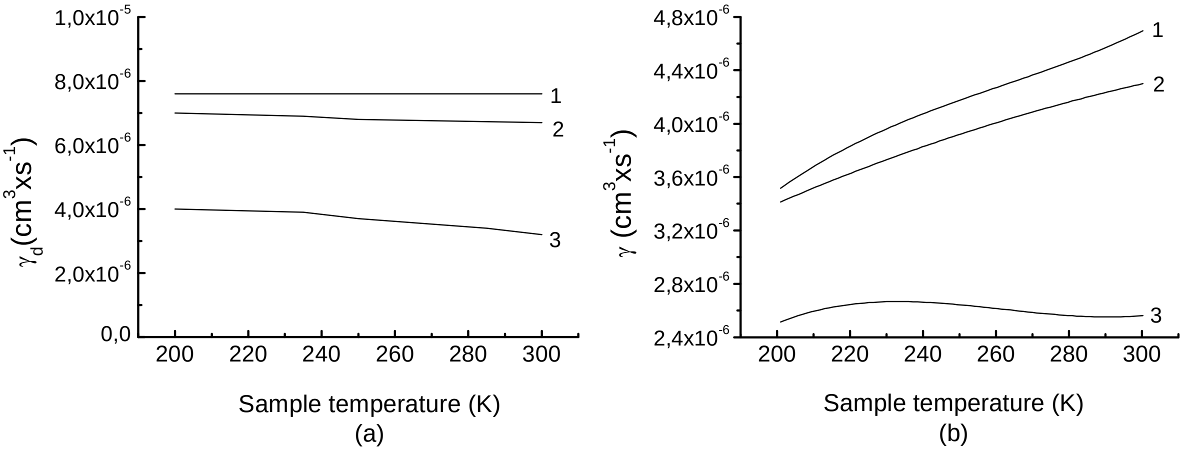

Fig. 7.2: Dependence of specific trapping coefficient of the diffusion phase of the reaction γ_d and specific trapping coefficient γ of positrons on negatively charged accumulations of vacancies on measurement temperature T in the GaAs:Te. Curves 1 have been obtained for $Q=\infty$, curves 2 – for $Q=10$, curves 3 – for $Q=1$ ($Q-$ is the excessive amount of electrons located on accumulations of vacancies if compared to the number of electrons in a neutral accumulation). (a) γ_d.(b) γ.

Comparison of results from fig. 7.1 and fig. 7.2(b) gives: if supposing that for accumulations of vacancies $Q \approx (1 \div 10)$ (which is quite reasonable since the number of vacancies in accumulations ~10) natures of dependencies of the trapping rate and specific trapping coefficient of positrons with accumulations of vacancies on measurement temperature lying in the interval from $200K$ to $300K$ are almost the same. It follows from the said that:

1. Expressions (7.10) and (7.11) can be used for determination γ if $n = 5 \times 10^{17} cm^{-3}$.
2. When determining γ for accumulations of vacancies one should take into account both coefficient γ_d and γ_{tr}.
3. Concentration of accumulations can be determined using (7.1) at any measurement temperature in the interval from $200K$ to $300K$, and the result is almost independent on the value of temperature.

Calculations based on (7.1), (7.10) and (7.11) show that the nature of dependence of γ on measurement temperature for $Q = 1, Q = 10$ and $Q = \infty$ (see fig. 7.2(b)) stays the same with increase of measurement temperature to $400K$.

Expressions (7.10) may be used to determine γ_d beyond the limits of the values interval of measurement temperature ($T = 200K \div 400K.$) as well but first one must fix $D_+(T)$ for $T < 200K$ and for $T > 400K.$ Here a qualitative analysis of dependence of γ_d and γ on T at $T < 200K$ may be given. In a strongly doped sample in the interval of $\mathrm{T} \approx 100K \div 200K$ charged doping impurities and acoustic phonons contribute to scattering of free charge carriers (positrons in this case) [Bon77]. When concentration of doping impurity $\approx (10^{17} cm^{-3} \div 10^{18} cm^{-3})$ drift mobility of charge carriers μ_d slightly changes in the interval of $T \approx 100K \div 200K$ [Bon77], so we may roughly assume $\mu_d = const.$ Then, using the known equation between drift mobility and diffusion coefficient for a mobile particle (for a positron in this case) $\mu_d = D_+ q/(k_B T)$ (q is the charge of the patricle) we get $D_+(T) \sim T.$ As a result if we increase T from $100K$ to $200K$ γ_d will increase (see (7.10)). Taking into account that γ_{tr} also increases with increase of T (see (7.11)) we get that increase of T from $100K$ to $200K$ gives increase of γ. Hence, natures of dependencies of γ and k_d on T in the interval of $T = 100K \div 200K$ are the same (see fig. 7.1).

We draw your attention that at other values of electrons concentration (not $5 \times 10^{17} cm^{-3}$) to determine γ one should take (7.1), (7.7) and $\gamma_{tr} = \pi r_d^2 \upsilon_+$ (here r_d is found from (7.3) for every electrons concentration), because (7.10) and (7.11) have been derived for a specific case when $n = 5 \times 10^{17} cm^{-3}$.

Fig. 7.3 represents data for dependence of trapping rate k_d of positrons on point defects on measurement temperature for GaAs:Te deformed at $200^0 C$ and $300^0 C.$ Point defects have been viewed in these two cases: mixed component from monovacancies and divacancies (see chapter 6.1). It follows from the data on fig. 7.3 that the nature of dependence of k_d on T for strongly doped and undoped GaAs samples is completely different.

If to determine the specific trapping coefficient γ of positrons on negatively charged point defects we use (3.23) that holds for γ_d in case of undoped samples, and $\gamma_{tr} = A_d / T^{1/2}$, we'll have a monotonous decrease of γ from measurement temperature.

This contradicts that which is shown on fig. 7.3(b). If to determine γ_d we use (7.10) (at $Q \sim 1$, which is true for point defects) which holds for $n = 5\times10^{17}cm^{-3}$ (at this $\gamma_{tr} = A_d / T^{1/2}$), we'll be able to explain data shown on fig. 7.3:

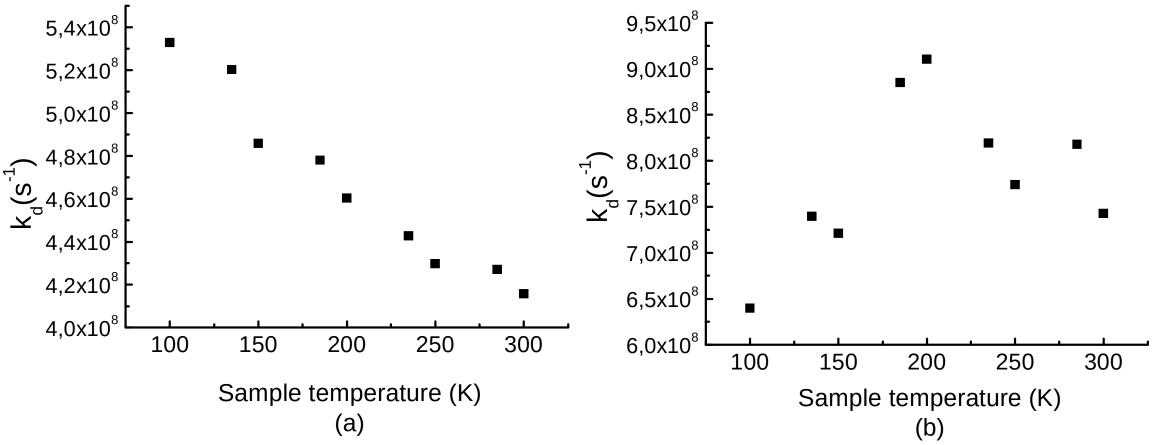

Fig. 7.3: Dependence of trapping rate k_d of positrons on point defects (monovacancies and divacancies) on measurement temperature in GaAs:Te samples. Samples have been deformed in the [110] direction. (a). Deformation temperature is 200^0C, strain rate is $2.23\times10^{-5}s^{-1}$, total stretching value is 5%. (b). Deformation temperature is 300^0C, strain rate is $2.23\times10^{-5}s^{-1}$, total stretching value is 4.5%. The error of trapping rate is $\pm(7-10)\%$.

1. Choosing A_d parameter so that in the viewed values interval of measurement temperature $\gamma_{tr} << \gamma_d$, holds we get $\gamma \approx \gamma_{tr} \sim T^{-1/2}$. This dependence of γ on T qualitatively coincides with that of k_d on T shown on fig. 7.3(a).
2. Choosing A_d parameter so that in the viewed values interval of measurement temperature $\gamma_d << \gamma_{tr}$, holds we get $\gamma \approx \gamma_d$. In the interval $100K \div 200K$ γ_d doubles with increase of temperature (at $T = 100K \div 200K$ $D_+ \sim T$ - see above).

   In the interval $200K \div 300K$ γ_d decreases with increase of temperature (see curve 3 on fig. 7.2(a)). Hence, γ depends on T nonmonotonously (there is a maximum). Such a dependence of γ on T qualitatively coincides with the dependence of k_d on T shown on fig. 7.3(b).

Earlier when analysing the dependence of γ on T for point defects we stated that A_d can take different values at different deformation conditions. The fact that the process of capture of positrons by point defects is influenced by electric and deformation field of dislocations serves an explanation for this. At different conditions of deformation these fields may have different values in the localities of point defects. From the above analysis for point defects results that:

1. Values of γ obtained from (7.1), (7.10) and $\gamma_{tr} = A_d T^{-1/2}$, can be used to determine concentration of defects.
2. Diffusion phase of the reaction and the capture phase of positrons by defects influence on the value of γ.

7.3 Concentration of defects

This chapter contains information on dependence of concentration of accumulation of vacancies n_{cl} and concentration of vacancies (supposing that anglomerated vacancies in an accumulation are evenly distributed in the crystal) n_V on deformation parameters, i.e. on temperature of deformation and stretching velocity as well as on total stretching value.
According to (7.1) we have:

$$n_{cl} = \frac{1}{\gamma} k_d . \tag{7.13}$$

Concentration of accumulation of vacancies has been determined at measurement temperature $T = 300^0 K$. Chapter 7.2 showed that values of concentration of accumulations are hardly dependances on temperature because dependencies of k_d and γ on T are very similar. Concentration of vacancies is determined by

$$n_V = n_{cl} N_V , \tag{7.14}$$

where $N_V -$ is the average amount of vacancies in an accumulation. The values of N_V have been calculated according to [Hub98]:

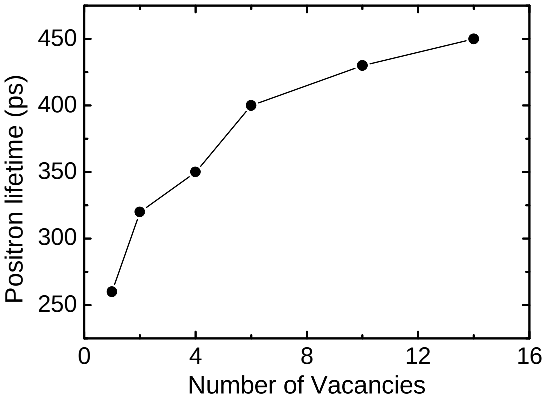

Fig. 7.4: Dependence of positrons lifetime from number of vacancies in accumulation for GaAs [Hub98].

Then, if experimental conditions for measuring positron lifetime are chosen so that k_d increases monotonously with increase of measurement temperature (see fig. 7.1(b)) it is taken $Q \sim 10$ when determining γ (see curve 2 on fig. 7.2(b)). In this case at $T = 300K$ $\gamma \approx 4.3 \times 10^{-6} cm^3 s^{-1}$ (according to (7.1), (7.10), (7.11)). If κ_d decreases in the interval of $T = 200K \div 300K$ (see fig. 7.1(a)) it is taken $Q \sim 1$ when determining γ (see curve 3 on fig. 7.2(b)). In this case at $T = 300K$ $\gamma \approx 2.54 \times 10^{-6} cm^3 s^{-1}$ (according to (7.1), (7.10), (7.11)).

Dependence of concentration of defects on total stretching value

Fig. 7.5 represents dependencies of concentrations of accumulations and vacancies on total stretching value for GaAs:Te samples.

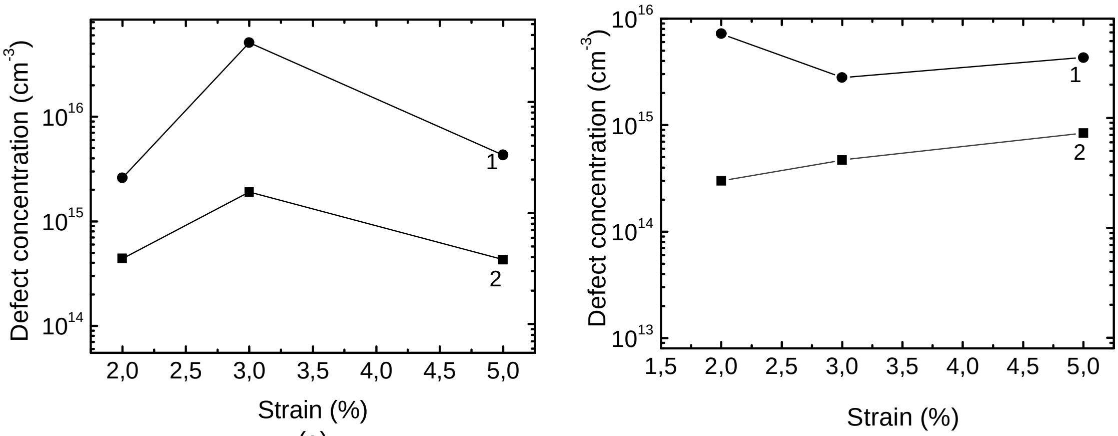

(a) (b)

Fig. 7.5: Dependence of concentration of defects in GaAs:Te samples on rate of stretching. Samples have been deformed in the [110] direction. Curves 1 show concentration of vacancies n_V (it's assumed that anglomerated vacancies in an accumulation are evenly distributed in the crystal), curves 2 show concentration of accumulation of vacancies n_{cl}. (a). Deformation temperature is $800^0 C$, strain rate is $2.23\times10^{-4} s^{-1}$. (b) Deformation temperature is $900^0 C$, strain rate is $2.28\times10^{-4} s^{-1}$.

Tables 7.1, 7.2 contain data for calculation of concentration of defects.

Table 7.1

$T_{def} = 800^0 C$	$\varepsilon = 5\%$	$\varepsilon = 3\%$	$\varepsilon = 2\%$
k_d	$k_d \approx 0.11\times10^{10} s^{-1}$	$k_d = 0.48\times10^{10} s^{-1}$	$k_d \approx 0.19\times10^{10} s^{-1}$
γ	$\gamma \approx 2.54\times10^{-6} cm^3/s$	$\gamma \approx 2.54\times10^{-6} cm^3/s$	$\gamma \approx 4.3\times10^{-6} cm^3/s$
Q, N_V	$(Q \sim 1), N_V \approx 10$	$(Q \sim 1), N_V \approx 27$	$(Q \sim 10), N_V \approx 6$
τ_2	$\tau_2 \approx (430 \pm 11) ps$	$\tau_2 \approx (496 \pm 1) ps$	$\tau_2 \approx (398 \pm 37) ps$

Table 7.2

$T_{def} = 900^0 C$	$\varepsilon = 5\%$	$\varepsilon = 3\%$	$\varepsilon = 2\%$
k_d	$k_d \approx 0.36\times10^{10} s^{-1}$	$k_d \approx 0.2\times10^{10} s^{-1}$	$k_d \approx (0.51\times10^{9} s^{-1}$
γ	$\gamma \approx 4.3\times10^{-6} cm^3/s$	$\gamma \approx 4.3\times10^{-6} cm^3/s$	$\gamma \approx 2.54\times10^{-6} cm^3/s$
Q, N_V	$(Q \sim 10), N_V \approx 24$	$(Q \sim 10), N_V \approx 6$	$(Q \sim 1), N_V \approx 24$
τ_2	$\tau_2 \approx (479 \pm 3) ps$	$\tau_2 \approx (338 \pm 10) ps$	$\tau_2 \approx (481 \pm 7) ps$

Dependence of concentration of defects on stretching velocity

Fig. 7.6 represents dependencies of concentration of accumulations and vacancies on stretching velocity of the GaAs:Te sample.Here for $\dot{\varepsilon} \approx 1.08\times10^{-4} s^{-1} \kappa_d \approx 0.79\times10^{9} s^{-1}$ and $\gamma \approx 2.54\times10^{-6} cm^3/s$ (Q~1), $N_V \approx 24$ ($\tau_2 \approx (481 \pm 5) ps$).

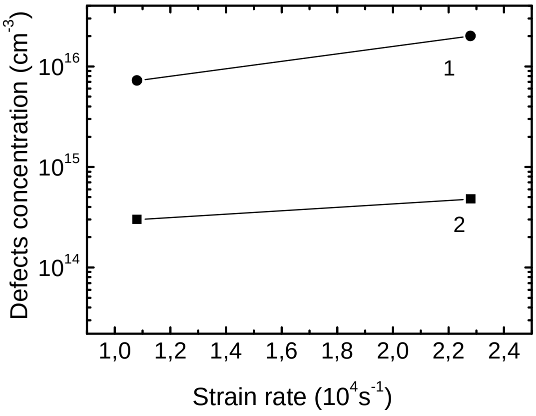

Fig. 7.6: Dependence of concentration of defects in the GaAs:Te sample on stretching velocity. Samples have been deformed in the [110] direction at $900^0 C$ to stretching value of 5%. Curve 1 shows concentration of vacancies n_V (it's assumed that anglomerated vacancies in an accumulation are evenly distributed in the crystal). Curve 2 shows concentration of accumulation of vacancies n_{cl}.

For deformation temperature of 800^0C at strain rate equal to $2.23\times10^{-4}s^{-1}$ accumulations of vacancies are viewed (see fig. 6.1(a)) being $n_V \approx (4.3\pm0.28)\times10^{15}cm^{-3}$ (see fig. 7.5(a)). At strain rate equal to $1.06\times10^{-4}s^{-1}$ vacancies and divacancies are viewed (see fig. 6.3(a)). At that k_d decreases monotonously with increase of measurement temperature (such a dependence of k_d on T is similar to that shown on fig. 7.3(a)). Chapter 7.2 showed that in this case $\gamma_{tr} << \gamma_d$ and $\gamma \approx \gamma_{tr}$. Hence, concentration of defects meets this condition:

$$n_d = \frac{k_d}{\gamma} = \frac{k_d}{\gamma_{tr}} >> \frac{k_d}{\gamma_d}. \tag{7.15}$$

As point defects are viewed in this case $(Q \sim 1)$, $\gamma_d \approx 2.54\times10^{-6}cm^3/s$ when measurement temperature is $300K$ (according to (7.10)). As a result from (7.15) we get: $n_d >> (0.18\pm0.028)\times10^{16}cm^{-3}$. Taking into account that here $N_V \sim 1(\tau_2 \approx (302\pm18)ps)$, we get $n_V >> (1.8\pm0.28)\times10^{15}cm^{-3}$ (as for a mixed component of vacancies and divacancies γ_{tr} is unknown, we cannot determine the value of n_V). Comparing this with $n_V \approx (4.3\pm0.28)\times10^{15}cm^{-3}$ at $\dot{\varepsilon} \approx 2.23\times10^{-4}s^{-1}$, we may conclude that at deformation temperature equal to $800^0 C$ concentration of vacancies, most likely, decreases with increase of stretching velocity. Thus, dependencies of n_V on stretching velocity at deformation temperatures of $800^0 C$ and $900^0 C$ are qualitatively different.

Dependence of concentration of defects on deformation temperature

Fig. 7.7 represents dependencies of concentration of accumulations and vacancies on deformation temperature for GaAs: Te samples. For deformation temperature of $1000^0 C$ we have: for $\varepsilon \approx 5.0\%$ $k_d \approx (0.35\pm0.03)\times10^{10}s^{-1}$ and $\gamma \approx 4.3\times10^{-6}cm^3/s$ $Q \sim 10$, $N_V \approx 9$ $(\tau_2 \approx (421\pm7)ps)$. Similar data for other cases have been considered above.

For deformation temperatures of 200^0C and 300^0C at strain rate of $2.23\times10^{-5}s^{-1}$ (total stretching value is $(4.5\div5)\%$) point defects are viewed i.e. monovacancies and divacancies (see chapter 6.1). At deformation temperature of $200^0 C$ k_d decreases monotonously with increase of measurement temperature (see fig. 7.3(a)) and in this case $\gamma_{tr} << \gamma_d$ and $\gamma \approx \gamma_{tr}$ (see chapter 7.2).

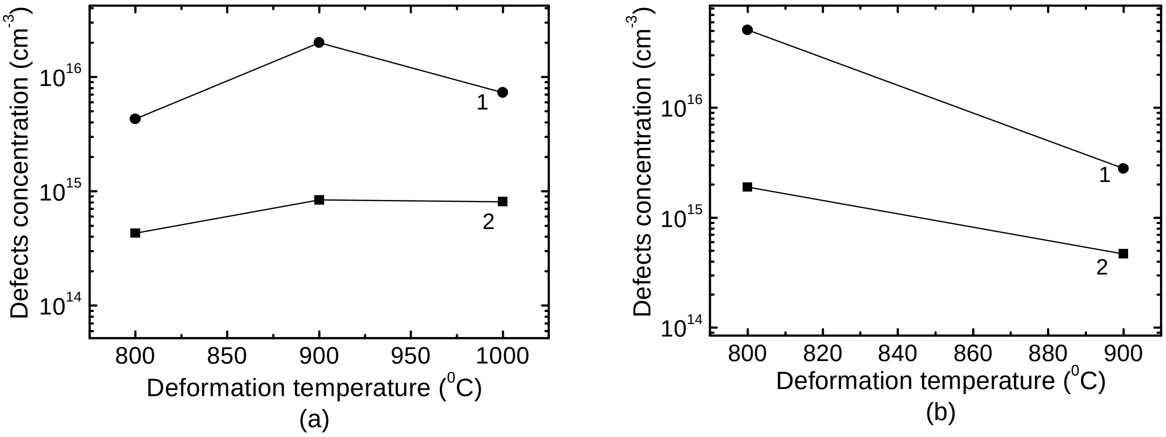

Fig. 7.7: Dependence of concentration of defects in GaAs: Te samples on deformation temperature. Samples have been deformed in the [110] direction at strain rate of $(2.23 \div 2.3) \times 10^{-4} s^{-1}$. Curves 1 show concentration of vacancies n_V (t's assumed that anglomerated vacancies in an accumulation are evenly distributed in the crystal), curves 2 show concentration of accumulation of vacancies n_{cl}. (a). Total stretching value is 5% (b). Total stretching value is 3%. (c). Total stretching value is 2%.

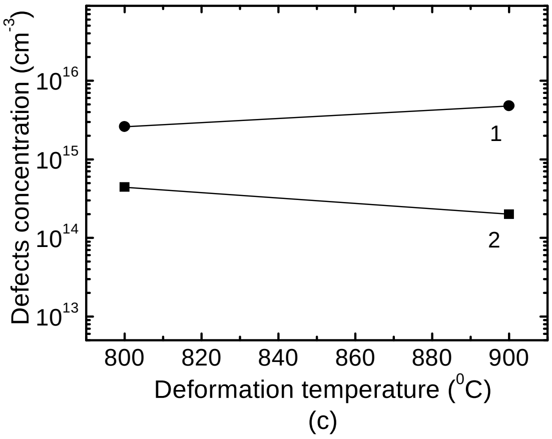

Hence, concentration of defects meets condition (7.15). Taking into account that at measurement temperature of $300K$ $k_d \approx (0.44 \pm 0.046) \times 10^9 s^{-1}$ and $\gamma_d \approx 2.54 \times 10^{-6} cm^3/s$ ($Q \sim 1$, because defects are point ones) we get: $n_d >> (0.17 \pm 0.018) \times 10^{15} cm^{-3}$. For deformation temperature of $300^0 C$ $\gamma_d << \gamma_{tr}$ and $\gamma \approx \gamma_d$ (see chapter 7.2). Taking into account that at measurement temperature of $300K$ $k_d \approx (0.7 \pm 0.11) \times 10^9 s^{-1}$ and $\gamma \approx \gamma_d \approx 2.54 \times 10^{-6} cm^3/s$ ($Q \sim 1$) we get: $n_d \approx (0.27 \pm 0.043) \times 10^{15} cm^{-3}$. In these two cases the values of τ_2 at measurement temperature of $300K$ are the same within the error: $\tau_2 \approx (325 \pm 12) ps$ ($200^0 C$) and $\tau_2 \approx (338 \pm 15) ps$ ($300^0 C$). That's why the number of vacancies N_V, in point defects is the same. Hence, here concentration of vacancies decreases with increase of deformation temperature from 200^0C to 300^0C. If when determining concentration of defects and vacancies one uses the same (any) value of γ in all cases, values of concentration themselves will be different, but dependencies of concentration of defects and vacancies do not change from parameters of deformation values shown on fig. $7.5 \div 7.7$.

The error of defects concentration is $\pm(8 \div 12)\%$.

Analysis of results for dependence of concentration of defects on parameters of deformation values

Vacancies are formed as a result of movement of dislocations with jogs. There are three main mechanisms of formation of jogs on the screw dislocation:

1. Thermal formation of jogs (thermal energy of atoms vibration is transfered on a dislocation which may result in formation of jogs; at this the number of jogs increases with increase of deformation temperature). The posibility of thermal formation of jogs is discussed in [Mie93] and [Mil94].
2. As a result of double cross slip (see chapter 2.3).
3. As a result of crossing of dislocations (see chapter 2.5).

As a rule, in case of complex dislocations glide (that in several slip systems, in particular, when deformation runs in [110] and [100] directions) the third mechanism dominates the second [Cui96]. In case of easy glide (that in one system, for example, in the [213] direction) the second mechanism dominates the third [Cui96].

On concentration of vacancies critical influence is exerted by density of mobile dislocations and their velocity, as well as by velocity of transportation of a jogs along the dislocation line and the number of such jogs on it. (see chapter 2.5.2). Relationship between velocity and density of mobile dislocations and concentration of vacancies is evident: with increase of density and (or) velocity of dislocations concentration of vacancies also increases. Influence of number of jogs and velocity of their transportation along the dislocation line is clear : with increase (decrease) of velocity of jogs the possibility of their mutual annihilation increases (decreases) which leads to decrease (increase) in concentration of vacancies; increase (decrease) of number of jogs gives increase (decrease) of concentration of vacancies.

When rate of stretching of samples is higher (deformation temperature and stretching velocity are assumed constant) the stress σ applying to mobile dislocations increases $(\sigma = m_s \tau)$. According to (2.15) mobile dislocations velocity rises. General density of dislocations, according to (2.10), rises as well. This increases the probability that a mobile dislocation will cross with a motionless one (or with a mobile, too). As a result during to the crossing of dislocations mechanism the number of jogs increases. Due to thermal mechanism the number of jogs stays the same because the temperature of the sample is the same. Thus, as stretching increases the number of jogs also increases which leads to increase of concentration of vacancies.

Increase of stretching velocity (deformation temperature and rate of stretching are assumed constant) results in increase of general density of dislocations according to (2.10) which leads to higher probability that a mobile dislocation will cross with a motionless one (or with mobile as well). As a result, higher stretching velocity gives rise to concentration of vacancies. Here, as well, thermal mechanism does not contribute to changes in number of jogs because deformation temperature stays the same.

Increase in deformation temperature (total stretching value and stretching velocity being constant) the general density of dislocations decreases according to (2.10). This reduces the probability that a mobile dislocation will cross with a motionless one (or with a mobile, too). As a result the number of jogs on a mobile dislocation decreases with increase of deformation temperature. On the other hand, due to thermal mechanism of generation of jogs they increase in number with increase of deformation temperature. Hence, there may be a complex dependence of the number of jogs and, consequently, concentration of vacancies on deformation temperature: different values intervals of deformation temperature may increase or decrease concentration of vacancies.

Processes of generation of vacancies as a result of movement of dislocations with jogs (primary processes) have been considered above. Supposing that accumulations are constituted from vacancies appearing close to each other (and not as a result of secondary processes, i.e. long-distanced diffusion of vacancies in the crystal with subsequent formation of accumulations due to interaction of vacancies) then the dependencies of concentration of accumulations and vacancies anglomerated in accumulations on parameters of deformation with help of primary processes only. Hence, these dependencies will be the same as those for the number of jogs on parameters of deformation:

1. Increase of total deformation value and (or) stretching velocity results in increase of anglomerated vacancies;
2. Increase of deformation temperature results in increase or decrease of concentration of anglomerated vacancies depending on the temperature interval viewed.

Such dependencies of concentration of anglomerated vacancies on parameters of deformation have been viewed in experiments results for which can be found in [Hub98]:

1. For doped GaAs: Te samples $(n = 2.5\times10^{18} cm^{-3})$, deformed in the [110] direction at $500^0 C$, concentration of anglomerated vacancies increases both with increase of stretching velocity and with increase of total deformation value. Increase of deformation temperature in the interval of $450^0\mathrm{C} \div 800^0\mathrm{C}$ reduces concentration of anglomerated vacancies.
2. For undoped GaAs samples deformed in the [110] direction at temperatures of $500^0\mathrm{C}$ and $800^0\mathrm{C}$, and in the [100] direction at $600^0\mathrm{C}$, and in the [213] direction at $500^0\mathrm{C}$, concentration of anglomerated vacancies increases with increase of stretching velocity. Increase of total stretching value of undoped samples deformed in the [100] direction at $600^0\mathrm{C}$ results in increase of concentration of anglomerated vacancies. When deformation temperature changes from $350^0\mathrm{C}$ to $550^0\mathrm{C}$ concentration of anglomerated vacancies in undoped samples deformed in the [100] direction changes nonmonotonously (having its maximum): temperature rise from $350^0\mathrm{C}$ to $450^0\mathrm{C}$ gives rise to concentration of vacancies; temperature rise from $450^0\mathrm{C}$ to $550^0\mathrm{C}$ reduces concentration of vacancies.

These dependencies of concentration of anglomerated vacancies on parameters of deformation prove that under the experimental conditions primary processes of generation of vacancies during movement of dislocations with jogs play a decisive part in kinetics of formation of defects (the author of [Hub98] also came to this conclusion).

Chapter 2.5.2 contains quantitative models of kinetics of formation of vacancies taking into account only primery processes: the Mott model [Mot60] (see (2.23)), the Popov model [Pop90] (see (2.25)), the Estrin-Mecking model [Mec80] (see (2.26)). The Mott and Popov models have ξ and P_j parameters ($P_j -$ is the ratio of density of tree-like dislocations creating jumps on a screw dislocation to general density of dislocations; ξ is the ratio of density of tree-like dislocations to general density of dislocations). Dependencies of ξ and P_j on parameters of deformation are unknown. Thus we cannot use these models to analyse experimental data contained in [Hub98]. But let's consider the Estrin-Mecking model. According to (2.26) we have:

$$\frac{\partial n_V}{\partial \gamma} = \frac{\chi \tau \dot{\varepsilon}}{\alpha_1 \mu b^3}. \tag{7.16}$$

Using $\gamma = \varepsilon / m_s$ and integrating (7.16) we get:

$$n_V \sim \dot{\varepsilon} \int_0^{\varepsilon} \tau(\varepsilon) d\varepsilon. \qquad (7.17)$$

It’s evident from (7.17) that increase of total stretching value and (or) of stretching velocity (higher streching velocity increases $\tau(\varepsilon)$) results in increase of concentration of vacancies n_V which agrees with experimental data of [Hub98]. Increase of deformation temperature leads to, according to (7.17), monotonous decrease of n_V (because $\tau(\varepsilon)$ reduces with increase of deformation temperature) which agrees with experimental data of [Hub98] for dependence of n_V on doped samples’ deformation temperature. However, the model fails to explain nonmonotonous dependence (with a maximum) of n_V on deformation temperature for undoped samples ([Hub98].

If in the Mott and the Popov models we assume that parameters ξ and P_j are constants, we’ll have the same dependencies of concentration of vacancies on parameters of deformation based on these models as the ones based on the Estrin-Mecking model.

Results of the present paper for dependence of concentration of defects on parameters of deformation (fig. $7.5 \div 7.7$), prove that at high-temperature deformation $(800^0 C \div 1000^0 C)$ secondary processes play a decisive part in kinetics of formation of defects. The significance of secondary processes is expressly illustrated by dependence of concentration of defects on total stretching value at different deformation temperatures (fig. 7.5). Considering only primery processes concentration of defects can only increase with increase of total stretching value. This doesn’t agree with data shown on fig. 7.5. Fig. $7.8 \div 7.10$ represents the dependence of the avarege number of vacancies N_V in an accumulation on parameters of deformation. It results from the data of fig. $7.8 \div 7.10$ that number of vacancies in accumulations is strongly dependable on parameters of deformation. Hence, changes in parameters of deformation restructure accumulations (apart from changing concentration of accumulations). We’d like to draw your attention that when one (any) of the parameters of deformation changes (other parameters maintaining their constant value) the maximum number of vacancies in accumulations is approximately the same: $(24 \div 27)$. Hence, accumulations that contain a larger number of vacancies are unstable at any parameters of deformation here considered. At different parameters of deformation stability of accumulations can be achieved with different number of vacancies.

One can imagine kinetics of formation of accumulations this way. For example, when rate of stretching becomes higher concentration of vacancies, due to primery processes, increases. At that concentration of accumulations and number of vacancies in them will increase until accumulations will stability. Further increase of rate of stretching may unstable accumulations. As a result, accumulations will dissociate, partly or totally. Released vacancies and those generated as a result of primery processes will annihilate mainly with interstitial atoms (or will enter into reactions with other components). This will lead to decrease in concentration of accumulations and in number of vacancies. Generally, increase of concentration of accumulations and of number of vacancies in accumulations when this or that parameter of deformation grows can be explained within the framework of primery processes of generation of vacancies supposing that accumulations are stable.

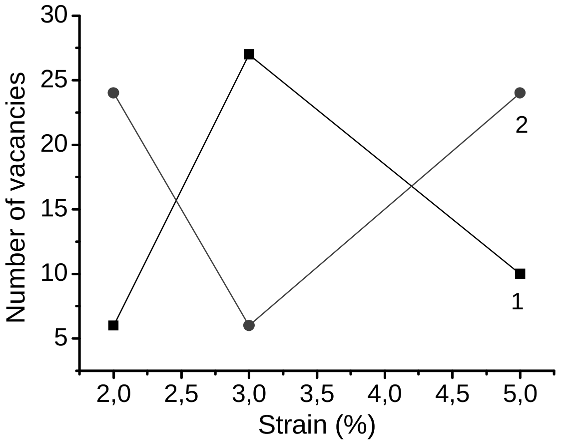

Fig. 7.8: Dependence of number of vacancies N_V in an accumulation on rate of stretching of GaAs: Te. Samples have been deformed in the [110] direction. Curve 1: deformation temperature is $800^0 C$, strain rate is $2.23 \times 10^{-4} s^{-1}$. Curve 2: deformation temperature is $900^0 C$, strain rate is $2.28 \times 10^{-4} s^{-1}$.

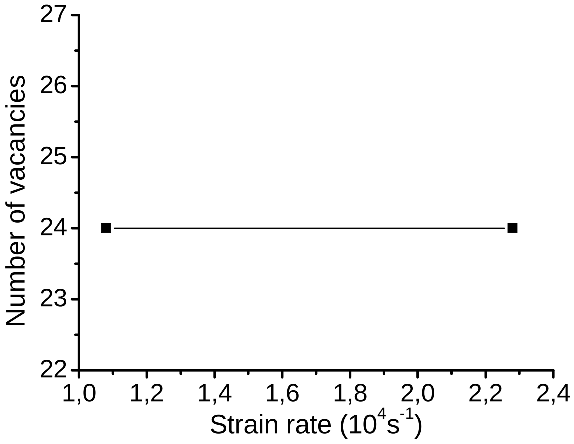

Fig. 7.9: Dependence of number of vacancies N_V in an accumulation on stretching velocity of GaAs: Te. Samples have been deformed in the [110] direction at $900^0 C$ until total value of 5%.

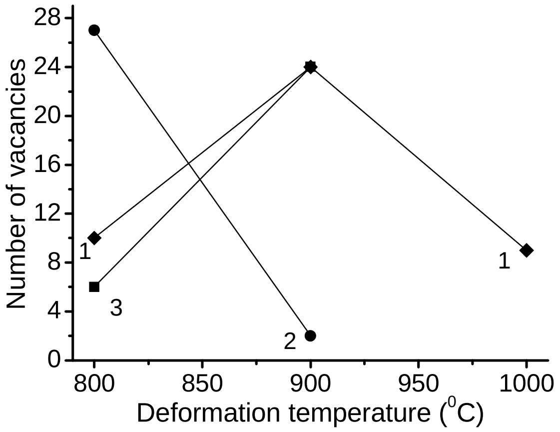

Fig. 7.10: Dependence of number of vacancies N_V in an accumulation on deformation temperature of GaAs: Te. Samples have been deformed in the [110] direction at a strain rate of $(2.23 \div 2.3) \times 10^{-4} s^{-1}$. Curve 1: total stretching value is 5%. Curve 2: total stretching value is 3%. Curve 3: total stretching value is 2%.

Decrease of concentration of accumulations and number of vacancies in accumulations can be explained by secondary processes, i.e. by dissociation of accumulations (partial or total). When concentration of accumulations decreases the number of vacancies in an accumulation also decreases see fig. $7.5 \div 7.10$). This argues for dissociation of accumulations.

Taking into consideration primery processes of generation of vacancies (during movement of dislocations with jogs) and secondary processes (dissociation of accumulations of vacancies) we can qualitatively explain data shown on fig. $7.5 \div 7.7$.

It has been clarified earlier that if deformation temperature changes from $200^0\mathrm{C}$ to $300^0\mathrm{C}$ concentration of defects decreases. This dependence is explained by primery processes (see above).

Taking into account that in intervals of deformation temperature from $200^0 C$ to $300^0 C$ (findings of the present paper) and from $400^0 C$ to $800^0 C$ (findings of [Hub98]) dependencies of concentration of defects on parameters of deformation can be interpreted only within primery processes, the following conclusion is made: secondary processes play an important part in kinetics of formation of defects at high-temperature deformation of the GaAs (at $\mathrm{T} \geq 800^0 C$).

Conclusions

1. It results from analysis of data for dependence of concentration of defects on deformation conditions of GaAs:Te samples that at high-temperature deformation $(\mathrm{T} = (800 \div 1000)^0\mathrm{C})$ on kinetics of formation of defects is influenced both by primery processes (generation of vacancies during movement of dislocations with jogs), and secondary ones (dissociation of accumulations of vacancies). However, kinetics of formation of defects at $T < 800^0 C$ can be described only by means of primery processes.
2. During high-temperature deformation (stretching) of GaAs:Te samples not only concentration of accumulation of vacancies change, but also accumulations restructure: the number of vacancies in stable accumulatins changes.
3. Nature of dependence of trapping rate k_d of positrons on accumulations of vacancies on temperature T of the crystal in case of strongly doped GaAs:Te samples $(n = 5\times10^{17} cm^{-3})$ and in case of undoped samples is totally different: in undoped samples k_d decreases monotonously with increase of T; in strongly doped samples k_d either increases monotonously or changes nonmonotonously (having its maximum).
4. An expression has been obtained for the specific trapping coefficient of positrons by negatively charged defects taking into account the diffusion phase of the reaction and the capture phase of positrons by defect. It has been shown that using this expression one can qualitatively explain the dependence of trapping rate k_d of positrons by defects on crystal temperature both for undoped and for strongly doped GaAs samples.Thus one can use the expression when calculating values of concentration of defects.

8. Summary

1. When increasing deformation temperature (in the interval from $800^0\mathrm{C}$ to $1000^0\mathrm{C}$) and (or) decreasing strain rate (from $2.2\times10^{-5}s^{-1}$ to $2.2\times10^{-4}s^{-1}$) of GaAs:Te samples $(n=5\times10^{17}cm^{-3})$ we view:
    a) increase in the number of phases of a plastic deformation;
    b) decrease of the values of stretching at which this or that plastic deformation phase begins;
    c) decrease of values of strengthening coefficients in the dislocations glide phase and hardening phases.
2. It has been shown that using (2.10), (2.11), (2.15), (2.19) which are generally used in the theory of plastic deformation it's possible to qualitatively explain the above mentioned regularities.
3. The expression that relates liquidity limits to deformation temperature and strain rate (2.19)is not to be applied to determine rate of stress exponent and activation energy of movement of dislocations.
4. In all deformed samples either accumulations of vacancies or point defects (monovacancies and divacancies) have been found. Both point defects and accumulations have not been detected simultaneously. When changing deformation temperature and stretching velocity type of positron traps changes: with decrease of deformation temperature and stretching velocity formation of point defects becomes more preferential.
5. During the process of high-temperature deformation of GaAs:Te samples not only concentration of accumulation of vacancies changes but accumulations themselves restructure: the number of vacancies in stable accumulations changes.
6. At high-temperature deformation $(T=800^0C\div1000^0C)$ of GaAs:Te samples kinetics of formation of accumulations of vacancies in influenced both by primery processes (generation of vacancies during movement of dislocations with jogs), and secondary ones (dissociation of accumulations of vacancies). However, kinetics of formation of defects at $T<800^0C$ can be described only within the framework of primery processes.
7. Nature of dependence of trapping rate k_d of positrons on accumulations of vacancies on temperature T of the crystal in case of doped GaAs:Te samples $(n=5\times10^{17}cm^{-3})$ and in case of undoped samples is totally different: in undoped samples k_d decreases monotonously with increase of T, in doped samples k_d either increases monotonously or changes nonmonotonously (having its maximum).
8. Expression (7.7),(7.10),(7.11) have been obtained for specific trapping coefficient of positrons on negatively charged defects taking into account the diffusion phase of the reaction and the capture phase of positrons by defect. It has been shown that using this expression one can qualitatively explain the dependence of trapping rate of positrons on defects (with accumulations of vacancies and point defects) on

crystal temperature both for undoped and for doped GaAs samples $(n = 5\times10^{17}cm^{-3})$. Thus one can use the expression when calculating values of concentration of defects.

9. In the future conduction of similar systematic research using other concentrations of doping impurity (and using other doping admixtures) seems appropriate. This will help determine the influence of concentration of impurities and of types of impurities on kinetics of formation of defects.

Appendix A

Slip systems of dislocations

There are twelve slip systems of dislocations in the gallium arsenide (see chapter 2.6). These are they:

1. In (111) planes there are three slip directions: $[0\bar{1}1],[\bar{1}10],[10\bar{1}]$.
2. In $(1\bar{1}1)$ planes there are three slip directions: $[\bar{1}01],[0\bar{1}\bar{1}],[110]$.
3. In $(\bar{1}11)$ planes there are three slip directions: $[\bar{1}0\bar{1}],[0\bar{1}1],[110]$.
4. **4.** In $(\bar{1}\bar{1}1)$ planes there are three slip directions: $[101],[\bar{1}10],[0\bar{1}\bar{1}]$.

The actual number of slip systems can be less. This depends on direction of deformation of the sample. If for any slip system $m_s = 0$, there's no dislocations glide in this system because there $\sigma = 0$ and, according to (2.15), dislocations velocity $\upsilon = 0$). Hence, to find the actual number of slip systems in this or that direction of deformation we need to determine the Schmidt factor for all 12 theoretically possible slip systems. The Schmidt factor is $m_s = \cos\Phi \times \cos\Psi$ [Hir72], where $\Phi -$ is the angle between the deformation axis and the unit vector that is perpendicular to the slip plane; $\Psi -$ is the angle between the deformation axis and the slip direction. Slip direction coincides with the Burgers vector because in (2.3) for the Peierls potential $W_0 \sim b^2$ [Hir72] and dislocations glide in the direction where the value of the Burgers vector length is minimal, i.e. in the direction in the slip system where atoms are most densely packed. Thus we may take the angle Ψ as an angle between the deformation axis and the Burgers vector.

$$\cos\Phi = \frac{(\vec{d}\,\vec{n})}{\left|\vec{d}\right|\left|\vec{n}\right|}, \quad \cos\Psi = \frac{(\vec{d}\,\vec{l})}{\left|\vec{d}\right|\left|\vec{l}\right|}.$$

Here $\vec{d} -$ is the vector in the direction of deformation; $\vec{n} -$ is the vector that is perpendicular to the slip plane; $\vec{l} -$ is the vector in the slip direction.

Let a sample be deformed in the $[h_1h_2h_3]$. direction. Considering slip in the $(g_1g_2g_3)$ plane in the $[m_1m_2m_3]$ slip direction, we may write $\vec{d} = h_1\vec{a}_1 + h_2\vec{a}_2 + h_3\vec{a}_3$, $\vec{l} = m_1\vec{a}_1 + m_2\vec{a}_2 + m_3\vec{a}_3$, $\vec{n} = g_1\vec{a}_1 + g_2\vec{a}_2 + g_3\vec{a}_3$ (vector which is perpendicular to the plane with Miller indices $(g_1g_2g_3)$, has the same indices $(g_1g_2g_3)$ [Ans78]). Here $\vec{a}_1, \vec{a}_2, \vec{a}_3 -$ are unit and mutually perpendicular lattice vectors.

Table A1 lists values of m_s that are mostly used in experiments for direction of deformation. It's evident from the table that when deformation runs in the [110] direction there are actually four equal slip systems (with values of $m_s \approx 0.408$).

Table. A1: Values of m_s for different slip systems of dislocations and for different directions of deformation of GaAs samples.

			Slip systems											
			(111)			$(1\bar{1}1)$			$(\bar{1}11)$			$(\bar{1}\bar{1}1)$		
			$[0\bar{1}1]$	$[\bar{1}10]$	$[10\bar{1}]$	$[\bar{1}01]$	$[0\bar{1}\bar{1}]$	$[110]$	$[\bar{1}0\bar{1}]$	$[0\bar{1}1]$	$[110]$	$[101]$	$[\bar{1}10]$	$[0\bar{1}\bar{1}]$
Direction of deformation	[110]	m_s	0.408	0	0.408	0	0	0	0	0	0	0.408	0	0.408
	[100]	m_s	0	0.408	0.408	0.408	0	0.408	0.408	0	0.408	0.408	0.408	0
	[213]	m_s	0.35	0.175	0.175	0.117	0.467	0.35	0.29	0.117	0.175	0	0	0

Here dislocations glide in four slip systems. When deformation runs in the [100] direction there are actually eight equal slip systems (with values of $m_s \approx 0.408$). Here dislocations glide in eight slip systems. When deformation runs in the [213] direction there are actually nine unequal slip systems (with different values of m_s). The slip system where the Schmidt factor is the highest is preferential ($m_s \approx 0.467$). Here dislocations glide only in one slip system (for it $m_s \approx 0.467$).

Appendix B

Conventional signs

A	Point defects annihilation velocity
a	The lattice constant and the Bohr radius of positronium
a_p	The Peierls potential period
b	The Burgers vector length
C	Concentration of defects
C_I	Concentration of interstitials
C_V	Concentration of vacancies
d	Stretching amplitude of a dialocation element and the average distance traveled by the dislocation line before annihilation (with another dislocation) during its entrance
D_V	Diffusion coefficient of vacancies
D_+	Diffusion coefficient of positrons
E_a	Energy level of acceptor impurity
E_b	Bond energy of a positron in a trap
E_C	Bottom energy of the conducting band
E_d	Energy level of a donor impurity
E_F	The Fermi level

E_0	Bond energy of a positronium in vacuum
E_S	Bond energy of a positronium in the crystal
E_υ	Valence zone ceiling energy
f	Oscillations frequancy of the dislocation line
G	The Gibbs enthalpy
I_i	Intensity of the *i-th* component of positron lifetime
k_B	The Boltzmann constant
k_d	Trapping rate of a positron on a defect
$\tilde{k}_d$	Coefficient of the diffusion phase of reaction of a positron with a defect
k_{tr}	Coefficient of the capture phase of a positron by a defect
L	The average distance traveled by the dislocation line before annihilation (with another dislocation) during its glide
m	Stress exponent
m_+	Effective mass of the positron
m_-	Effective mass of the electron
m_e	Mass of the electron
m_c	Mass of density of states of electrons
m_s	Schmidt factor
m_υ	Mass of density of state of holes
n	Concentration of electrons
N_{a_z}	Concentration of charged acceptors
N_d	Number of traps with positrons and density of dislocaions
N_{d_z}	Concentrations of charged donors
n_{a_z}	Concentration of acceptor-type defects
n_{dz}	Concentration of donor-type defects
N_{dm}	Density of mobile dislocations
N_p	Number of free positrons
P	Formation of point defects velocity
p	Concentration of holes
P_f	Probability that the condition f in a trap is not taken by a positron
P_i	Probability that a positron is in free condition i
T	Crystal temperature
U	Activation energy of dislocation motion
V_A	Activation volume
υ	Dislocation velocity and relative velocity of an electron and a positron in a positronium
υ_j	Velocity of jogs glide on dislocations
W	The Peierls potential
α	Constant (in different formulas)
α_1	Constant
α_+	Linear damping coefficient
β	Constant
χ	Constant

χ_S	Constant
ε	Deformation (relative change in length of the sample)
ε_0	Static permittivity of the crystal
γ	Shear and specific trapping coefficient of a positron in a defect
γ_d	Coefficient of the diffusionally limited reaction
γ_0	Constant
γ_{tr}	Coefficient of the capture phase of a positron by a defect
Γ_0	Positronium level width
δ_d	Thermal shooting velocity of a positron located on a dislocation
δ_{st}	Thermal shooting velocity of a positron located on a shallow point trap
λ	Average distance between capture centres of vacancies and interstitials and annihilation rate of positrons
λ_b	Annihilation rate of positrons in a non-defective crystal
λ_j	Distance between jogs on the dislocation line
μ	Shear modulus
ν	The Poisson coefficient
ρ	Density of crystal
σ	Internal stress and section of capture of a positron by a cluster of defects
σ_{eff}	Effective stress
σ_i	Stress created by dislocations
τ	External stress and positron lifetime
τ_{aV}	Average lifetime of positrons
τ_b	Bulk lifetime
τ_i	Components of positron lifetime
ξ	Ratio of density of tree-like dislocations to the general density of dislocations
θ	Hardening coefficient

References

[Ale68a] H.Alexander und P.Haasen. In: Solid State Physics, herausgegeben von F.Seitz. D.Turnbull und H.Ehrenreich, Bd. 22 (S.27) (Academic Press, New York,1968).

[Ale68b] H.Alexander, P.Haasen. Solid State Phys. 22(1968), p.27.

[Ans78] A.I.Anselm. In: Vvedenije v teoriyu poluprovodnikov (Nauka, Moscow, 1978).

[Are83] K.P.Arefjev, S.A.Vorobjov, E.P.Prokopjev. In:Pozitronika v radiacionom materialovedenii ionikh struktur i poluprovodnikov (Energoatomizdat, Moscow, 1983).

[Ash79] N.Ashcroft, N.Mermin. In:Solid State Physics, part 2 (Mir, Moscow, 1979).

[Ask85] B.M.Askerov. In:Elektronie yavleniya perenosa v poluprovodnikakh (Nauka, Moscow, 1985).

[Bar65] C.Barrett, W.Nix. Acta metal.13 (1965), p.1247.

[Bar85] G.A.Baraff, M.Schluter. Phys.Rev.Lett. 55(1985), p.1327.

[Ber68] V.B.Berestetsky, E.M.Lifshis, L.P.Pitaevsky. In:Relativistskaya kvantovaya mekhanika (Nauka, Moscow, 1968).

[Bon77] V.L.Bonch – Bruyevich, S.G.Kalashnikov. In: Physics of Semiconductors (Nauka, Moscow, 1977).

[Bra72] W.Brandt, R.Paulin. Phus.Rev.B 5(1972), p.2430.

[Bra77] W.Brandt, R.Paulin. Phus.Rev.B 15(1977), p.2511.

[Bro87] M.Brohl, C.Kisielowski – Kemmerich, H.Alexander. Appl.Phys. Lett. 50(1987), p.1733.

[Cor90] C.Corbel, F.Pierre, P.Hautojarvi, K.Saarinen, P.Moser. Phys.Rev.B 41(1990), p.10632.

[Cui96] A.Cuito, M.Ortiz.Acta Mater. 44 (1996), p.427.

[Dan91] S.Dannefaer, P.Mascher, D.Kerr. J.Appl. Phys. 69 (1991), p.4080.

[Die56] J.Diehl. Z.Metall. 47 (1956), p.331.

[Ent73] S.G. Entelis, R.P. Tiger. In:Kinetika reaktsy v zhidkoi faze (Chimija, Moscow, 1973).

[Fra74] W.Frank, A.Seeger. Appl. Phys. 3 (1974), p.61.

[Geb99] J.Gebauer, R.Krause – Rehberg, S.Eichler, F.Barnen.Appl. Surf. Sci. 149 (1999), p.110.

[Geb2000] J.Gebauer.Native Leerstellen in GaAs – der Einflus von Stoechiometry und Dotierung. Mathematisch – naturwissenschaftlicher Bereich (Halle (Saale), Martin – Luther – Universitate, 2000).

[Ger86] D.Gerthsen. Phys.Stat.Sol. (a), 97 (1986), p.527.

[Gri91] Fizicheskiye velichini. Spravochnik pod red. I.S.Grigoryeva, E.Z.Meilikhova (Energoatomizdat, Moscow, 1991).

[Gyu28] Z.Gyulai, D.Hartly. Zeits. Phys.51 (1928), p.378.

[Haa62] P.Haasen. Z.Physik. 167 (1962), p.461.

[Haa89] P.Haasen. Phys.France. 50 (1989), p.2445.

[Hir72] J.Hirth, J.Lothe. In: Theory of Dislocations (Atomizdat, Moscow, 1972).

[Hub98] C.Hubner. Punktdefektgeneration bei der Versetzungsbewegung (Dissertation, Halle (Saale), Martin – Luther – Universitate, 1998).

[Jan89] R.W.Jansen, O.F.Sankey. Phys.Rev. B 39 (1989), p.3192.

[Koz81] V.P.Kozhevnikov, V.V.Mikhnovitch. J.Tekhnicheskoi Fiziki. 51 (1981), p.153.

[Kra84] V.A.Krasilnikov, V.V.Krylov. In: Vvedenije v fizicheskuyu akustiku (Nauka, Moscow, 1984).

[Kra94] R.Krause – Rehberg, H.Leipner, A.Kupsch, A.Polity, T.Drost. Phys. Rev. B 49 (1994), p.2385.

[Kra99] R.Krause – Rehberg, H.S.Leipner. In: Positron annihilation in semiconductors (Berlin, Springer – Verlag, 1999).

[Lak80] Yu.M.Lakhtin, V.P.Leontyeva. In: Materialovedenie (Maschinostroenie, Moscow, 1980).

[Lan87] L.D.Landau, E.M.Lifshis. In: Teoriya uprugosti (Nauka, Moscow, 1987).

[Man81] M.Manninen, R.Nieminen. Appl. Phys. A 26 (1981), p.93.

[Mat74] H.F.Matare. In: Defect Electronics in Semiconductors (Mir, Moscow, 1974).

[Mec80] H.Mecking, Y.Estrim. Scripta metal. 14 (1980), p.815.

[Mec81] H.Mecking, U.Kocks. Acta Met., 29 (1981), p.1865.

[Mil93] M.Militzer, W.Sun, J.Jonas. Mater. Sc. For. $111 \div 115$ (1993), p.163.

[Mil 94] M.Militzer, W.Sun, J.Jonas. Acta Metall. Mater. 42 (1994), p.133.

[Mog95] O.E. Mogensen. In: Positron annihilation in chemistry. Springer Series in Chemical Physics (Springer – Verlag, Berlin, 1995).

[Mot60] N. F.Mott. Trans. Met. Soc. AIME. 218 (1960), p.962.

[Oro34] E. Orowan. Z. Phys. (1934), p.614.

[Oro40] E .Orowan. Proc. Phys. Soc. 52 (1940), p.8.

[Pei40] R. Peierls. Proc. Phys. Soc. 52 (1940), p.23.

[Per70] A. Perkins, J.Carbotte. Phys. Rev. B1 (1970), p.101.

[Pog84] A. Pogrebnyak. Phys. Stat. Sol. (a). 86 (1984), p.191.

[Pol34] G. Polyani. Z. Phys. (1934), p.660.

[Pop90] L.E. Popov, V.A. Starenchenko, I.I. Shalygin. Fizika Metalov i Metalovedenie. 6 (1990), p.31.

[Pus78] M.Puska. Non – linear regression program. Techn. Ber., Teknillinen Korkeakoulu. Ottaniemi, Finland, 1978.

[Pus83] M.J. Puska, R.M.Nieminen. J.Phys.F: Met. Phys. 13 (1983), p.333.

[Pus89] M.J. Puska. J.Phys. : Cond. Mat. 1 (1989), p.7347.

[Pus 90] M. Puska, C. Corbel, R. Nieminen. Phys. Rev. B 41 (1990), p.9980.

[Pus94] M. Puska, R. Nieminen. Reviews of Modern Physics. 66 (1994), p.841.

[Rab79] Yu.N. Rabotnov. In: Mekhanika deformiruemogo tverdogo tela (Nauka, Moscow, 1979).

[Saa89] K. Saarinen, P. Hautojarvi, A. Vehanen, R. Krause, G. Dlubek. Phys. Rev. B 39 (1989), p. 5287.

[Saa90] K. Saarinen,C.Corbel, P. Hautojarvi, P. Lanki, F. Pierre, D. Vignuad. J. Phys: Condens. Matter. 2 (1990), p. 2453.

[Sch65] G. Schoeck. Phys. Stat. Sol. 8 (1965), p.499.

[Sch67] S. Schafer. Phys. Stat. Sol. 19 (1967), p.297.

[Sch82] M.P. Shakolskaya. In: Akusticheskie kristaly (Nauka, Moscow, 1982).

[Sei 50] F. Seitz. Phys. Rev. 80 (1950), p. 239.

[Seo95] H. Seong, L.J. Lewis. Phys. Rev. B 52 (1995), p.5675.

[Sie93a] H. Siethoff. Phys. Stat. Sol. (a) 138 (1993), p. 591.

[Sie 93b] H. Siethoff, H. Brion, J. Volkl. J. Appl. Phys. 74 (1993), p. 153.

[Som96] B. Somieski, T. Staab, R. Krause – Rehberg. Nucl. Instr.and Meth. in Phys. Res. A 381 (1996), p. 128.

[Sta96] T. Staab, B. Somieski, R. Krause – Rehberg. Nucl. Instr. and Meth. in Phys. Res. A 381 (1996), p. 141.

[Ste33] A. Stepanov. Zeits. Phys. 81 (1933), p.560.

[Tay34] G.I. Taylor. Proc. Roy. Soc. (London) A 145 (1934), p. 362.

[Tru92] G. Trumpy, M. Bentzon. J. Phys. : Condens. Matter. 4 (1992), p. 419.

[Vin72a] V.L. Vinetsky, I.I. Yaskovets. Ukrainskii Fizicheckii Jurnal. 17 (1972), p.934.

[Vin72b] V.L. Vinetsky, I.I. Yaskovets. Fizika Tvjerdogo Tela. 14 (1972), p. 3046.

[Vin75] V.L. Vinetsky, I.I. Yaskovets. Fizika Tvjerdogo Tela. 17 (1975), p. 2518.

[Wee83a] J. Weertmann und J. Weertmann. In: Physical Mettallurgy, herausgegeben von R. Cahn und P. Haasen (p. 1259) (North – Holland Physics Publishing, Amsterdam, 1983).

[Wee83b] J. Weertmann und J. Weertmann. In: Physical Metallurgy, herausgegeben von R. Cahn und P. Haasen (p. 1309) (North – Holland Physics Publishing, Amsterdam, 1983).

[Wei64] H. Weisberg, S. Berko. Phys. Rev., 154 (1964), p. 249.

[Yon89] I. Yonenage, K. Sumino. J. Appl. Phys. 65 (1989), p. 85.

[Zha91] S.B. Zhang, J.E. Nortrup. Phys. Rev. Lett. 67 (1991), p. 2339.

[Zon94] I. Zongo, J. Farvacque. Phys. Stat. Sol. (a) 142 (1994), p. 383.

Erklärung

Hiermit erkläre ich, dass ich die vorliegende Arbeit selbständig und nur unter Verwendung der angegebenen Quellen und Hilfsmittel angefertigt habe. Wörtlich oder inhaltlich übernommene Stellen sind als solche gekennzeichnet.

Diese Arbeit habe ich an keiner anderen Universität oder Hochschule vorgelegt und mich zu keinem frühren Zeitpunkt um den Doktorgrad beworben.

V.V. Mikhnovich

Halle/Saale, September 2005

Curriculum Vitae of Vladimir V. Mikhnovich

1985-1995	Secondary school
1995-2001	Moscow State Engineering and Physics Institute (Technical University) Department of Experimental and Theoretical Physics Diploma thesis: “Quantitative analysis of electrons and holes mobility in Silicon and Gallium nitrides” (excellent)
Dec. 2002 – 2005 (till present)	Ph D student and a member of Graduiertenkolleg 415 “Defektstrukturbestimmte physicalische Eigenschaften” at Martin-Luther University Halle-Wittenberg Supervisor: Dr. H.S Leipner

Personal data

Date of birth	October 3, 1978
Place of birth	Voskressensk, Moscow region, Russia
Present address	Lutherstr. 43 06110 Halle (Saale)
Citizenship	Russia

Halle (Saale), September 5, 2005 Vladimir Mikhnovich

Acknowledgements.

The primary acknowledgement must be to PD Dr. Hartmut S. Leipner, gave me the opportunity to conduct scientific research in the field of plastic deformation. I’m grateful to him for defining the problem, discussing results of the research and friendly and encouraging criticism.

I’m thankful to Prof. Dr. Reinhard Krause - Rehberg for the opportunity to conduct experimental research using the positron annihilation spectroscopy method. He was always willing to discuss matters concerning positron lifetime spectroscopy.

I’d like to thank Mr Prof. Dr. Peter Grau for the opportumity to subject samples to deformation on test equipment.

I must also thank Mr Dr.Wolfgang Fräinzel for being very helpful during plastic deformation experiments.

Acknowledgement must also go to Mr Dr. Ludovic Thilly for his assistance at conducting a part of plastic deformation experiments.

I’d like to thank all laboratory personnel for creating a pleasant and creative working atmosphere.

I’m thankful to German Research Society for financial support.

I must thank my parents for continuous support and trust in me.